CALIFORNIA INSTITUTE OF TECHNOLOGY
EARTHQUAKE ENGINEERING RESEARCH LABORATORY
AND
UNIVERSITY OF CALIFORNIA AT LOS ANGELES
EARTHQUAKE ENGINEERING AND
STRUCTURES LABORATORY

FORCED VIBRATION OF A 22-STORY STEEL FRAME BUILDING

BY
PAUL C. JENNINGS, R. B. MATTHIESEN AND J. BRENT HOERNER

EERL 71-01

A REPORT ON RESEARCH CONDUCTED UNDER
GRANTS FROM THE NATIONAL SCIENCE FOUNDATION

PASADENA, CALIFORNIA

FEBRUARY 1971

ACKNOWLEDGMENTS

The authors wish to acknowledge the excellent cooperation of the personnel of the San Diego Gas and Electric Company. Without their assistance and their tolerance of the inconveniences associated with the testing it would not have been possible to perform the experiments described herein. The contributions of Joseph Sinnott, President, and John C. Burton, Associate Civil Engineer, are especially appreciated. The authors are grateful also for the interest and advice of the engineering firm of Ferver, Dorland and Associates of San Diego.

Vibration tests of major structures require the efforts of a large number of people. The authors wish, in particular, to acknowledge the work of Roy Relles, Rafael Ronderos, Ed Reuben, Harry Gobler, Knut Skattum, Rudolpho Saragoni, Michel Flandrin, Robert Shanman, Paul Ibañez, M. D. Trifunac and J. S. Benya, as well as Professors Gary C. Hart and Donald E. Hudson.

The initial stages of the testing program were coordinated through Caltech's Earthquake Research Affiliates Program, of which the San Diego Gas and Electric Company is a member. The research was supported in part by grants from the National Science Foundation.

INTRODUCTION

The 22-story steel frame structure that houses the offices of the San Diego Gas and Electric Company is a well-known feature of the skyline of San Diego and is a good example of modern, high-rise office construction. Designed by the architectural firm of R. G. Wheeler and Associates, with structural design by Ferver, Dorland and Associates, the building was completed in April 1968. The building, shown in Figure 1, is owned and occupied solely by the San Diego Gas and Electric Company.

Because this building typifies many buildings in the major cities of the seismic west coast, and because a multistory office building may hold a thousand people or more during business hours, it is important that the dynamic properties of structures such as this be measured. Experimentally determined dynamic properties are required both to improve the techniques by which such properties are calculated for purposes of design, and to permit interpretation of the measured response of the building in the event of a strong earthquake. As information on the dynamic properties of tall buildings and their earthquake response accumulates, it should be possible to develop better procedures for determining the appropriate levels of earthquake loading for design. The need for special attention to the tall buildings becomes clear when it is realized that the seismic provisions of building codes are not as applicable to the newer tall buildings as they are to older types of construction.

In the tests reported below, the San Diego Gas and Electric Company Building was excited by two eccentric-mass vibration generators located on the 20th (equipment) floor and measurements of the structural response were

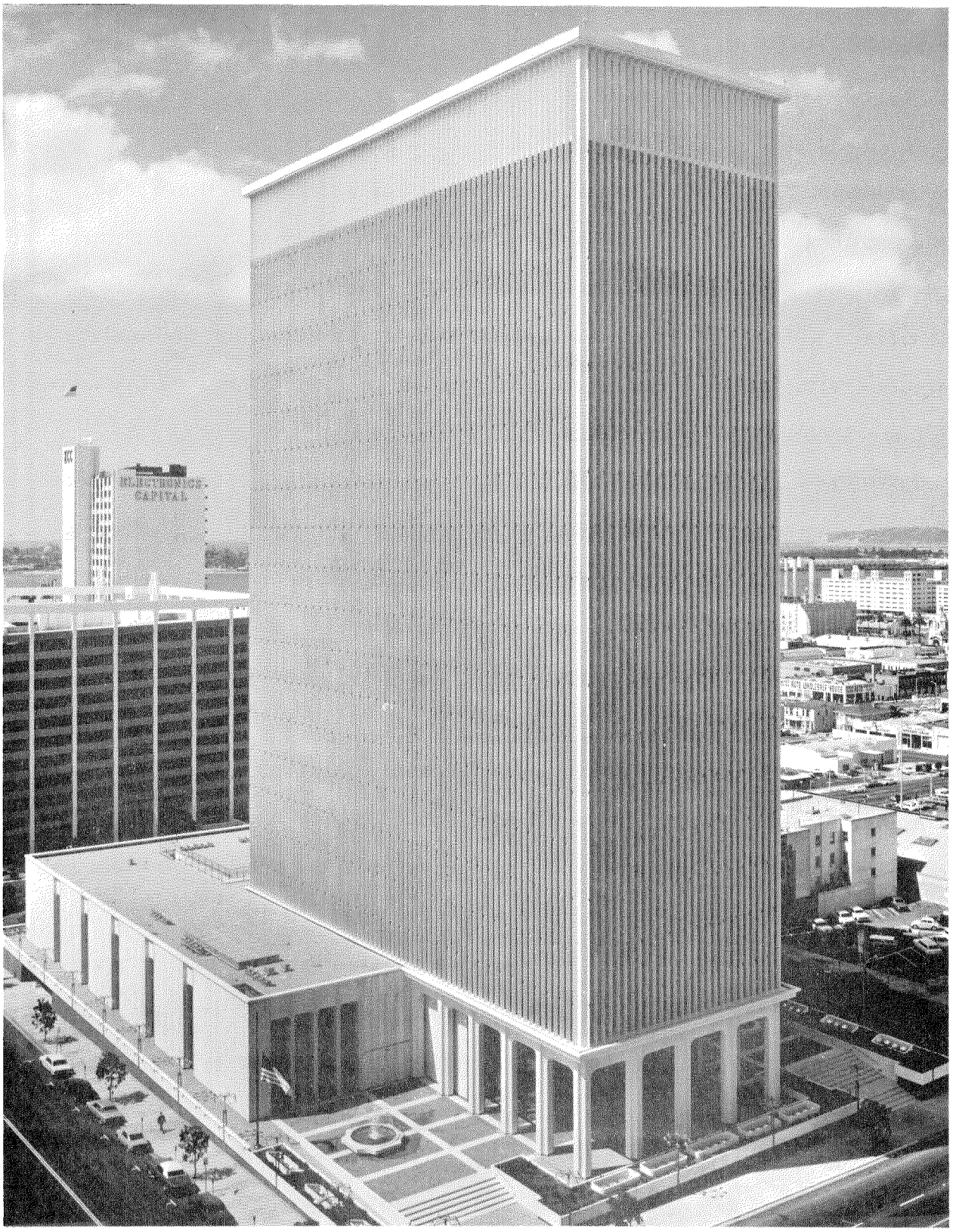

FIGURE 1. SAN DIEGO GAS AND ELECTRIC COMPANY BUILDING

made throughout the building from the roof to the second basement. From these measurements, which are more extensive than in previous tests of this type, it has been possible to determine frequencies, mode shapes and damping values for the first 18 modes of the structure; six each in N-S translation, E-W translation and in torsion. In another portion of the testing program the dynamic properties of the building also were determined by analysis of the measured response of the building to ambient vibration (Trifunac, 1970a). The results of these two experiments and the analytical determination of the building properties (Gobler, 1969) complete the research efforts devoted to the structure.

The experimental program was a cooperative effort between the research groups in earthquake engineering at the California Institute of Technology and the University of California at Los Angeles. The testing, conducted on weekends to minimize disturbance to the occupants, extended over a period of approximately two months and required a crew varying between four and eight.

The building has already experienced minor earthquake shaking, being completed just a few days before the Magnitude 6.5 Borrego Mountain Earthquake of April 9, 1968. Although the epicenter of the shock was about 65 miles from the site, the building vibrated enough to exercise the seismic joints of the structure and the earthquake response substantially exceeded that of the subsequent vibration tests. The earthquake response was well below design levels, however, and, as expected, no structural damage occurred. The response to this earthquake was not recorded, but two strong-motion accelerographs were purchased and installed by the company after the vibration tests were completed and future earthquake motions will be

measured.

Description of the Building

The San Diego Gas and Electric Company office complex occupies a city block in downtown San Diego at 101 Ash Street. As seen in Figure 1, the complex consists of two buildings: a 22-story tower and a two-story U-shaped building. The two-story building envelops the tower on three sides but is structurally separated from the tower by 3-inch seismic joints. Together, the buildings have over 325,000 sq. ft. of floor space and are occupied by nearly 1000 employees.

The 291-ft tower portion is the major building and was the subject of the test program. The overall dimensions of the tower are approximately 180 ft by 70 ft. The structural system of the tower is a moment-resistant, ductile steel frame supporting 21 floor levels and a roof above grade and two levels below. Figure 2 shows sections of the tower and the adjacent structure. A plan section of a typical floor of the tower is shown in Figure 3 in which it is seen that there are seven frames aligned E-W and three frames in the N-S direction. The columns are joined by girders in the N-S and E-W directions. In the N-S direction, intermediate beams, which support the floor system, are framed into the girders. The girders and beams are rolled shapes whereas the columns are 24-in. built-up sections. The framing changes at the top two levels of the structure, but it should be noted that the framing of the tower is essentially symmetrical. A36 steel is used throughout the frame.

The typical floor system for the office portions of the tower consists of cellular steel decking intermittently welded to the structural frame. The decking is topped with approximately 2 in. of concrete. Five-inch reinforced concrete slabs cast over the floor beams are used in areas where the loading

SAN DIEGO GAS AND ELECTRIC BUILDING

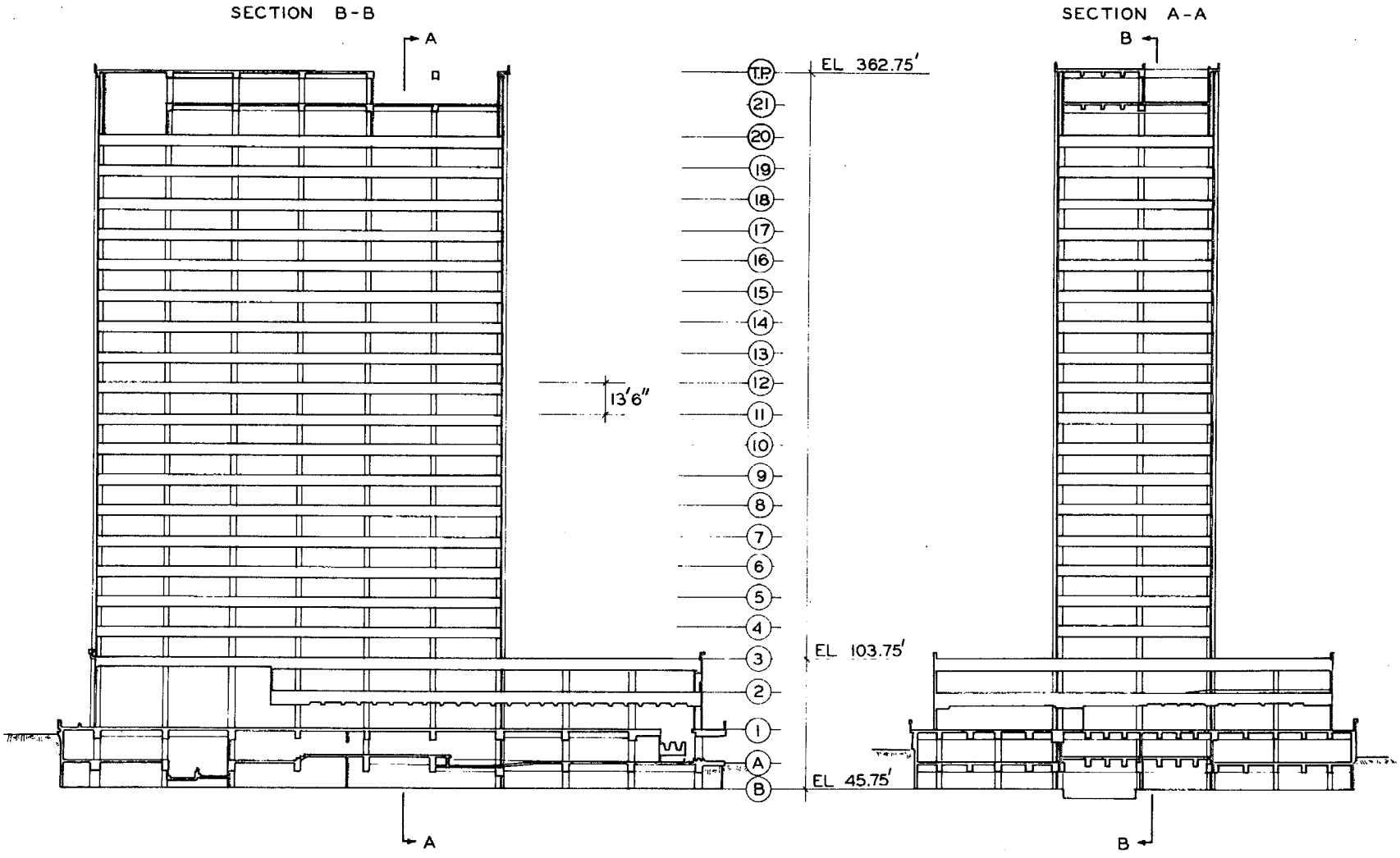

FIGURE 2. N-S AND E-W SECTIONS OF THE SAN DIEGO GAS AND ELECTRIC COMPANY BUILDING

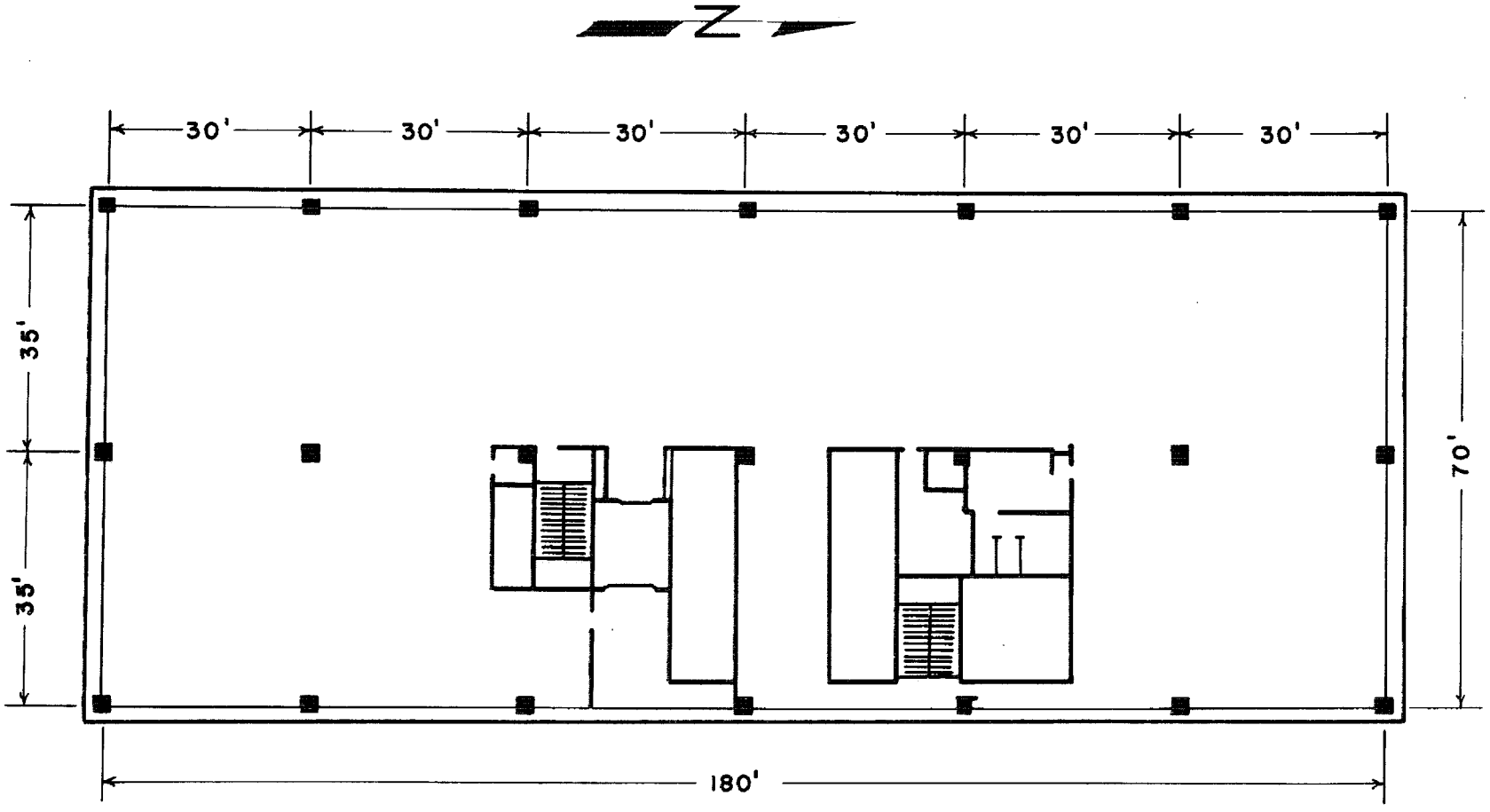

TYPICAL PLAN, 4th - 17th FLOORS

SAN DIEGO GAS & ELECTRIC BUILDING

FIGURE 3. TYPICAL FLOOR PLAN

is heavier, and a reinforced concrete slab, composite with the floor system, is used to support the heavy mechanical equipment on the 20th and 21st floors.

All steel framing below the first floor of the structure is encased in reinforced concrete. Above this level, fireproofing is achieved by metal lath and plaster facing on the columns and by a sprayed layer of Zonolite plaster on the beams, girders and undersides of the steel decking of the floors. The fireproofing undoubtedly contributes to the stiffness of the structure, especially for small displacements (Gobler, 1969). Some of the features of the frame and fireproofing are shown in Figure 4A, a photograph taken during construction.

The interior walls of the structure are of 4- and 6-in. metal lath and plaster construction, the latter thickness being used for the walls which surround the elevator cores (Figure 3). Although these asymmetrically located walls are not structural, they may influence the structural response. The exterior curtain walls are also nonstructural and consist mainly of glass and lightweight metal panels.

All four sides of the tower are faced with precast, reinforced concrete fins which are attached to the structural frame at each floor level (Figure 1). These fins, which measure approximately 6 in. by 18 in. by 27 ft-0 in. each contribute substantially to the mass and stiffness of the tower. Their purpose is architectural.

Another architectural feature can be seen in Figure 1 which shows the two-story columns on the lowest levels of the north portion of the tower. The columns are encased in reinforced concrete and covered with a ceramic veneer. For architectural purposes, additional dummy columns of reinforced

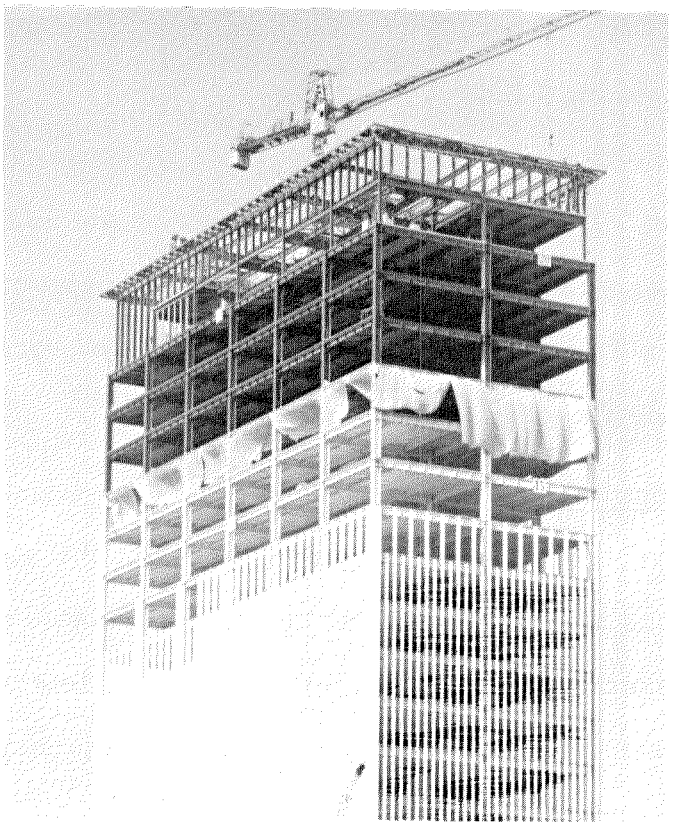

A. FRAMING OF THE TOWER

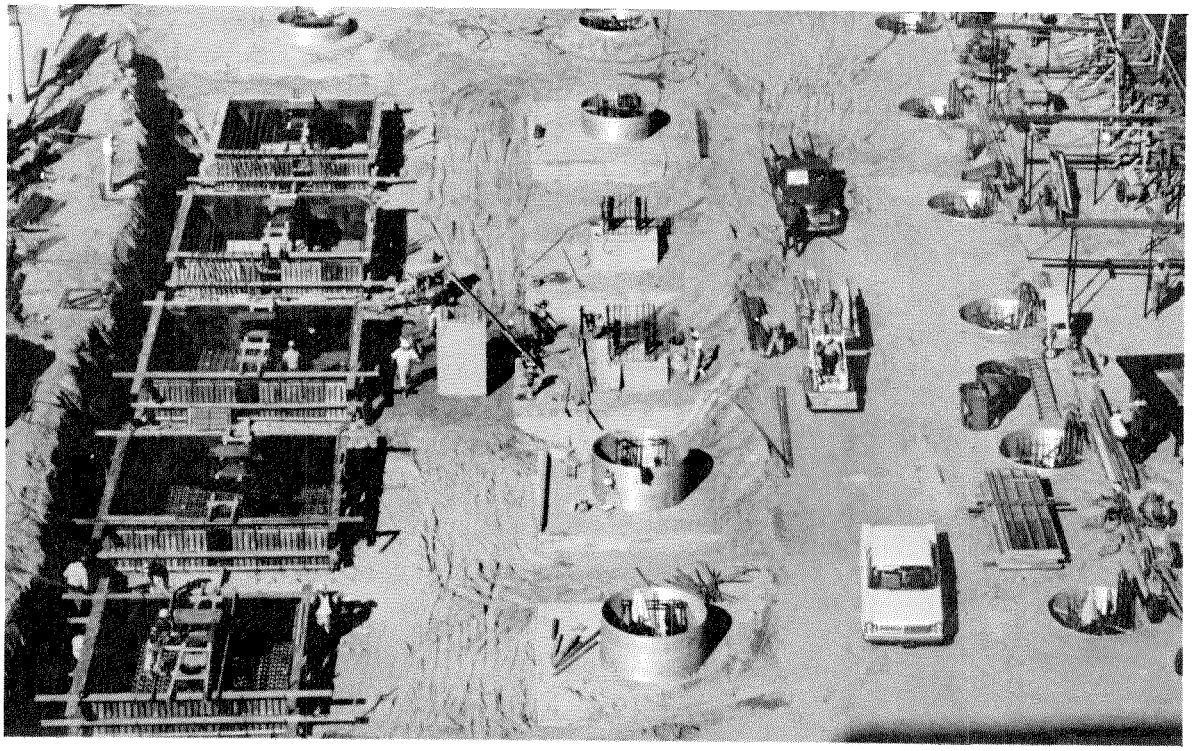

B. FOUNDATION DETAILS

FIGURE 4. CONSTRUCTION OF THE BUILDING

concrete have been added between the actual columns. The dummy columns can be located by comparing Figures 1 and 3.

The foundation conditions at the site consist of irregular layers of firm to very firm silty sand, clayey sand, gravelly clayey sand and loose to compact sand containing gravel and cobbles (Benton Engineering, 1965). These relatively favorable conditions permitted the use of spread footings with dimensions varying from 14 to 22 ft. (Figure 4-B).

Test Procedures and Summary of Testing

Steady-state, sinusoidal vibrations were induced in the structure by two vibration generators placed on the 20th floor as indicated in Figure 5. The response of the structure was measured at points of interest with an accelerometer-amplifier-recorder system. At each frequency change, the vibrators were held at constant frequency long enough for all transient effects to decay, so only steady-state response was recorded. The transient effects were a problem only for the fundamental modes, for which the exciting forces were very low and the periods (approximately 2.4 seconds) were relatively long. The essential features of the equipment and test procedures are substantially the same as those for previous tests (Keightley, 1964; Nielsen, 1964; Rea, Bouwkamp and Clough, 1966; Benya, 1967; Jennings and Kuroiwa, 1968; Shanman, 1969; Smith and Matthiesen, 1969; Matthiesen and Smith, 1969, and Ibañez, Matthiesen, Smith and Wang, 1970) and only a brief summary is given herein. One notable improvement added since most of the tests cited above were made is the addition of equipment to measure the phase between the excitation and response. This feature permits a marked increase in the information gained from the tests.

In each vibrator the force is produced by eccentric masses which rotate about a vertical axis. Thus the exciting force is proportional to the eccentric mass, the amount of eccentricity and the square of the rotational frequency.

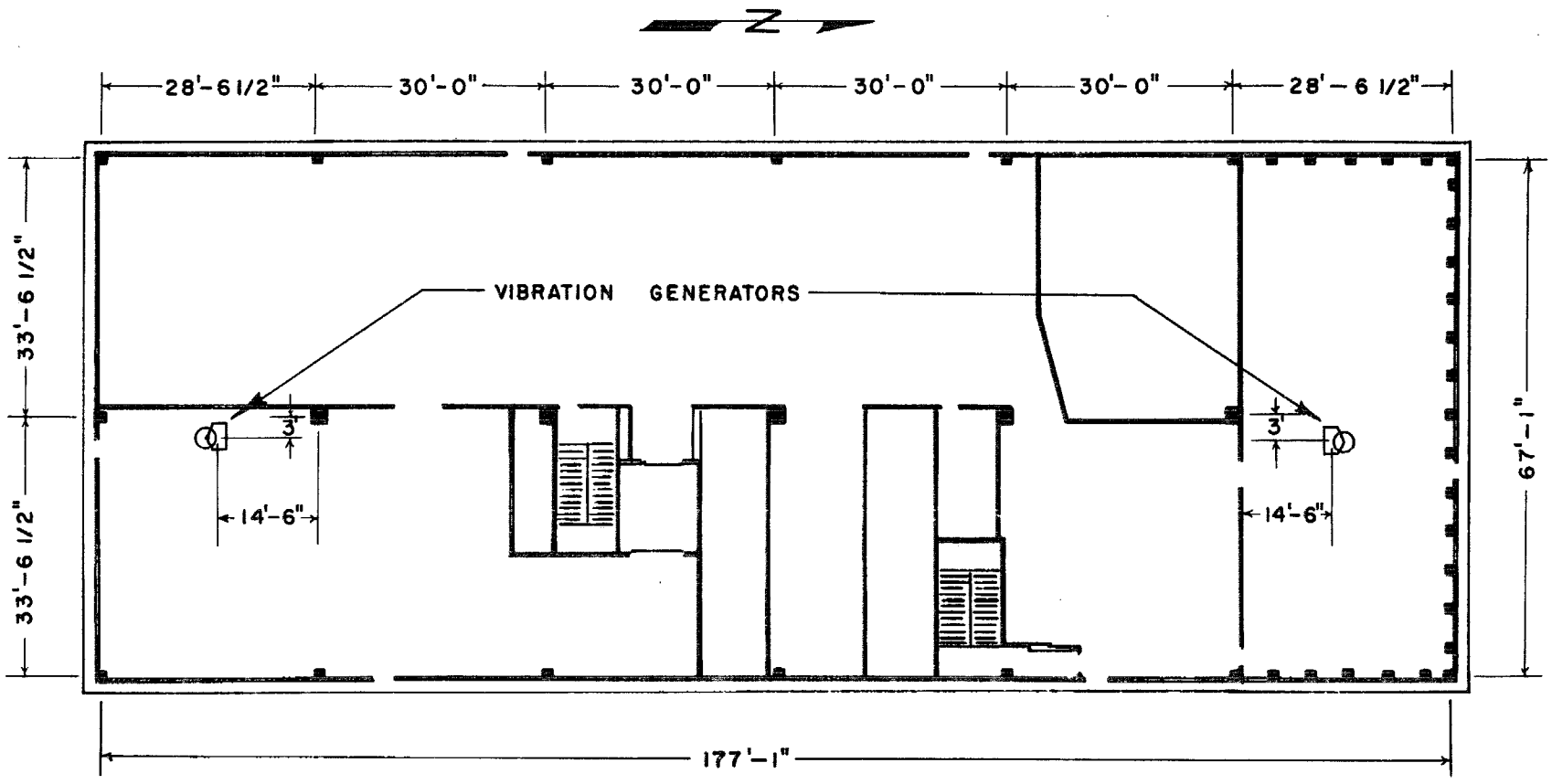

20th FLOOR PLAN

SAN DIEGO GAS & ELECTRIC BUILDING

FIGURE 5. PLAN OF 20th FLOOR, INCLUDING LOCATION OF VIBRATION GENERATORS

The force level is adjusted by changing the number of lead weights in the eccentric baskets and a high or low frequency range can be selected by the choice of the pulleys used on the shaft of the motor and on the drive shaft. The maximum force from each vibrator is limited to 5000 lbs. in order not to cause excessive stress in the machines.

The frequency of the vibrators is controlled by an amplidyne system which supplies power to the 1-1/2 horsepower, DC drive motors. In addition, feedback circuits are used to control the phase between units operated synchronously. The frequency control has an accuracy to within 0.003 cps for the range up to 3 cps and to within 0.01 cps in the range up to 10 cps. The phase control allows the vibrators to be operated with the force vectors in any desired phase relation. For example, either torsional or lateral motions can be excited. The error in phase between the two vibrators is indicated on an error meter on the control panel of the master unit. With this indicator, the error in phase can be kept to less than about four degrees.

The units are part of a four-unit, synchronized, vibration generation system originally developed at the California Institute of Technology under the sponsorship of the State of California, Office of Architecture, with advice from a special committee of the Earthquake Engineering Research Institute. The design and operation of the original system has been discussed by Hudson (1962). The ownership of the units subsequently has been transferred to the University of California.

The measuring system is essentially that used in previous tests and has been described in detail in other reports (Kuroiwa, 1967; Keightley, 1964). The vibratory response of the structure was measured using accelerometers and strip-chart recorders. The accelerometers utilize a four-arm, strain-gage bridge as the sensing element and are manufactured by the Statham

Instrument Company. They have natural frequencies varying from 12 to 21 cycles per second and ranges from ±0.20g to ±0.50g. The signals from the accelerometers were amplified by Miller C-3 carrier amplifiers and then recorded on a CEC recording oscillograph. The entire system was field calibrated using a tilt table giving a 0.05 g signal. Typically, the system was calibrated daily or at the beginning of a test. For some tests, additional dynamic calibrations were made at frequencies of interest by measuring motion at the same location with all the accelerometers. The dynamic calibrations were particularly useful for determining mode shapes, which only require relative values of response at different points, but at the same frequency.

To measure the phase between the force and the response, an additional stationary synchro was added to the circuit which maintains the relative phase between the two vibrators. Because this additional synchro is stationary, its signal is a measure of the absolute position of the eccentric weights of the master vibrator. The orientation of the stationary synchro may be adjusted to correlate the position signal with the direction of the force vector. The position signal was recorded on one channel of the oscillograph for comparison with the accelerometer records. By this technique the phase between the excitation and response can be determined to about 10° under favorable circumstances.

The details of the actual testing program are included in the tables and figures of Appendix I. In summary, the tests began with a series of frequency sweeps in the N-S and E-W directions and in torsion, with measurements taken only on the 20th floor. From these tests, a preliminary determination of the frequencies of the building was made in order to identify frequency bands over

which more detailed measurements were required. With an approximate knowledge of the resonant frequencies, finely-stepped frequency sweeps were made to make a closer determination of the natural frequencies of vibrations. These tests determined the damping in the various modes and the frequencies at which measurements at each floor level of the building were made. Measurements of the variation of response with height were taken by moving from one to four accelerometers from floor to floor; these records were used to determine mode shapes and centers of rotation.

TEST RESULTS

Preliminary Results

The data recorded during the vibration test consisted of steady-state response to sinusoidal excitation at selected points in the structure, plus a sinusoidal signal indicating the position of the exciting forces. Although the basic data could be presented in a variety of ways, the most common presentation is simply a plot of the steady-state amplitude of response versus the frequency of excitation. If the natural frequencies of the structure are well separated, and if the damping is small, this technique usually will serve to determine the lower natural frequencies and associated damping values. Such presentations are given in Figures 6, 7 and 8 for N-S, E-W and torsional excitation, respectively. In each case the accelerometers were located on the 20th floor, oriented to record the response in the sense of the excitation. The exact location can be found by reference to Appendix I. The discontinuities in the curves arise from the fact that different eccentric weights and different speed ranges are required to excite the structure with measurable amplitudes over the frequency range of interest.

Some structural properties can be found from analysis of Figures 6 - 8 and similar curves, but the interpretation is difficult because of two factors. First, the identification of the fundamental modes in the N-S, E-W and torsional senses is made awkward by the fact that all three of the fundamental modes have very nearly the same frequency and, as closer study will show, the fundamental mode shapes are combinations of translational and rotational deformations. This feature of the building's dynamic characteristics is examined in detail in a subsequent section of this chapter. Second, the resonant frequencies and damping values cannot be determined accurately from

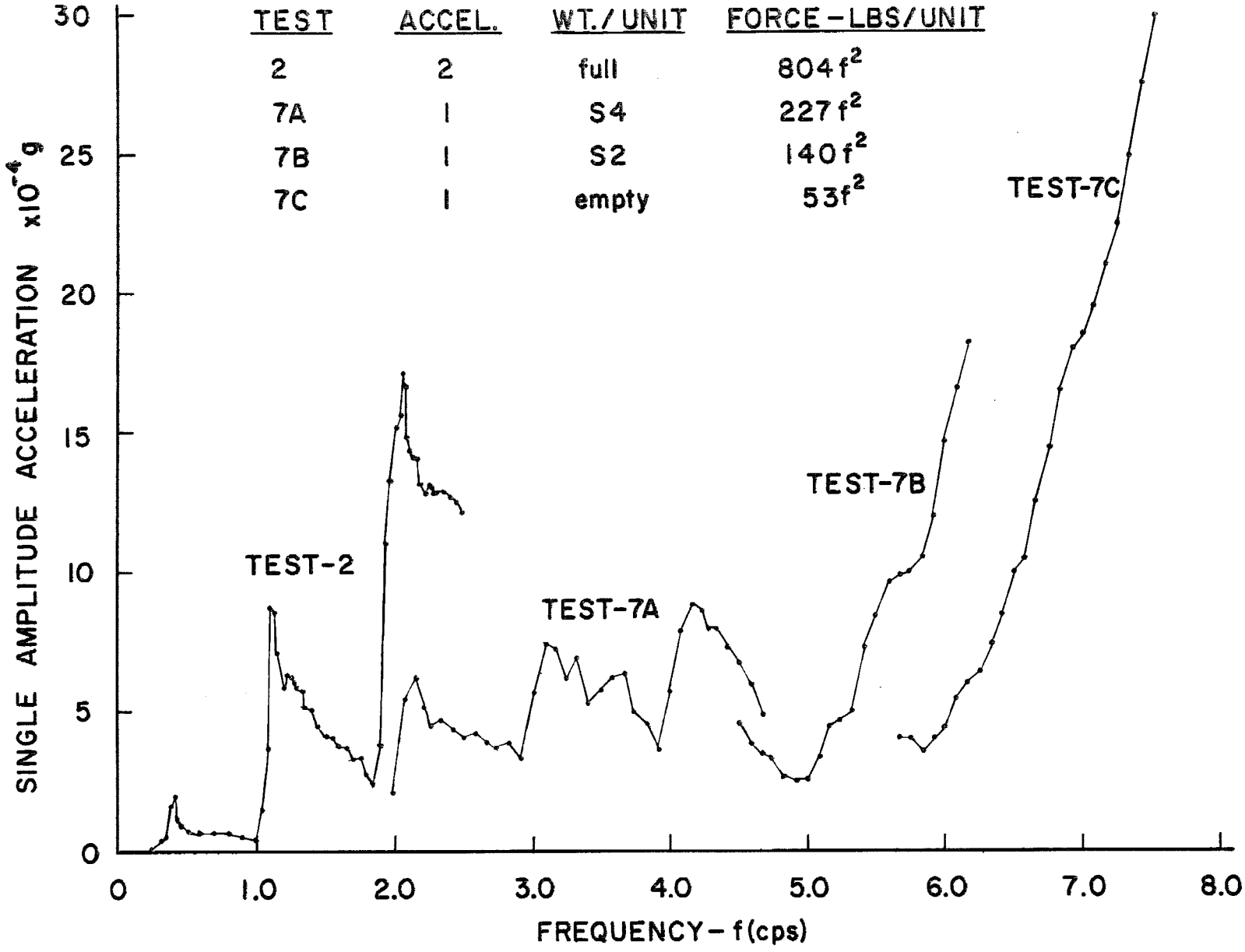

NORTH-SOUTH FREQUENCY SWEEP

FIGURE 6. N-S RESPONSE OF 20th FLOOR TO N-S EXCITATION

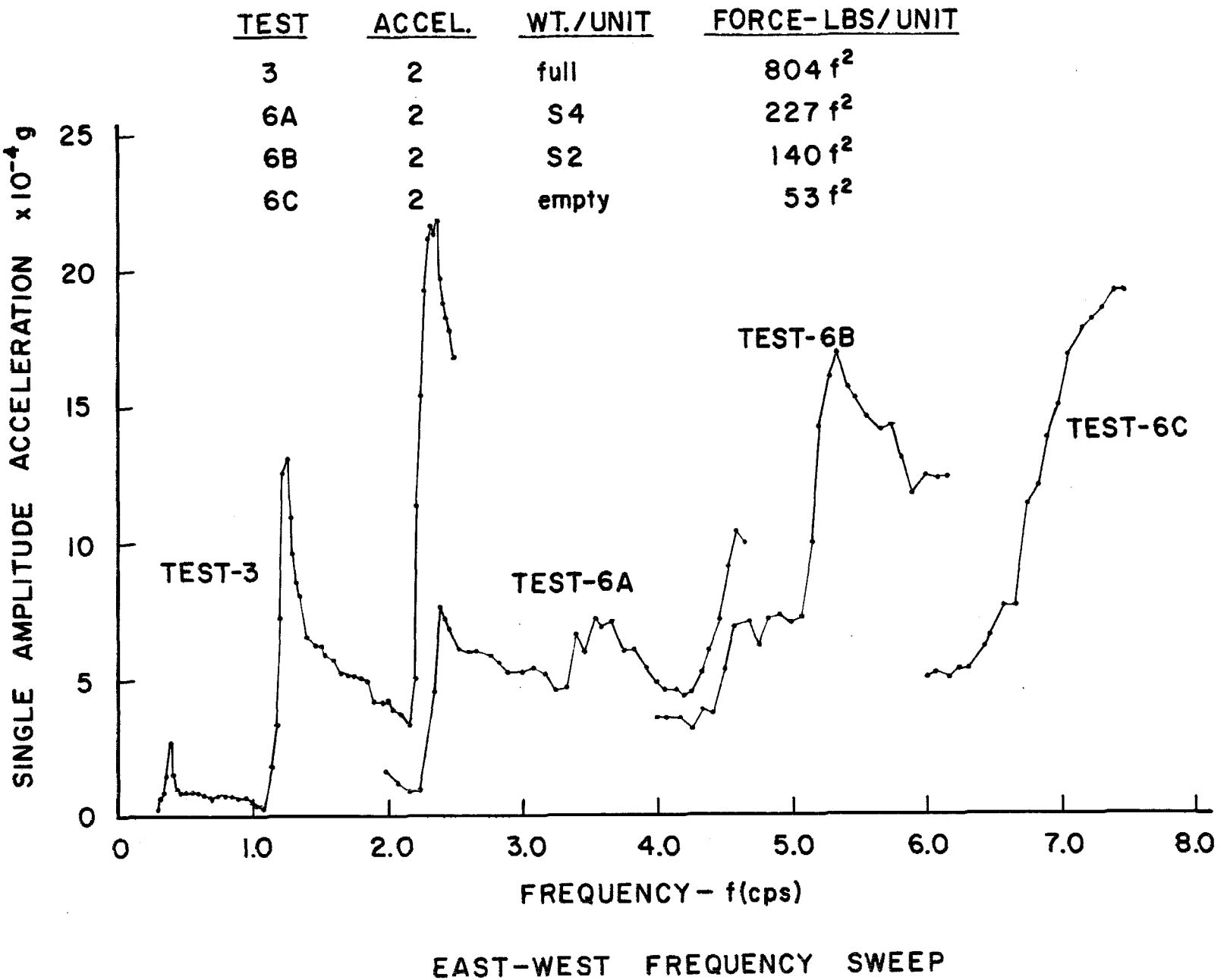

FIGURE 7. E-W RESPONSE OF 20th FLOOR TO E-W EXCITATION

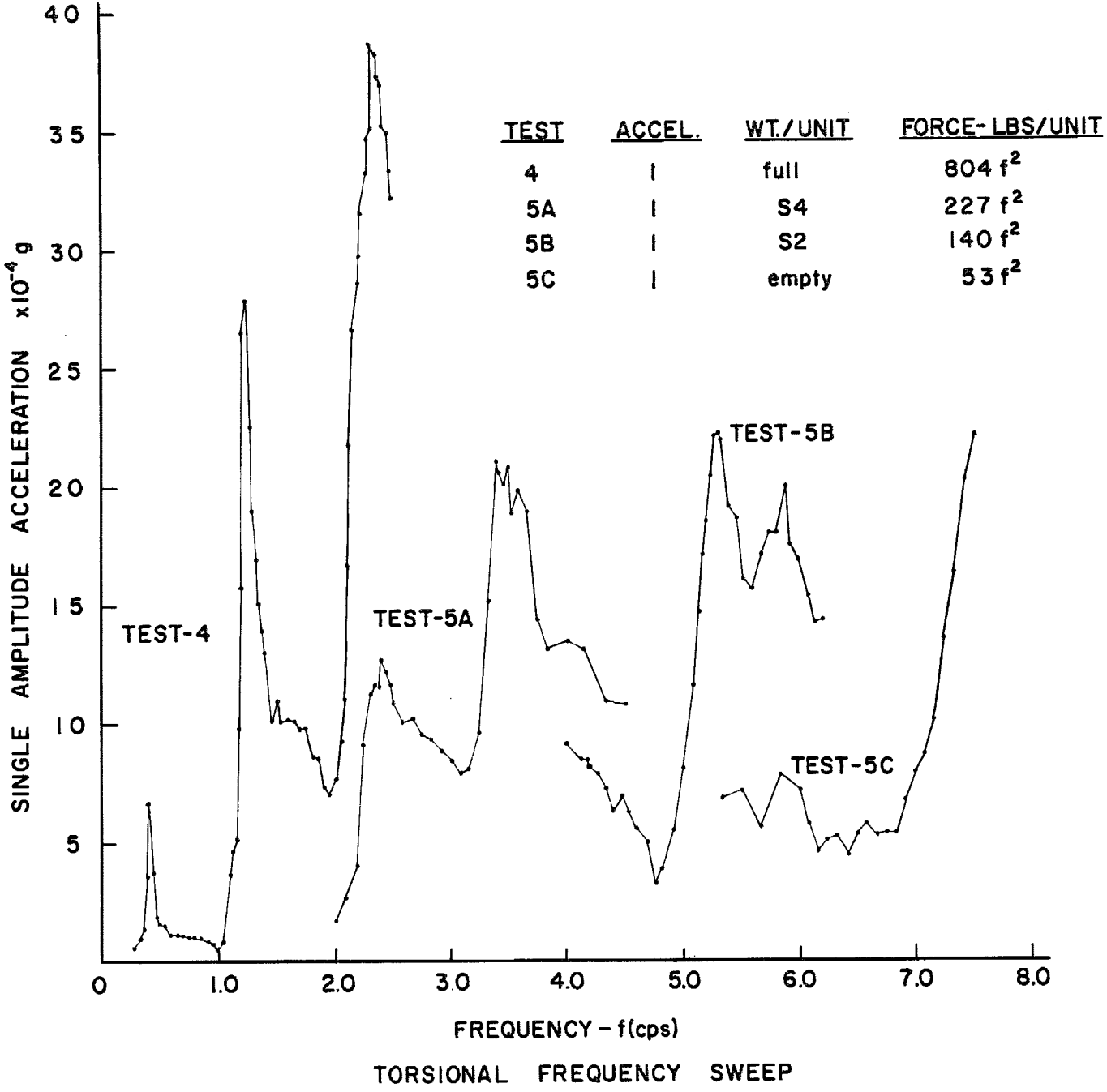

TORSIONAL FREQUENCY SWEEP

FIGURE 8. TORSIONAL RESPONSE OF 20th FLOOR TO TORSIONAL EXCITATION

Figures 6-8 for the higher modes because of the interfering response of other modes of the structure (Hoerner and Jennings, 1969). This difficulty can largely be overcome, however, by making use of the measured phase between the excitation and response.

Damping from Response Curves

Because of the presence in the response of other nearby modes, it is obvious from Figures 6 - 8 that the half-power method and other common approaches are not directly applicable for determining damping values from much of the data. In this test, however, the recorded phase of the force with respect to the response allows the response to be separated into its in-phase and 90° out-of-phase components. If the 90° out-of-phase component of the acceleration is plotted versus frequency, the resonances of the system become much more sharply defined and frequencies, dampings and mode shapes are more readily determined. This is illustrated by Figure 9 which gives the total response, the 90° out-of-phase response and the in-phase response for the second N-S mode. Figure 9 shows that the resonant frequency of the mode is found more precisely from the in- and out-of-phase components than from the total response,and the damping also is more accurately determined . The application of the half-power method to the total response gives a modal damping of 3. 7 percent whereas the damping from the out-of-phase component is found from a similar method outlined in the following pages to be 2. 7 percent. The overestimation of damping from the total response is an unfortunate consequence of modal interference. Another advantage of the use of in- and out-of-phase components is given in Figure 10 which shows that resonating modes can be identified when the total response is unclear. The use of the phase information in this manner appears new to resonant testing of building

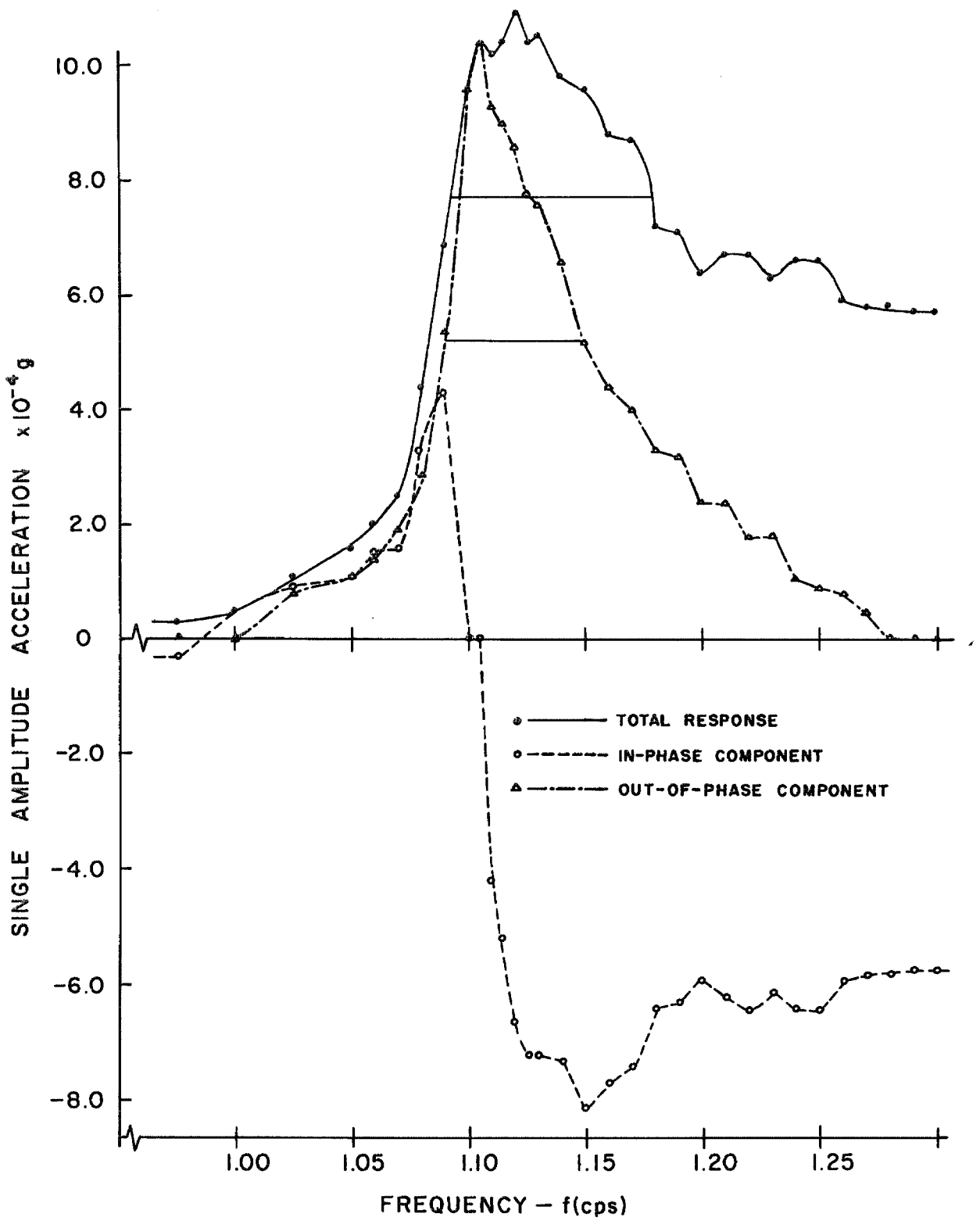

SECOND N-S MODE RESPONSE AT THE 20th FLOOR
(ACCELEROMETER NO. 1, TEST 8a)

FIGURE 9. TOTAL RESPONSE, IN-PHASE COMPONENT, AND 90° OUT-OF-PHASE COMPONENT OF RESPONSE FOR SECOND N-S MODE

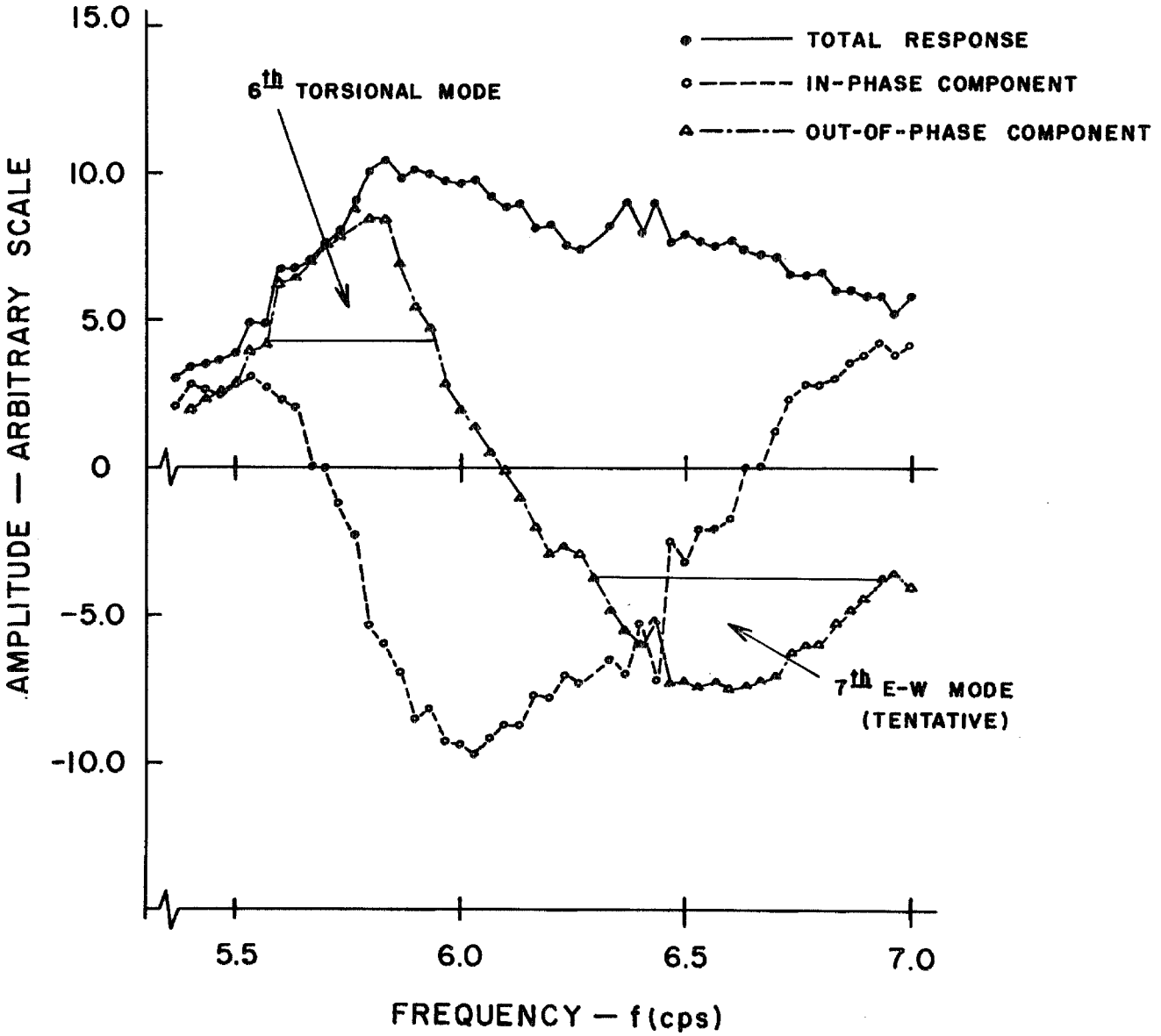

RESPONSE TO TORSIONAL EXCITATION AT THE 14th FLOOR
(ACCELEROMETER NO. 3, TEST 21a)

FIGURE 10. EXAMPLE OF THE USE OF PHASE COMPONENTS IN IDENTIFYING RESONANCE

structures, although related techniques are more common in mechanical and electrical engineering practice.

The essential feature of the technique is to take advantage of the fact that at resonance of a particular mode, the interfering response of lower modes is almost entirely in-phase with the excitation, and that of higher modes is almost all 180° out of phase. By concentrating on the 90° out-of-phase components of response, interference is greatly reduced, although light damping and some degree of frequency separation are still required for successful determination of frequencies and damping values.

To introduce the method, consider an n degree-of-freedom structure vibrating in a single plane. The method is applicable to more general response, but this system suffices for purposes of presentation.

For eccentric mass excitation, $mr\omega^2 \sin \omega t$, applied at the ℓth level, the steady-state acceleration of the ith level is given by Hoerner and Jennings, (1969).

$$\ddot{x}_i = -\sum_{j=1}^{n} \frac{\phi_{ij}\,\phi_{\ell j}\, mr\omega^2 \dfrac{\omega^2}{\omega_j^2}}{\left(1-\dfrac{\omega^2}{\omega_j^2}\right)^2 + \left(2\zeta_j \dfrac{\omega}{\omega_j}\right)^2} \left[\left(1-\frac{\omega^2}{\omega_j^2}\right)\sin\omega t - \left(2\zeta_j \frac{\omega}{\omega_j}\right)\cos\omega t\right] \qquad (1)$$

in which $\ddot{x}_i$ is the acceleration at the ith level, ϕ_{ij} is the component of the jth mode at the ith level, and ω_j and ζ_j are the frequency and damping, respectively, of the jth mode of vibration. In Equation 1, it is to be understood that the frequencies increase with increasing index j.

If the damping is small and some degree of modal separation exists, the acceleration $\ddot{x}_i$ for ω near the kth resonance frequency can be separated into three parts: the in- and 90° out-of-phase components of the response of the kth mode, and the response of all other modes. The latter portion is effectively in phase because the difference between in-phase response and

180° out-of-phase response is only an algebraic sign. This division into three parts is facilitated by the introduction of a parameter α defined by

$$\omega = \omega_k(1 + \alpha\zeta_k) \tag{2}$$

in which

$$|\alpha\zeta_k| << 1 \tag{3}$$

Within the range defined by Equation 3, Equation 1 becomes

$$\ddot{x}_i = -\sum_{\substack{j=1 \\ j\neq k}}^{n} \frac{\phi_{ij}\phi_{\ell j} mr\omega^2 \frac{\omega^2}{\omega_j^2}\left(1 - \frac{\omega^2}{\omega_j^2}\right)\sin\omega t}{\left(1 - \frac{\omega^2}{\omega_j^2}\right)^2 + \left(2\zeta_j \frac{\omega}{\omega_j}\right)^2} + \frac{\phi_{ik}\phi_{\ell k} mr\omega_k^2}{2\zeta_k(1 + \alpha^2)}(\alpha\sin\omega t + \cos\omega t) \tag{4}$$

Equation 4 shows the 90° out-of-phase component of the response to be

$$\ddot{x}_i^* = \frac{\phi_{ik}\phi_{\ell k} mr\omega_k^2}{2\zeta_k(1 + \alpha^2)} \tag{5}$$

From Equations 2 and 5 it is seen that $\ddot{x}_i^*$, the 90° out-of-phase component of the response near $\omega = \omega_k$, peaks at ω_k, the resonance frequency, where it takes the value

$$|\ddot{x}_i^*|_{max} = \frac{\phi_{ik}\phi_{\ell k} mr\omega_k^2}{2\zeta_k} \tag{6}$$

If the governing equations are examined in more detail, it can be shown that the resonance peak of the 90° out-of-phase component of response is significantly narrower than the peak of total response. This is a reflection of the fact that near resonance of a mode, the major portion of the response

is the 90° out-of-phase component, whereas off resonance the larger fraction of the response of the mode is either the in-phase or 180° out-of-phase component.

Equation 6 shows that the 90° out-of-phase response can be used to determine the mode shape from records obtained at different levels under the same excitation inasmuch as the response at each level is proportional to the mode shape, ϕ_{ik}, at that level.

The damping is found from a plot of the 90° out-of-phase response by noting that at $\alpha = \pm 1$, $\omega = \omega_k(1 \pm \zeta_k)$ and the response is

$$\ddot{x}_i^* \Big|_{\alpha = \pm 1} = \frac{\phi_{ik}\phi_{\ell k} m r \omega_k^{\,2}}{4\zeta_k} \tag{7}$$

which is seen to be one-half the peak response. The determination of damping then proceeds exactly like the familiar half-power method, with the exception that one-half the peak amplitude is used, rather than the usual $\sqrt{2}/2$. The procedure for determining the damping is illustrated in Figure 11.

The above analysis requires that the 90° out-of-phase components of the response be separated from the total response. One technique by which this can be done is illustrated in Figure 12 which is traced from test data. In this case the double amplitude is determined.

Fundamental Translational and Torsional Modes

Preliminary results such as those shown in Figures 6, 7 and 8 serve to identify the first few frequencies of the structure and the frequency ranges which require further examination. In Test 11 a detailed study was made of the response at the 20th floor under E-W excitation in the frequency range near 0.4 sec. which Figure 7 suggests is the E-W fundamental frequency. The positions of the accelerometers and their positive directions are shown in the

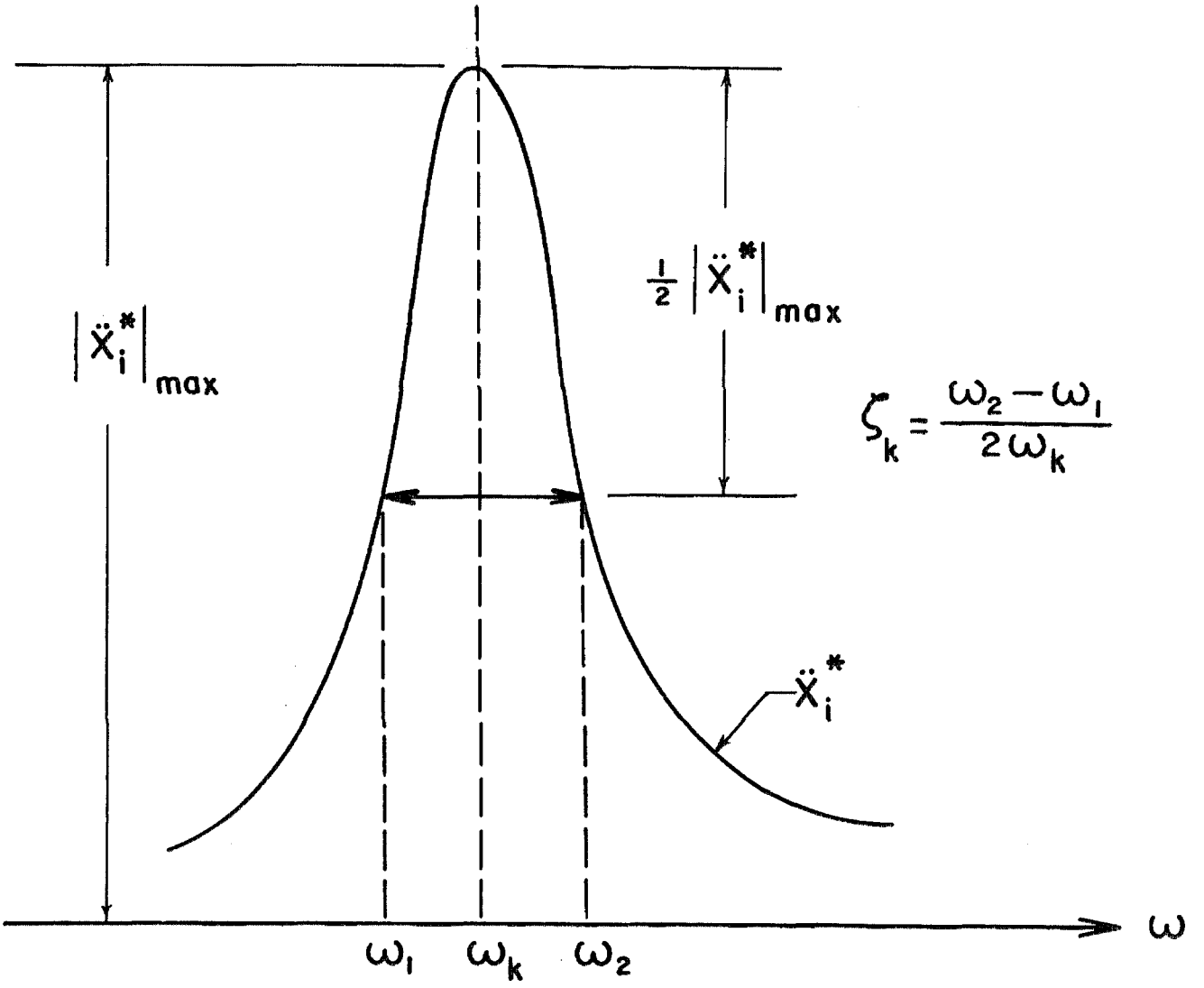

DETERMINATION OF DAMPING FROM OUT-OF-PHASE COMPONENT OF ACCELERATION

FIGURE 11. HALF-POWER METHOD APPLIED TO RESPONSE CURVES OF 90° OUT-OF-PHASE COMPONENT

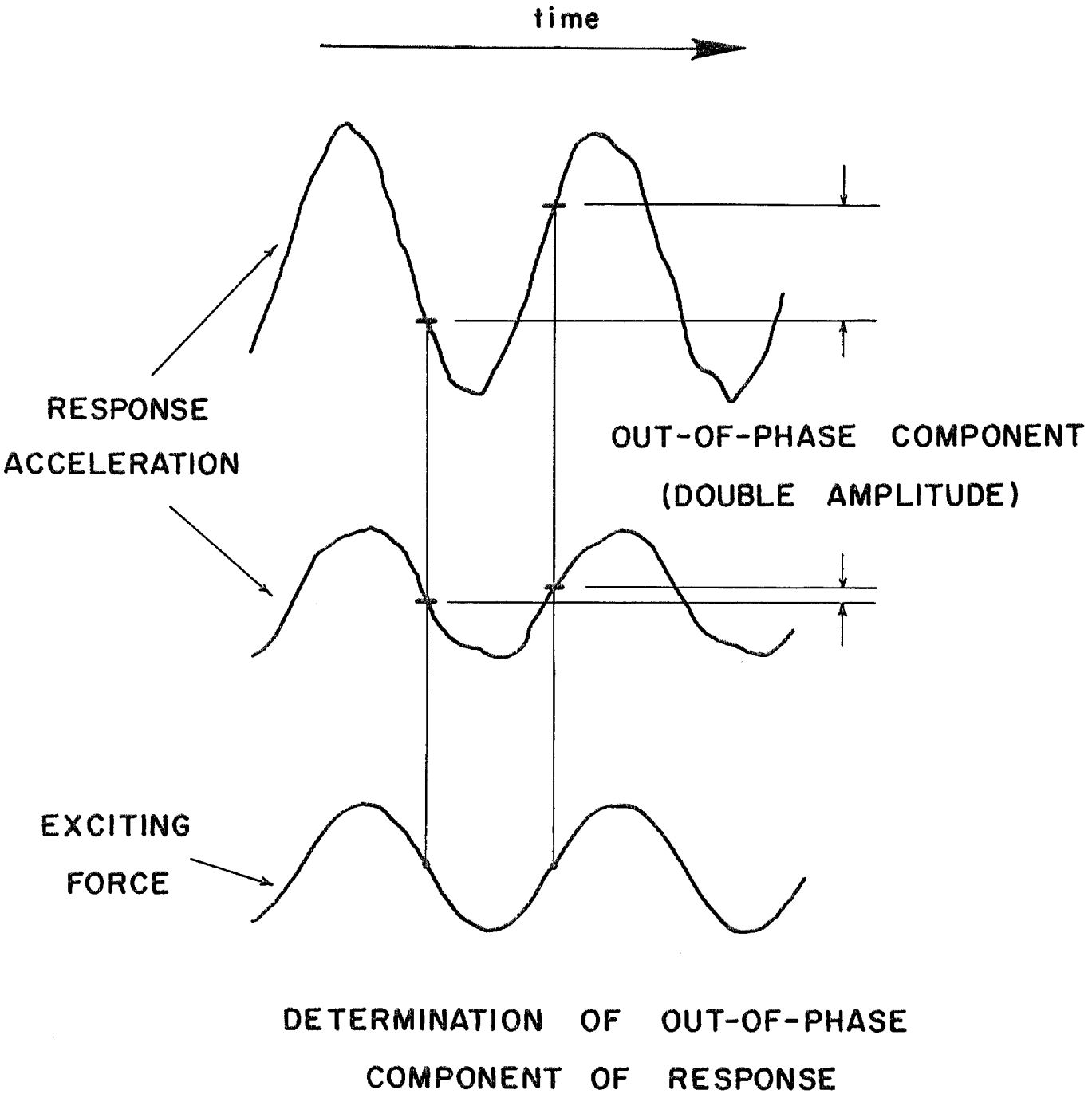

FIGURE 12. GRAPHICAL METHOD OF FINDING 90° OUT-OF-PHASE COMPONENT OF RESPONSE

upper portion of Figure 13. Also given in this figure are the total and 90° out-of-phase responses, the latter determined by the procedure discussed in the previous section. The frequencies f_1 and f_2 are values found subsequently to be the two primarily translational fundamental frequencies of the structure, and f_3 is the frequency of the fundamental mode that is primarily torsional. Note the usefulness of the 90° out-of-phase components of response in identifying the existence of three resonating modes in this relatively narrow frequency range.

The response to E-W excitation of these three fundamental modes at about the same level (Figure 13) indicates a complex modal geometry that is not expected if the structure is truly symmetrical. It is thought that the natural tendency of asymmetries and eccentricities to couple translational and rotational motions has been amplified strongly by the effects of the small differences among the three fundamental frequencies of the structure. These all lie between 0.380 and 0.425 cps.

If the three fundamental frequencies, f_1, f_2 and f_3 were to coalesce, structural dynamic theory states that the mode shapes corresponding to the single frequency would have rotational and translational components, in both directions, that are arbitrary within certain limitations. Experimentally, a structure with such repeated natural frequencies would appear to exhibit a variety of mode shapes at the same frequency. In the San Diego Gas and Electric Company building the three fundamental frequencies do not coincide, but are close enough that a much larger coupling of N-S, E-W and rotational displacements occurs in the mode shapes than would be the case if the frequencies were well separated. As a result of this coupling, E-W excitation caused all three of the fundamental modes of the building to respond significantly.

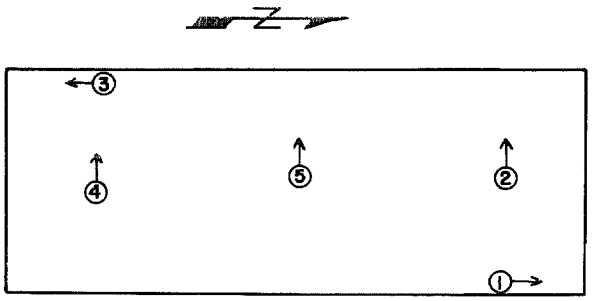

ACCELEROMETER LOCATIONS

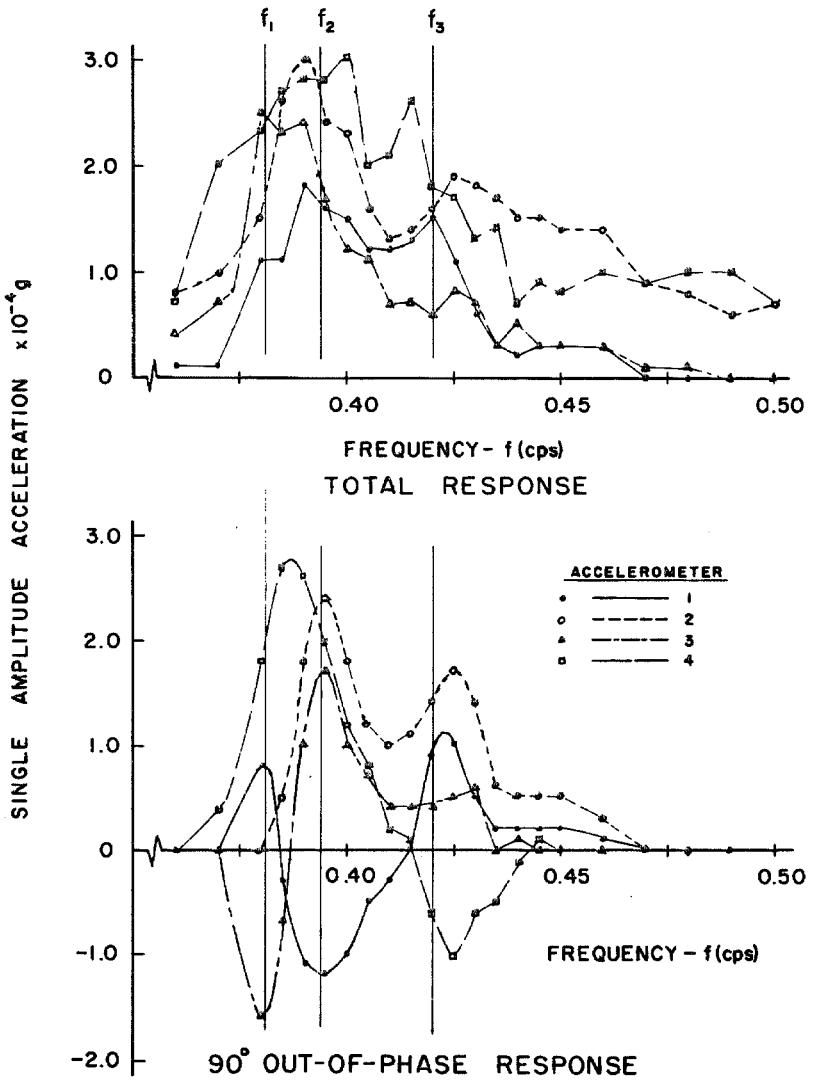

RESPONSE OF 20th FLOOR TO E-W EXCITATION (TEST II)

FIGURE 13.

It was observed in other tests that N-S and torsional excitation also caused the three fundamental modes to respond.

The basic features of the problem can be clarified by reference to Figure 14 which shows an idealized structure which possesses two translational modes which oscillate at directions skew from the N-S and E-W directions of the structural lines. For simplicity, rotational coupling has been omitted. If the simple structure in Figure 14 were excited in the 1-1 direction, only the first mode would respond in the frequency range f_1 - f_2. Consequently, only one resonance peak would appear on records from accelerometers oriented in the 1-1 direction and accelerometers oriented in the 2-2 direction would not show resonance. In a similar manner, excitation in the 2-2 direction would induce resonance only in the 2-2 direction and this response would be apparent in records obtained from accelerometers oriented in the 1-1 and 2-2 directions.

On the other hand, if E-W or N-S excitation were applied to the structure in Figure 14, both modes would respond and accelerometers oriented N-S and E-W would record resonances at f_1 and f_2 since both of these modes have N-S and E-W components. The recorded N-S and E-W motions would vary as a function of frequency depending on the degree of resonance of each mode.

The addition of rotational components to the mode shapes does not change the basic phenomenon, but further complicates the response because the rotational components of a mode can significantly reinforce or diminish, at a different resonant frequency, the translational components of the response of other modes. Thus, it becomes possible for accelerometers at different points on the same level to show only one resonant mode, two resonant modes

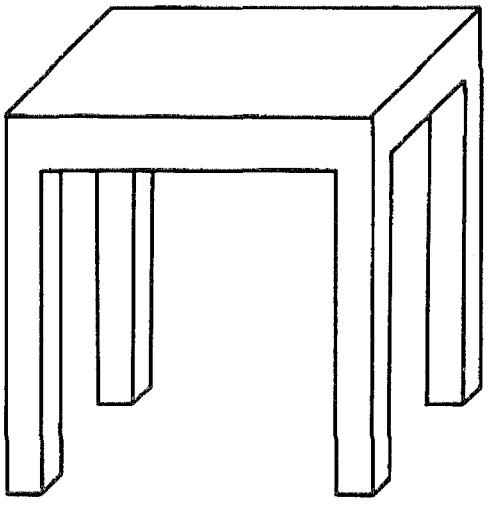

IDEALIZED STRUCTURE

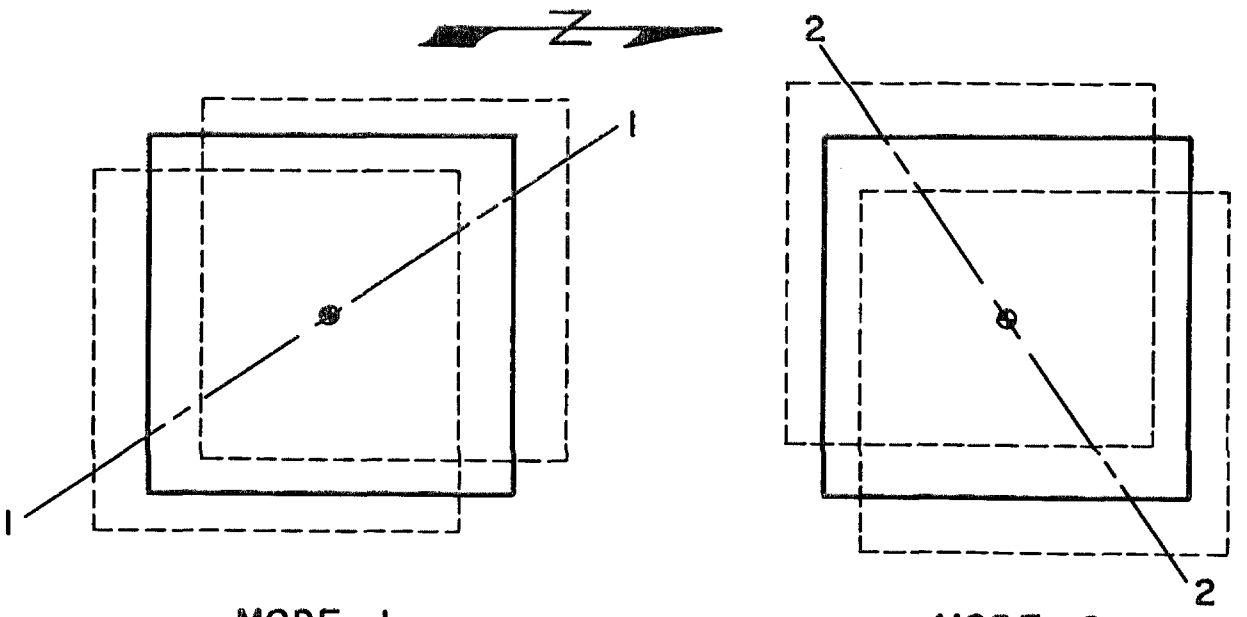

MODE 1
ω_1

MODE 2
ω_2

FIGURE 14. SIMPLE STRUCTURE SHOWING COUPLING OF MODAL DISPLACEMENTS

in phase, or two resonant modes with opposite phasing. Figure 13 shows many of these effects.

1. Determination of fundamental modes

To improve the determination of the dynamic properties from the test results, the motions recorded in Test 11 by accelerometers 1 through 4 were used to construct the N-S and E-W motions of the centroid of the 20th floor, and the rotation of the floor. This construction required the assumption that the floor moved very nearly as a rigid body and the expectation that the 20th floor response was to some degree representative of the response of the entire structure for the three fundamental modes. The N-S($\ddot{x}$), E-W($\ddot{y}$) and rotational ($\bar{r}\ddot{\theta}$) components of the motion at the centroid are given by the data points and narrow lines in Figure 15. In this figure, $\bar{r}$, the radius of gyration, is 55.7 ft (calculated on the basis of the nominal 70-ft x 180 ft plan).

The heavy lines in Figure 15 represent a decomposition of the 90° out-of-phase response into components associated with each mode. For example, the $\ddot{x}$ motion at the centroid in the f_1-f_2 frequency range is the sum of two opposite motions, one associated with f_1 and the other with f_2. The shape of each component of response is fixed by Equation 5. The $\ddot{y}$ and $\bar{r}\ddot{\theta}$ motions have been decomposed in a similar manner. The third fundamental frequency is somewhat removed from the other two, and the modal interference is much less. Consequently, in Figure 15 the heavy lines lie over the lighter lines in most of this frequency range. When the resolution is completed, the $\ddot{x}$, $\ddot{y}$ and $\bar{r}\ddot{\theta}$ components at each frequency determine the translational and rotational components of each mode at the 20th floor. The damping given in Figure 15 has been determined for each mode from the largest components

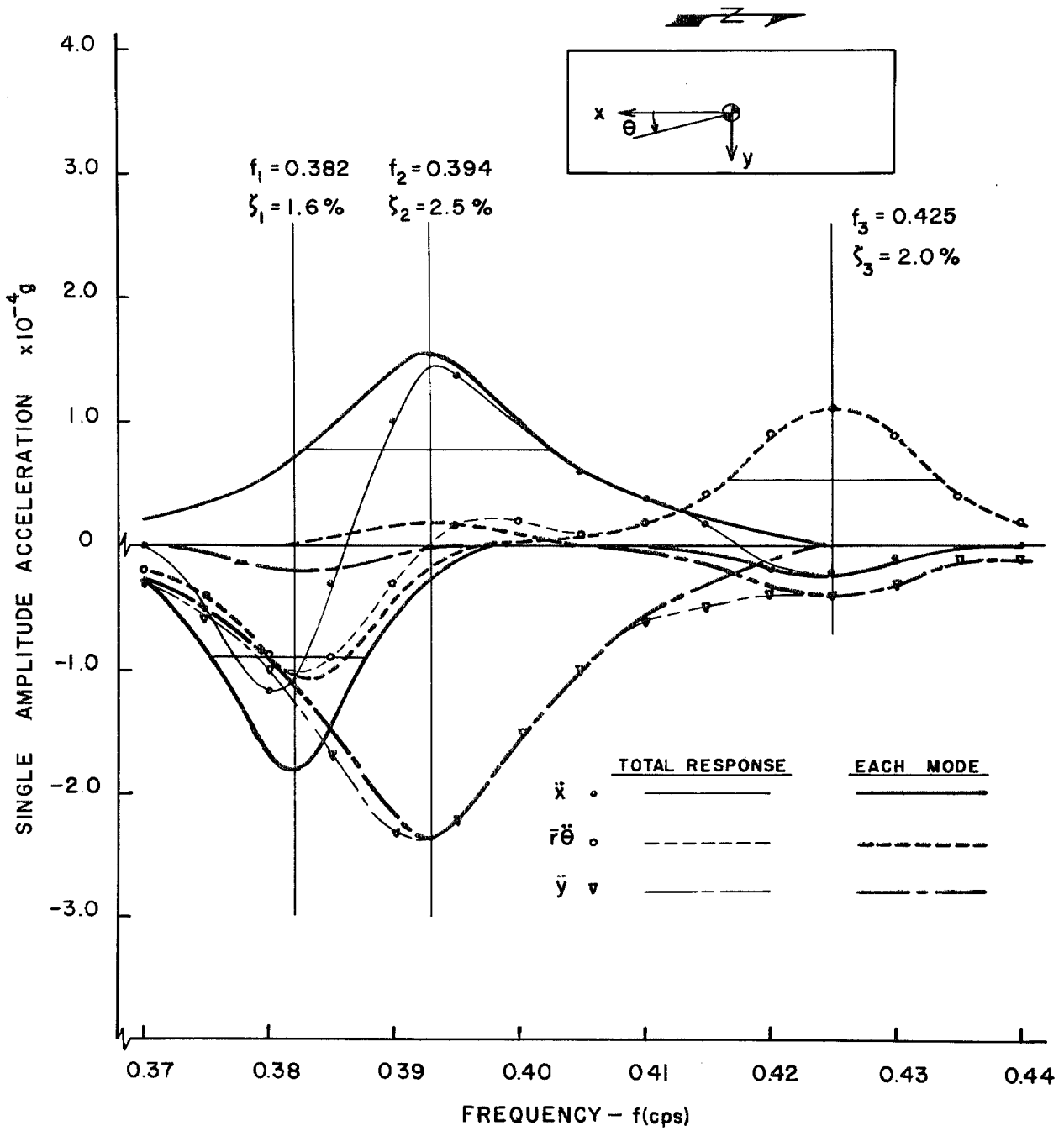

90° OUT-OF-PHASE RESPONSE OF FUNDAMENTAL MODES

AT CENTROID OF 20th FLOOR

E-W EXCITATION

FIGURE 15.

of the 90° out-of-phase response.

The mode shapes, damping and frequencies found above from E-W excitation are consistent with the measured response of the structure to N-S excitation. This response, which also includes all three modes, was measured at both the 20th and 12th floors by enough accelerometers to define the $\ddot{x}$ and $\bar{r}\ddot{\theta}$ motions at the centroid. E-W motion ($\ddot{y}$) was not measured. The results, decomposed in the same manner as in Figure 15, are given in Figure 16, which indicates that the relative values of the translational and rotational components of the modes are somewhat different for the 20th floor and the 12th floor. The different phasing of the modal response at f_2 in Figures 15 and 16 is a consequence of the different directions of excitation. Comparison of Figures 15 and 16 also shows that the relative values of the modal components at the 20th floor of the third fundamental (torsion) are slightly different, depending on whether they are determined from the E-W or N-S tests. In addition, Figures 15 and 16 show that modal interference is most significant in the response of the first two fundamental frequencies.

Damping values found from Figure 16 from the response of the 20th and 12th floors are 2.6 and 2.0 percent at f_1, 2.9 and 2.7 percent at f_2, and 2.2 and 1.9 percent at f_3. These values are judged to be consistent within the experimental error with the values given in Figure 15.

The results and analysis in Figures 15 and 16 are consistent in their major features although small inconsistencies do appear. Some inconsistencies are not surprising in view of the approximate determination of the modes, the rigid floor assumption, and the relatively low signal-to-noise ratio in the recorded response. In this regard it is found from Appendix I that the amplitude of the harmonic exciting force in Test 11 is only 129 lbs

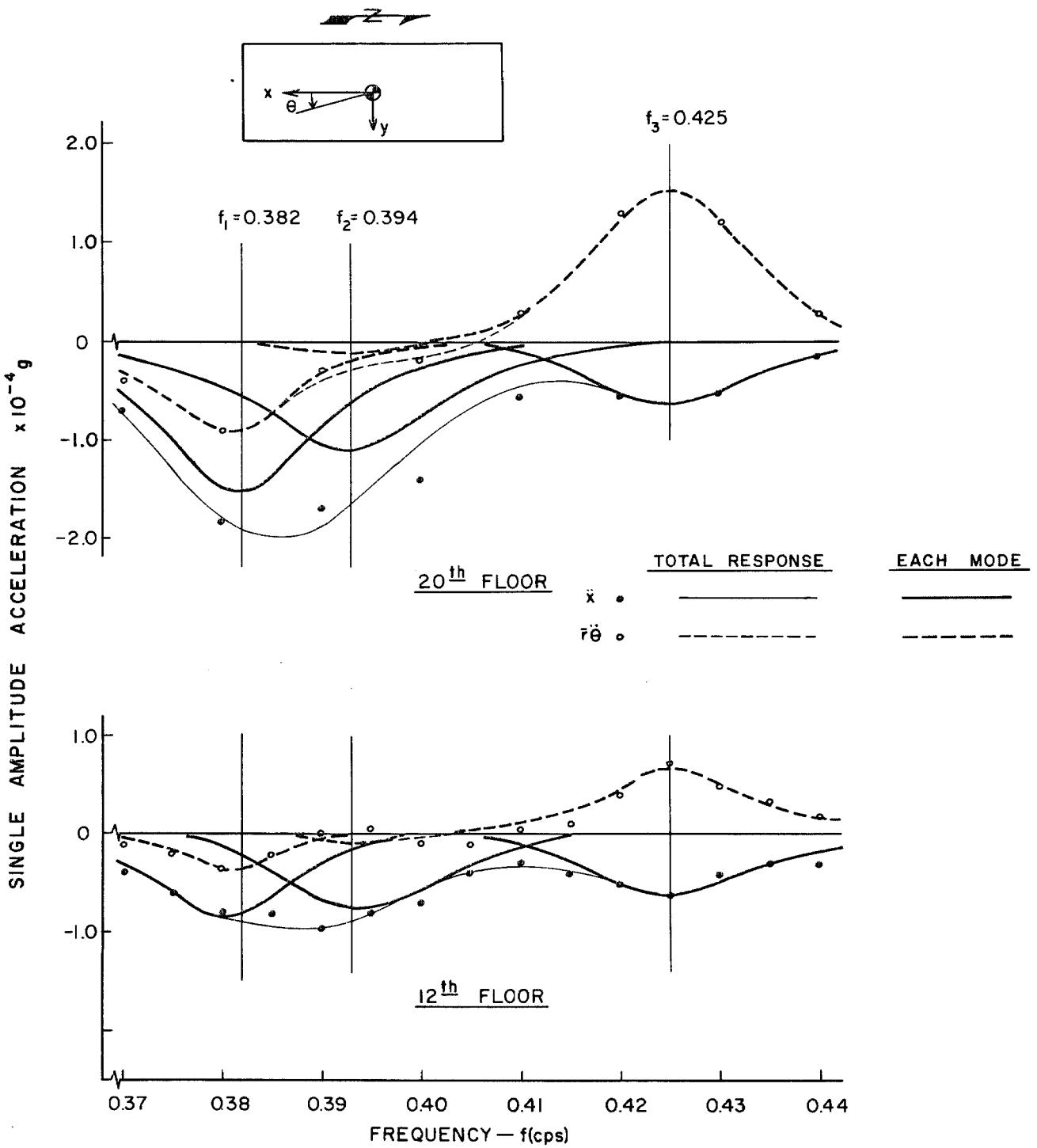

90° OUT-OF-PHASE COMPONENT OF RESPONSE OF FUNDAMENTAL MODES

N-S EXCITATION

FIGURE 16.

per machine at 0.40 cps.

The motion of the 20th floor in the three fundamental modes, as determined by the results shown in Figure 15, is given in Figure 17. When vibrating in a particular mode, the structure moves from one dashed outline to the other, passing through the equilibrium position indicated by the solid outline. The mode shapes are illustrated in a different manner in Figure 18 which shows the modes plotted as unit vectors with components in three mutually perpendicular directions. If the mode shapes were for a simple structure such as shown in Figure 14 so that the masses associated with each component of the motion were equal, the three modal vectors would have to be mutually orthogonal. The set of such orthogonal modes closest to those found for the motion of the 20th floor is shown also in Figure 18. The departure from orthogonality of the motion of the 20th floor in the three modes is attributed to uncertainties in the analysis and to the fact that the motion at a particular floor is not exactly representative of the motion of the entire building; the three fundamental modes are expected to be orthogonal over the entire structure, but the motions of each individual level need not be orthogonal.

Figure 18 indicates that a relatively large increase of small modal components can occur without much decrease in the major component of a mode. This implies, for example, that significant rotational components could occur in a mode without decreasing substantially the translational components. Geometrically, this is visualized in Figure 18 as a rotation of the modal triad about the origin, caused by a change in the properties of the structure from which the modes are derived.

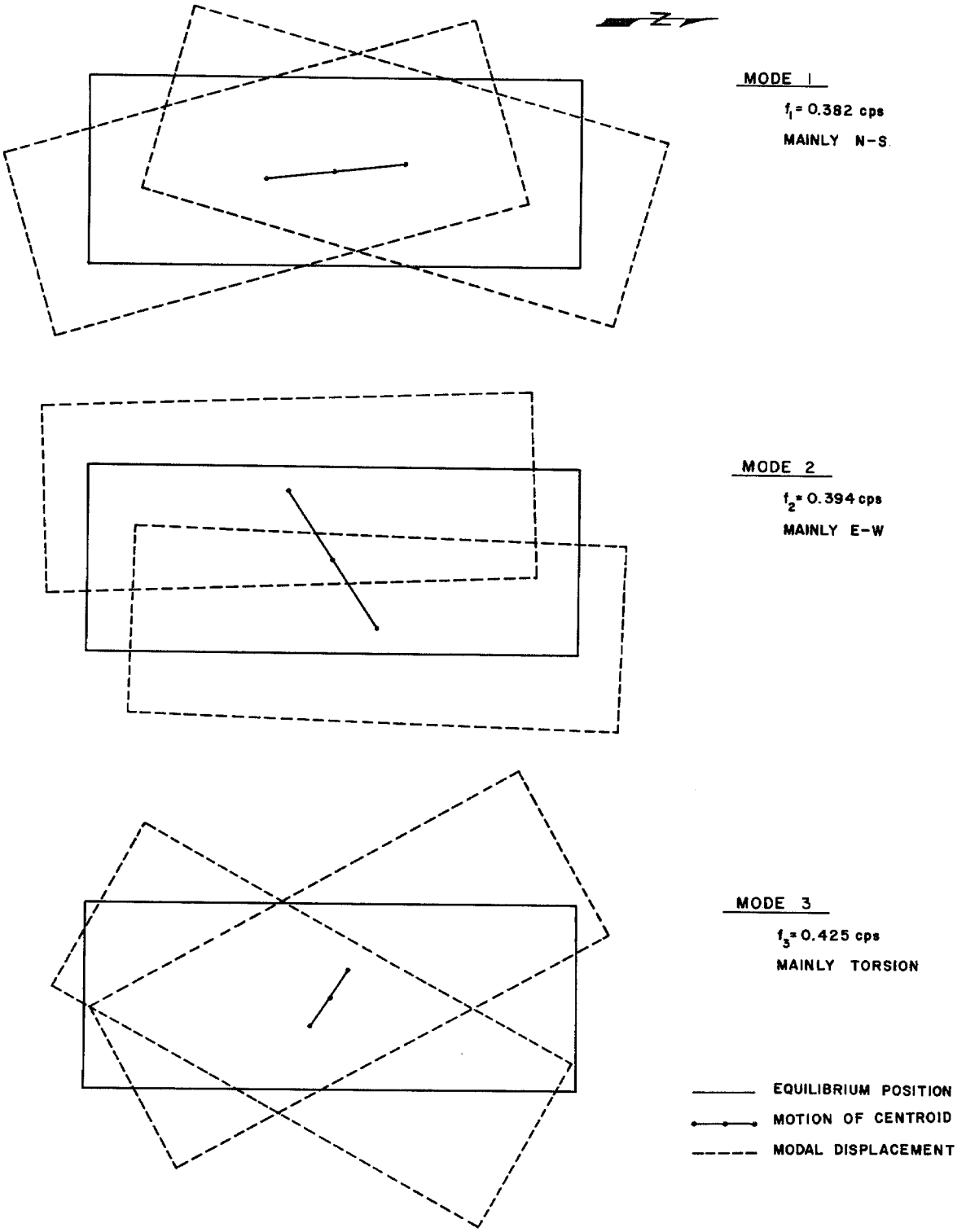

FIGURE 17. PLAN VIEW OF FUNDAMENTAL MODES AT 20th FLOOR

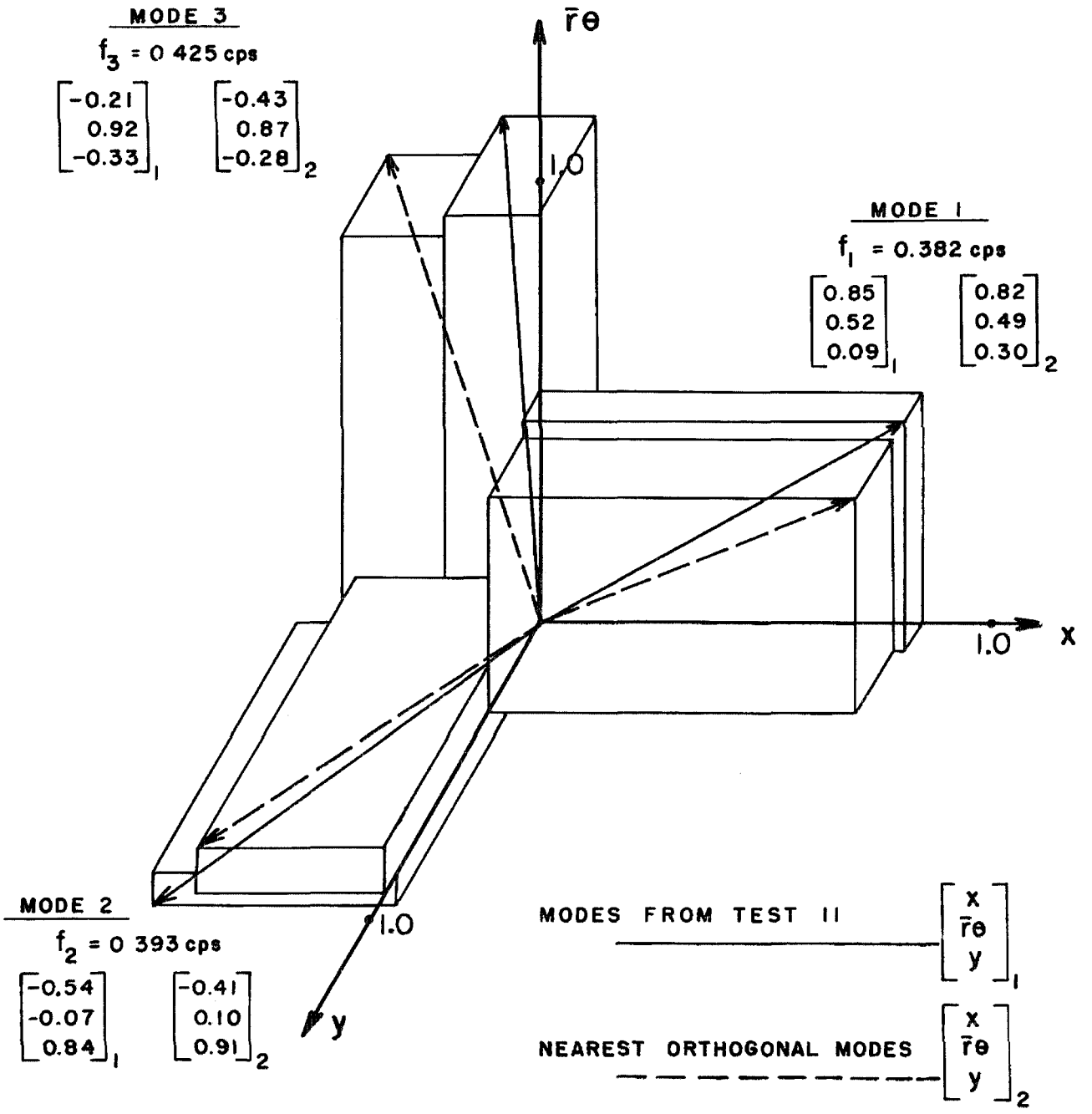

NORMALIZED FUNDAMENTAL MODES – 20th FLOOR

FIGURE 18. THREE-DIMENSIONAL REPRESENTATION OF COMPONENTS OF FUNDAMENTAL MODES

2. Computer-aided resolution of the fundamental modes

An independent attempt was made to obtain a mathematical model of the building using a computer program being developed at UCLA for this purpose (Ibañez et al., 1970). The supposition is made that the first three modes can be represented by a three-degree-of-freedom structure like Figure 14 in accordance with the usual assumptions for the dynamic response of linear, viscously damped, multi-degree-of-freedom systems. First an estimate of the natural frequencies, modal dampings, effective modal masses and mode shapes is made. Then the computer is used in an iterative process to improve the estimate of the mode shapes and modal masses by comparing the response of the initial, estimated model with the experimental data. The response of the improved model to the forces used in the tests is obtained by the computer and these response curves are visually compared to the experimental results. From this visual comparison, an improved estimate of the natural frequencies and modal dampings may be made. The computer program is used again to improve the estimate of the mode shapes and modal masses, and the computed response curves are again compared to the experimental results. The process is continued until the comparison with the experimental data is acceptable.

The existing computer program utilizes only the data from what are judged to be resonant peaks in the experimental results in the process of improving the mode shapes and modal masses. More sophisticated modeling techniques utilizing more of the experimental data are now being incorporated into the program to obtain better estimates of the natural frequencies and modal dampings.

The results obtained with this technique are shown in Figures 19 and 20, which compare total response. The curves are the results obtained from the computer model, whereas the data points represent the experimental results. A general correlation in the vicinity of the peaks in the response may be seen, but some significant differences exist in the regions away from the peaks. Although additional iterations could have been tried, it was thought that these results are satisfactory at this time. In obtaining these results, only the responses from E-W and torsional excitation were used since the N-S data were incomplete for this type of modeling. A subsequent comparison of the computer results with the experimental results for N-S excitation is shown in Figure 21. The comparison of results is discouraging and is thought to reflect the increasingly poor conditioning of the calculations as the resonant frequencies of the modes under study become closer.

The model which has been obtained from the iterative approach is indicated in Table I. The mode shapes (displacements of the 20th floor in the horizontal plane) are shown in Figure 22,in the same format as Figure 17.

Comparison of the modes and frequencies obtained by the two methods, as seen in Figures 17 and 22, shows agreement that is considered acceptable for most purposes. There are some differences that are judged to be consequences of uncertainties and insufficiencies in the data and differences in the two approaches. The basic conclusion is the same, however; the motion of the 20th floor in the three fundamental modes is a mixture of translational and rotational components to a degree that is surprising in view of the essential symmetry of the structural frame.

3. Presentation of results

The analyses of the 20th floor response were used to guide the data

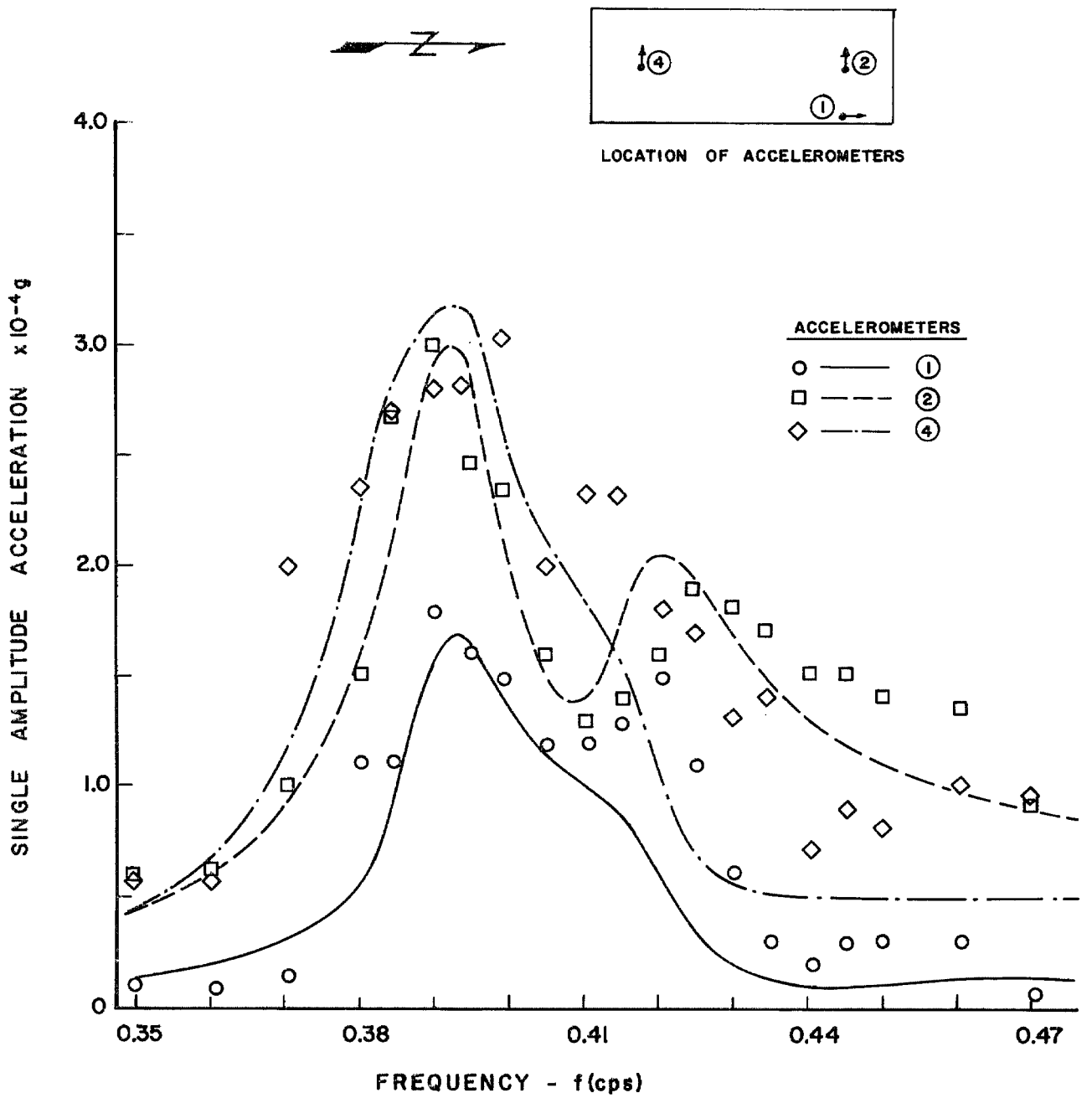

RESPONSE AT 20th FLOOR TO EAST-WEST EXCITATION

FIGURE 19. COMPARISON OF COMPUTED ACCELERATION OF SIMPLIFIED STRUCTURE WITH EXPERIMENTAL OBSERVATIONS. E-W EXCITATION

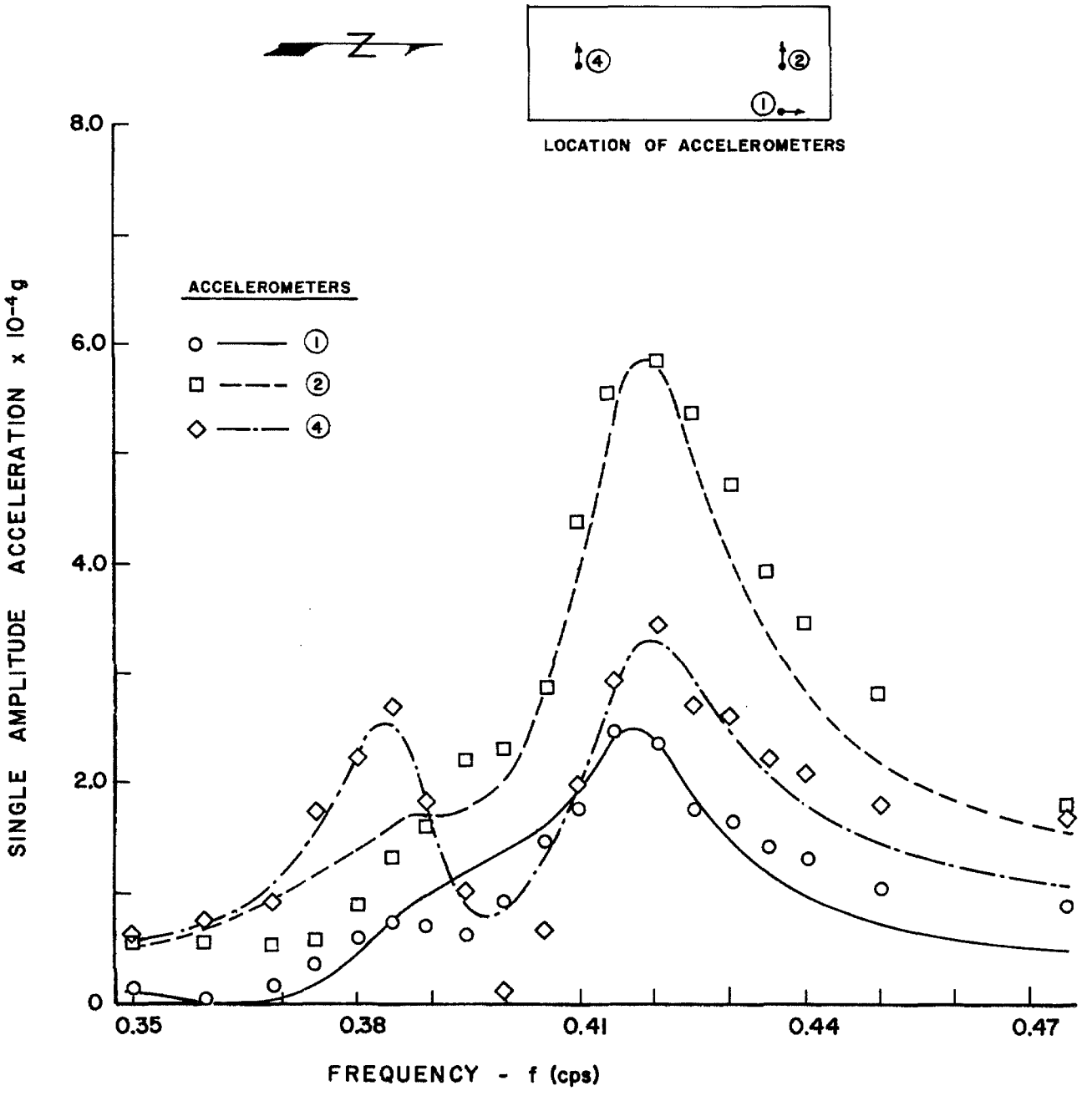

RESPONSE AT 20th FLOOR TO TORSIONAL EXCITATION

FIGURE 20. COMPARISON OF COMPUTED ACCELERATION OF SIMPLIFIED STRUCTURE WITH EXPERIMENTAL OBSERVATIONS. TORSIONAL EXCITATION

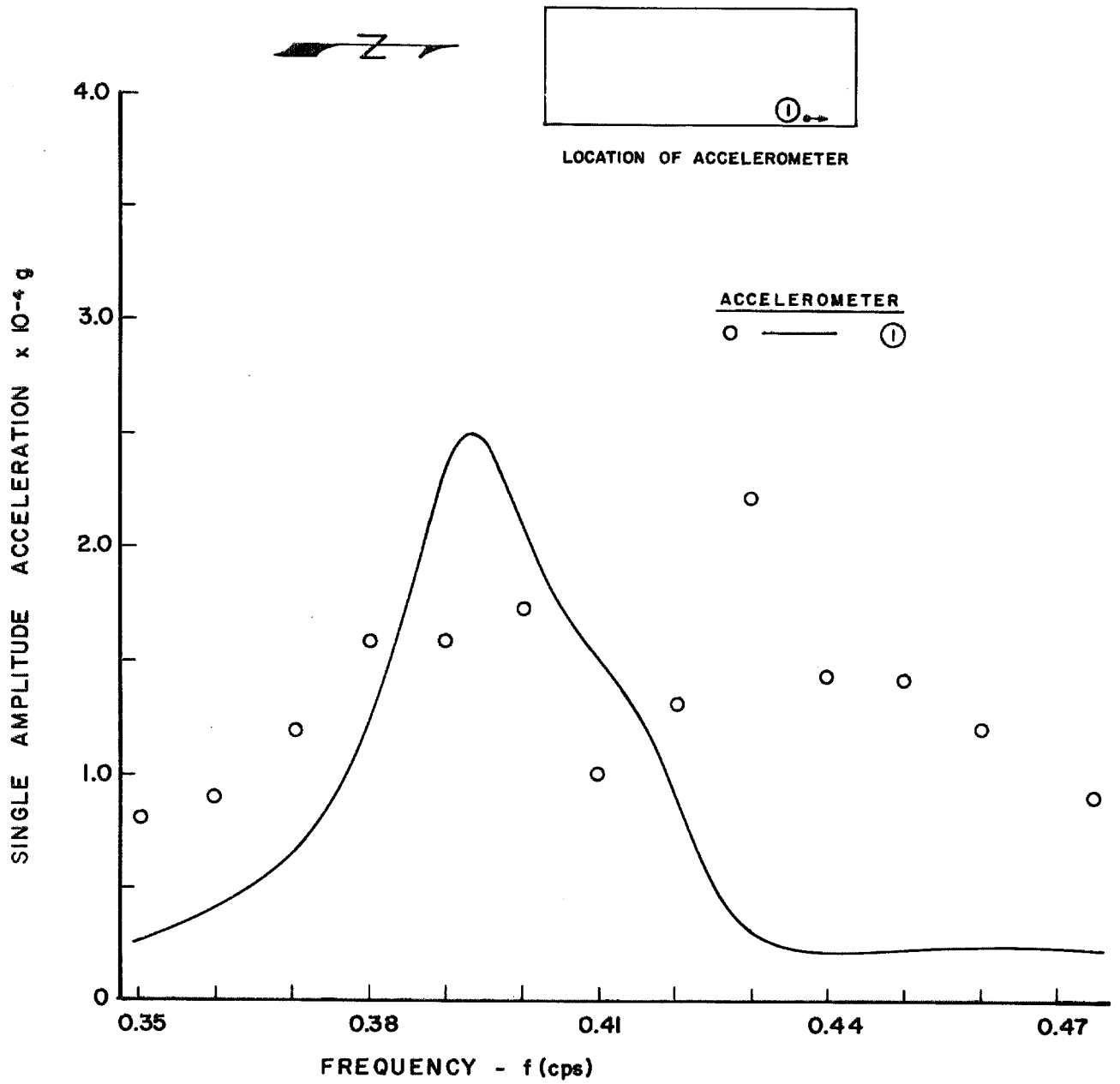

RESPONSE AT 20th FLOOR TO NORTH - SOUTH EXCITATION

FIGURE 21. COMPARISON OF COMPUTED RESPONSE OF SIMPLIFIED STRUCTURE WITH EXPERIMENTAL OBSERVATIONS. N-S EXCITATION

TABLE I

COMPUTER MODEL OF SAN DIEGO GAS AND ELECTRIC COMPANY BUILDING

Mode Number	Frequency (cps)	Damping (percent)	Effective Weight † (16×10^{-7})	Mode Shape * ϕ_2	ϕ_4	ϕ_1
1	0.385	1.8	1.77	-0.126	1.00	0.254
2	0.392	2.0	3.25	1.34	1.00	-0.882
3	0.420	2.2	3.54	-1.85	1.00	-0.882

† The mass associated with each vibration mode, see Ibañez, et al.,1970.

* Mode shapes are defined by the motions at points 1, 2 and 4, Figure 19.

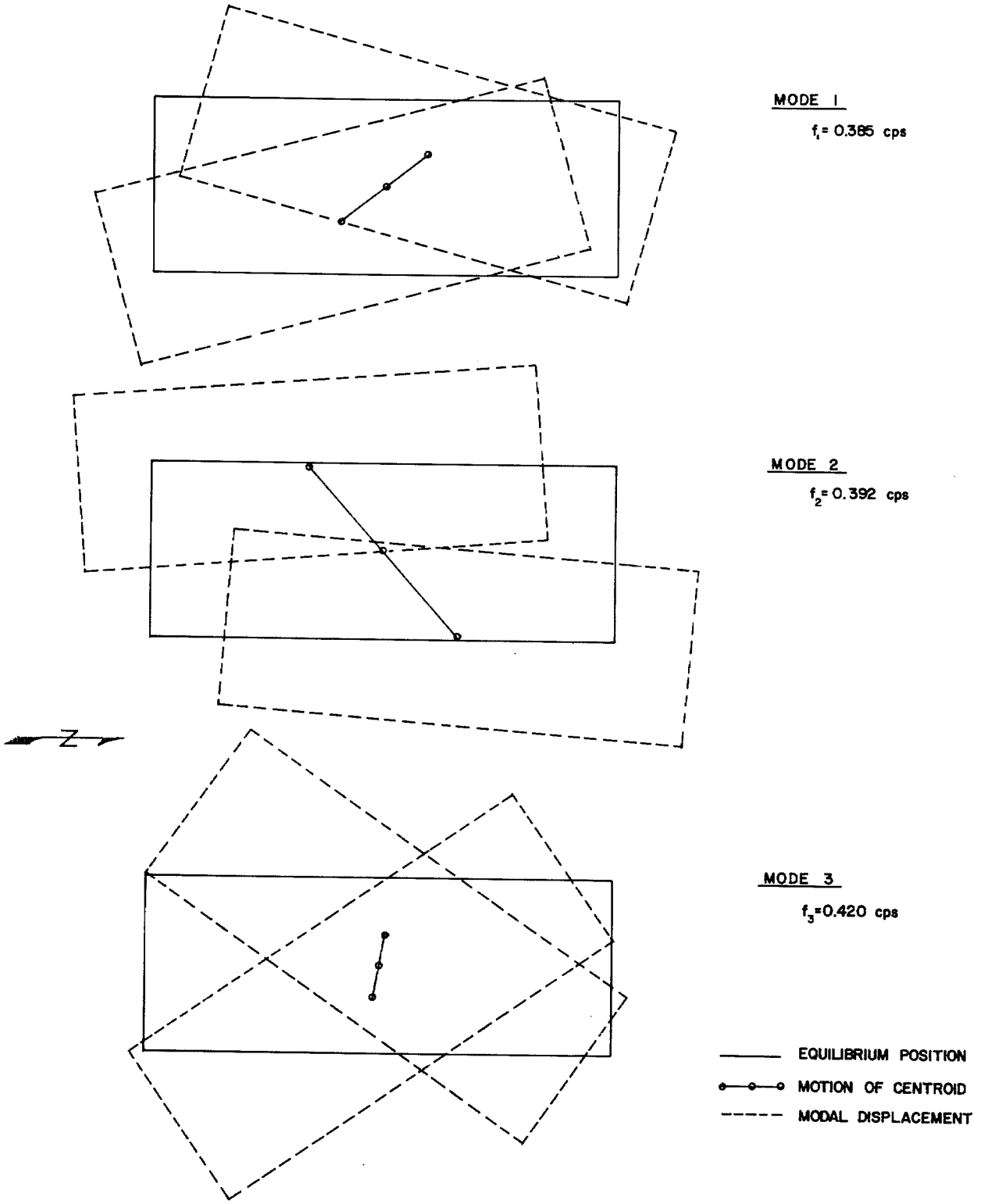

FIGURE 22. PLAN VIEW OF FUNDAMENTAL MODES AT 20th FLOOR AS DETERMINED FROM COMPUTER-AIDED RESOLUTION OF FUNDAMENTAL MODES. COMPARE WITH FIGURE 17

reduction techniques for determining the mode shapes for the three fundamental modes throughout the structure. The resulting mode shapes are given in Figures 23 and 24.

Insufficient data were available to determine the E-W and torsional components of the first fundamental mode and the results in Figure 23 show only the principal, N-S motion. The plotted points are the 90° out-of-phase components of the response to N-S excitation at f_1, which from Figure 16 is seen to be nearly equal to the mode shape at this frequency. There is some interference from the N-S component of the second mode under N-S excitation, but interference does not affect the modal component determined this way if the ratio of interfering response to total response is the same at each level of the structure. Since this is approximately the case, the error in mode shape is considered to be small.

The second mode shape, shown also in Figure 23, is determined from the 90° out-of-phase components of the response to E-W excitation at f_2. From Figure 15 it is seen that the shape as defined will differ only slightly from the true mode shape, with the rotational component showing the greatest error. The results in Figure 23 show that the relative values of the three modal components tend to be nearly the same throughout the structure.

The third, primarily torsional mode, is given in Figure 24 along with the center of rotation of each floor. From Figures 15 and 16 it is expected that distortion of the mode shape in Figure 24 by interference of the other two fundamental modes will be negligible. For the preparation of Figure 24, E-W sensing accelerometers were used to locate the center of rotation on the east face and N-S accelerometers were used for locating the coordinate on the south face. Only the values of rotation from the E-W records,

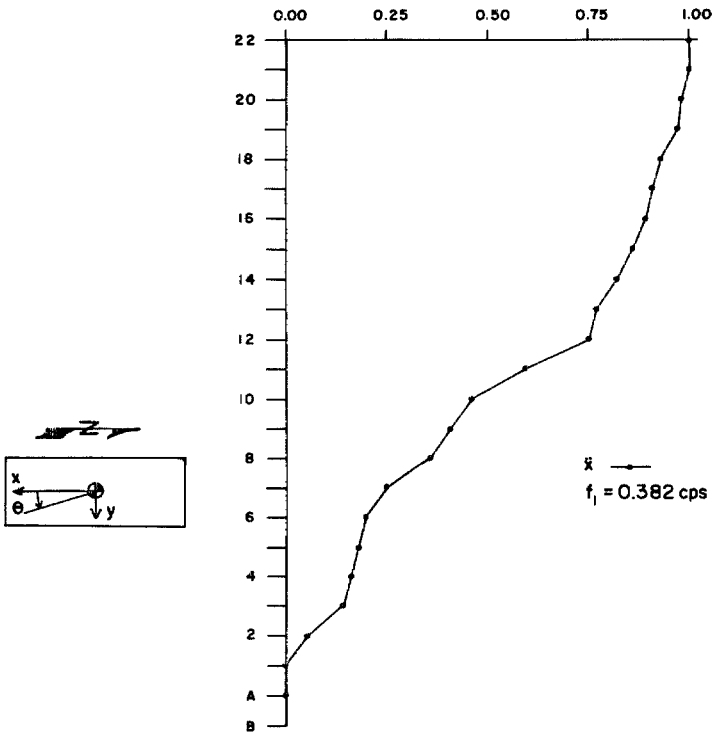

FIRST MODE SHAPE
(N-S MOTION ONLY)

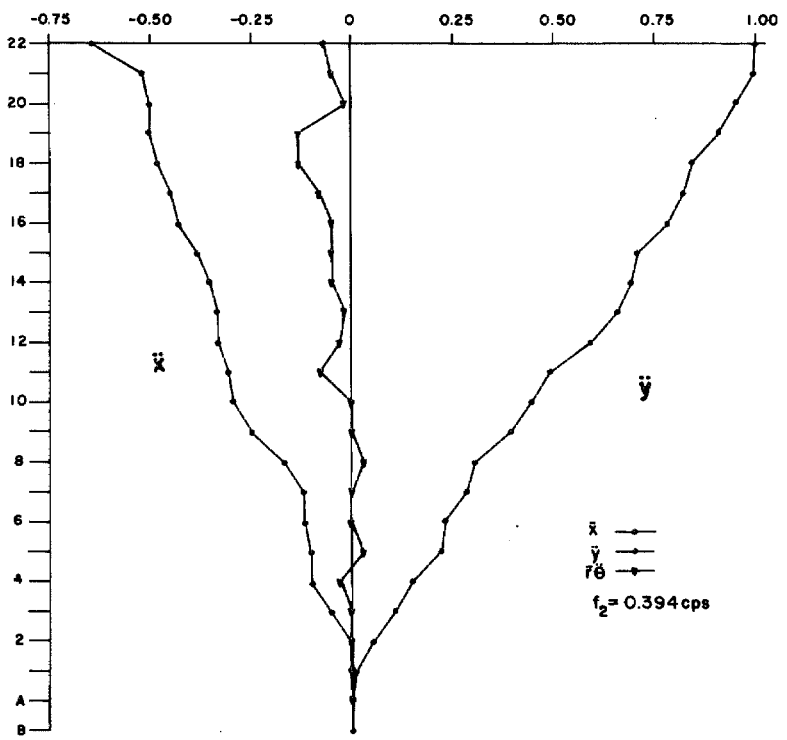

SECOND MODE SHAPE

FIGURE 23. COMPONENTS OF FIRST AND SECOND FUNDAMENTAL MODE SHAPES

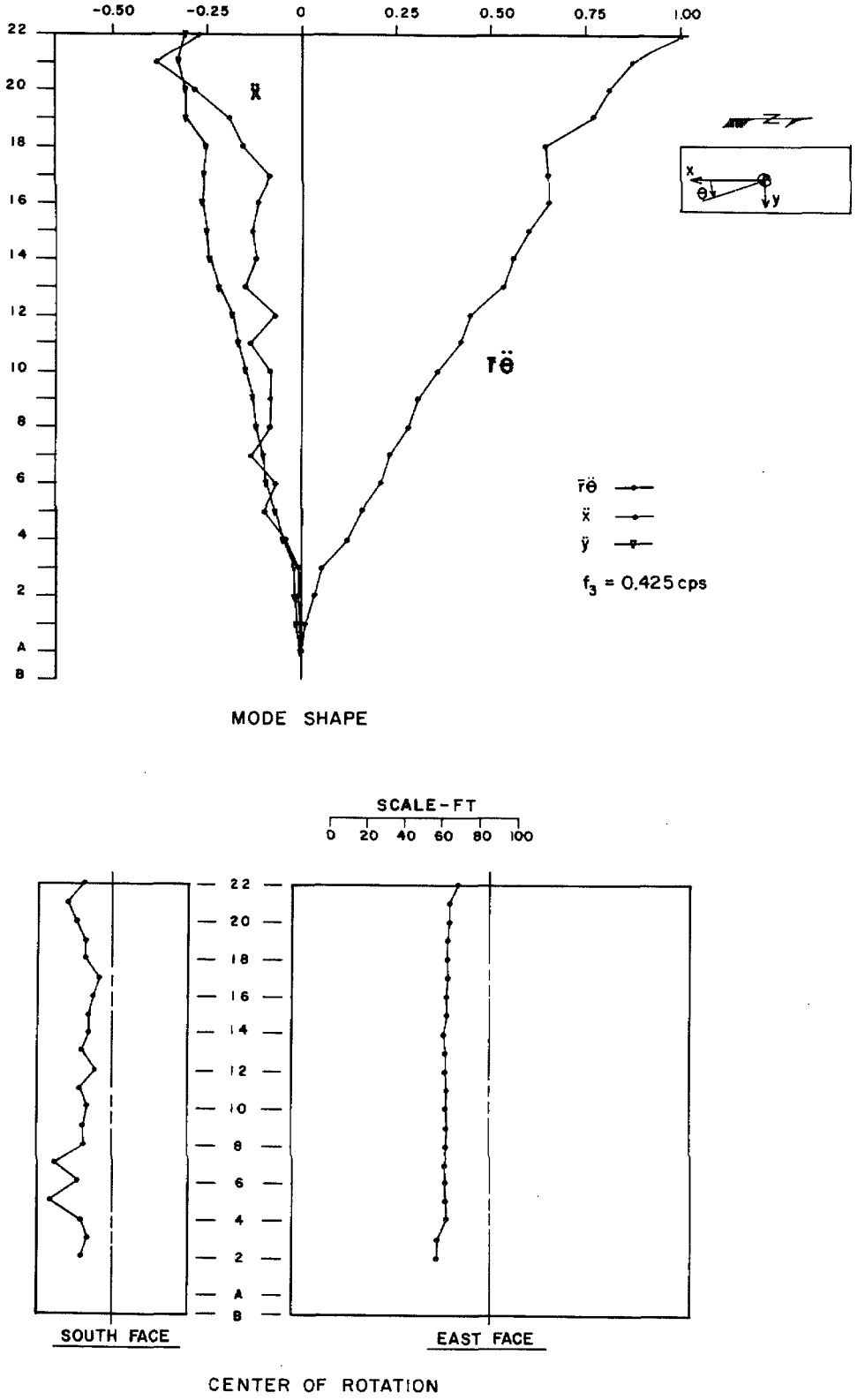

FIGURE 24. DETAILS OF THIRD FUNDAMENTAL MODE SHAPE

however, were used to determine $\bar{r}\ddot{\theta}$ at each floor because of the greater consistency of the results. The plotted values of $\ddot{x}$ and $\ddot{y}$ in Figure 24 are equal to the average translational components of motion in the two directions. Again the relative values of the modal contributions are nearly constant.

Although data are not available for the first, mainly N-S mode, it appears probable that the relative values of the modal components do not vary greatly with height for this mode either. Thus, the 20th floor motion probably is reasonably typical of other floors and the motions depicted in Figures 17 or 22 should give a good qualitative picture of the motions of the entire structure, adjusted, of course, by the amplitude vs. floor relations shown in Figures 23 and 24.

Properties of Higher Modes

The preliminary results shown in Figures 6, 7 and 8 indicate that 4 to 6 modes were excited by each of the frequency sweeps employing N-S, E-W and torsional excitation. In later tests, each of the resonant peaks was investigated further in enough detail to determine the resonant frequency, damping and major component of the mode shape.

The deformation pattern of the building at the resonant frequencies was measured throughout the building and the 90° out-of-phase component of the response was used to define the mode shapes. The measurements for the N-S modes typically consisted of two N-S records per floor, one at each stairwell, while for the E-W and torsional modes a N-S and an E-W record were taken in each stairwell for a total of four measurements per floor.

Table II summarizes the modal properties of the structure and Figures 25 through 28 give the mode shapes for the higher modes. The results in Table II

TABLE II

SUMMARY OF MODAL PROPERTIES
SAN DIEGO GAS AND ELECTRIC COMPANY BUILDING

Mode Number	N-S Modes*			E-W Modes*			Torsional Modes*		
	frequency (cps)	frequency ratio	damping (percent)	frequency (cps)	frequency ratio	damping (percent)	frequency (cps)	frequency ratio	damping (percent)
1	0.382	1	1.6	0.394	1	2.5	0.425	1	2.0
2	1.10	2.88	2.7	1.20	3.05	1.6	1.23	2.89	3.4
3	1.99	5.21	3.7	2.27	5.76	3.1	2.15	5.06	2.9
4	3.00	7.85	3.9	3.40	8.63	2.8	3.36	7.90	3.0
5	4.10	10.7	3.1	4.46	11.3	3.0	4.75	11.2	4.4
6	5.10	13.4	4.4	5.30	13.5	4.0	5.78	13.6	3.4

*Modes are identified by their primary component of motion.

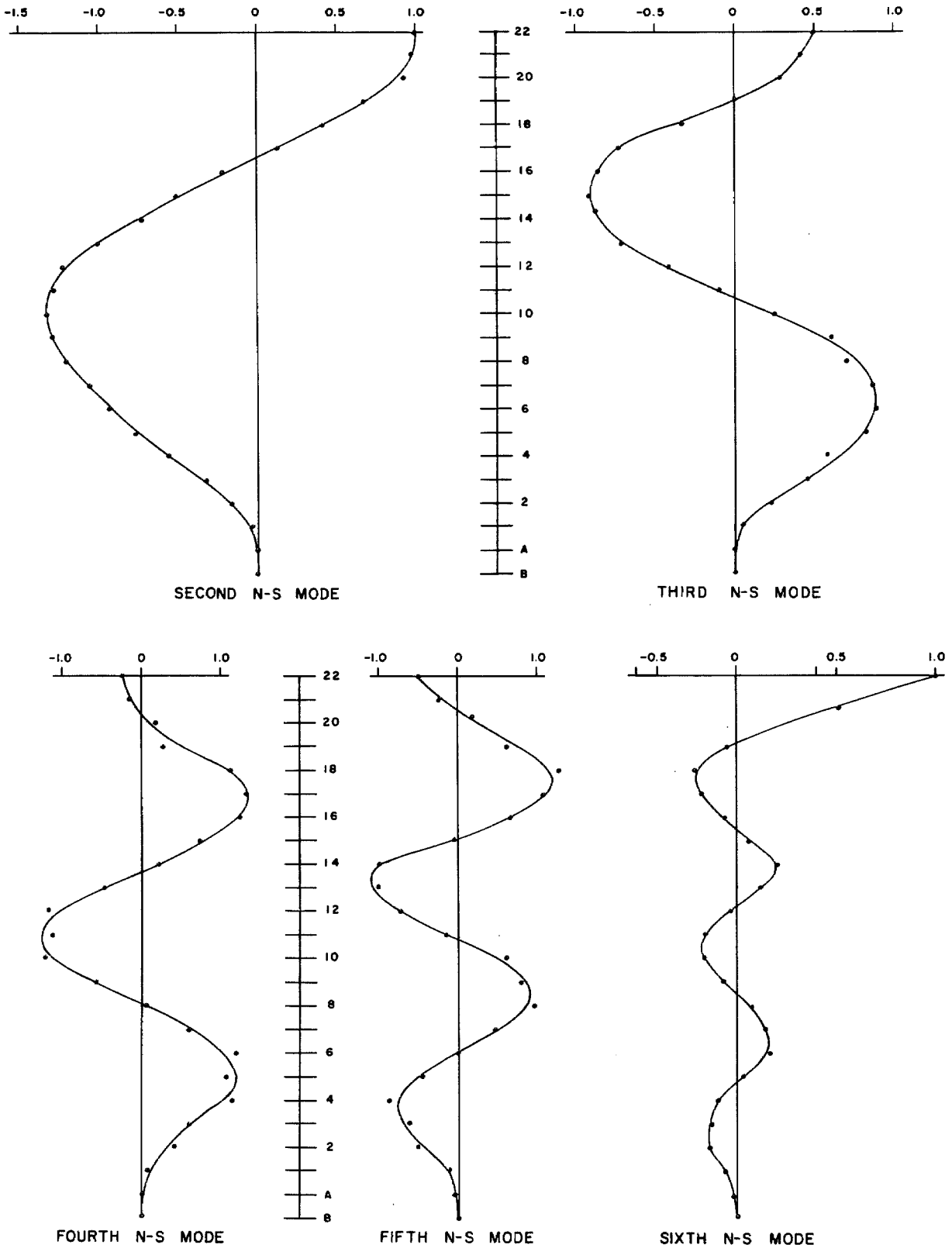

FIGURE 25. PRIMARY COMPONENTS OF HIGHER N-S MODES

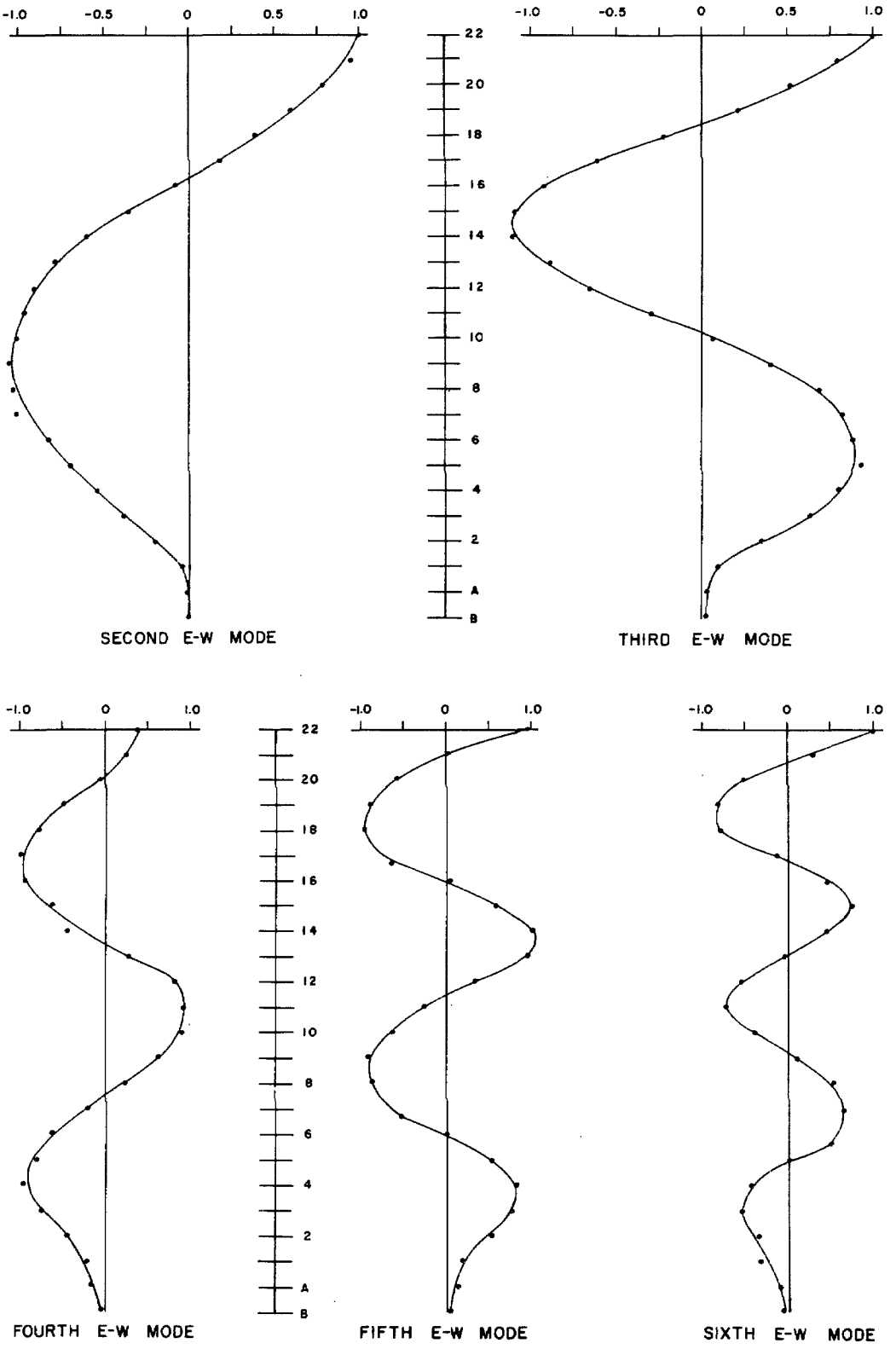

FIGURE 26. PRIMARY COMPONENTS OF HIGHER E-W MODES

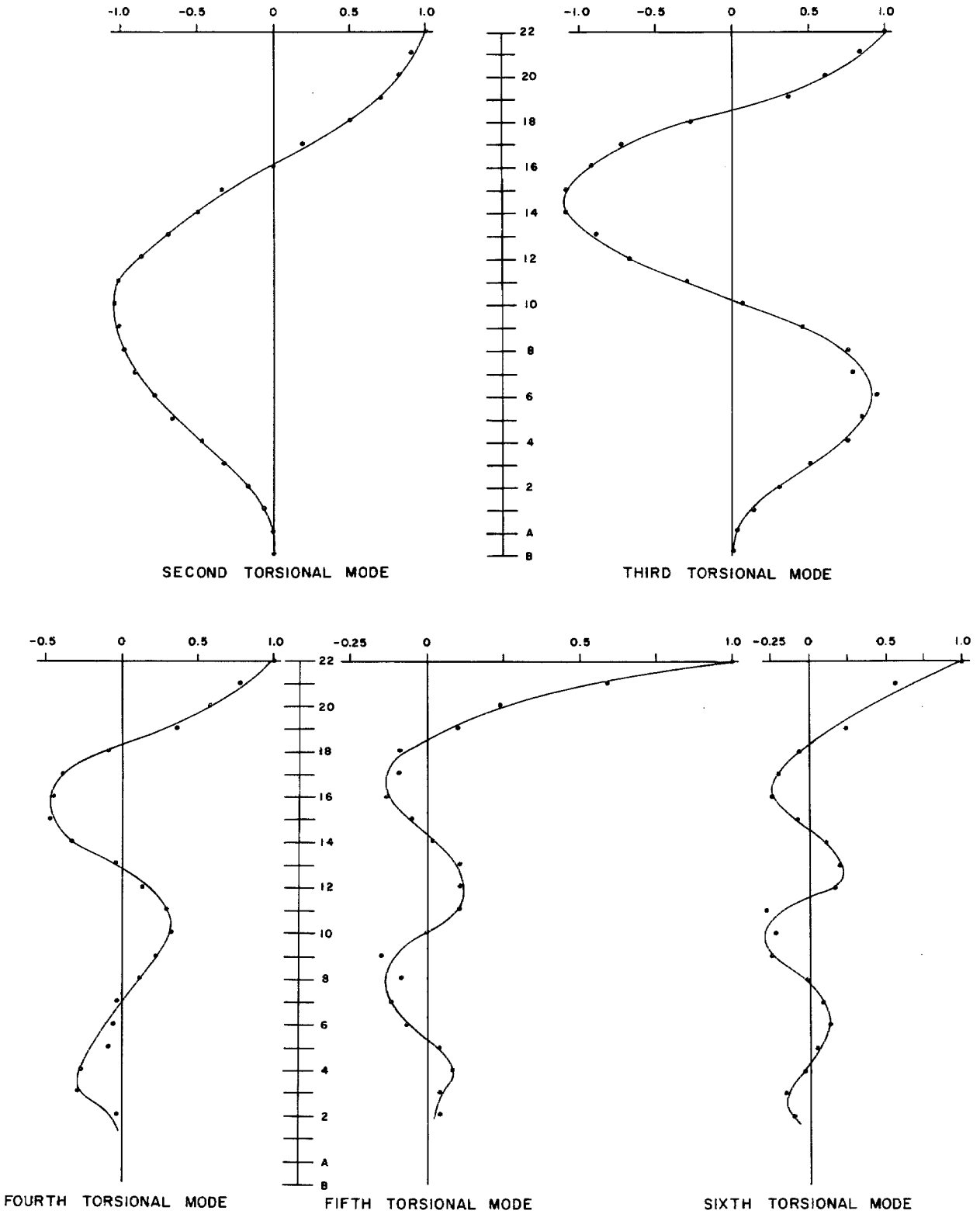

FIGURE 27. PRIMARY COMPONENTS OF HIGHER TORSIONAL MODES

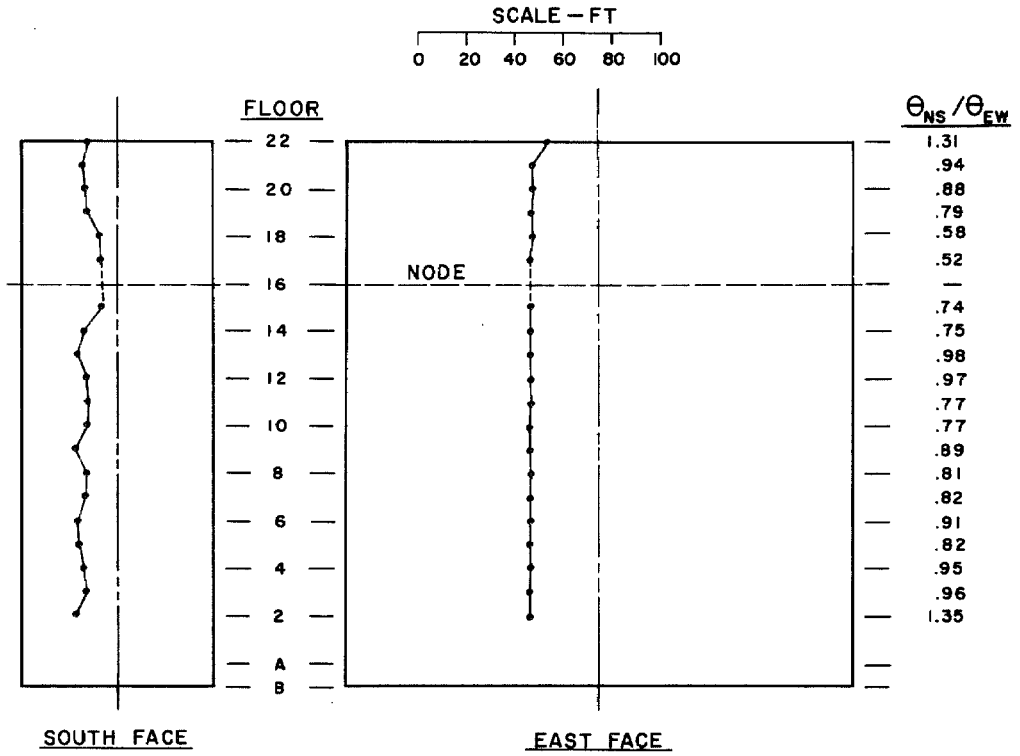

SECOND TORSIONAL MODE

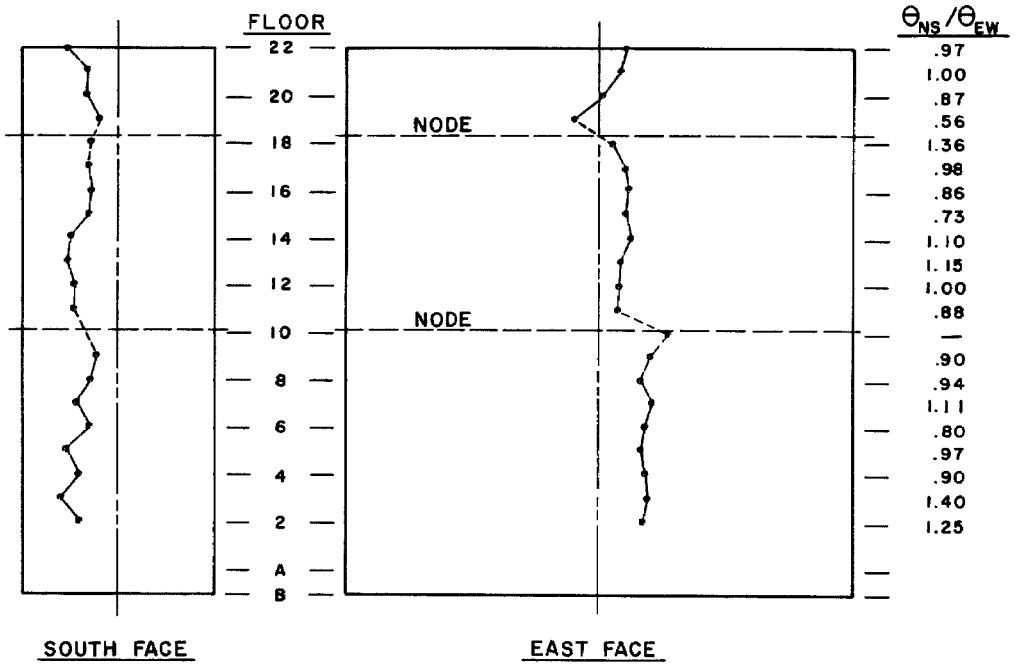

THIRD TORSIONAL MODE

CENTER OF ROTATION OF HIGHER TORSIONAL MODES

FIGURE 28.

include frequencies, damping values and frequency ratios for the first 18 modes of the structure, including the results for the fundamental modes presented above. The 18 modes include 6 each that are classified according to the principal component of motion as N-S, E-W or torsional in nature. The accuracy of the frequency determinations in Table II is about ±0.005 cps for the three fundamental modes and approximately ±0.05 cps for the higher modes. The accuracy of the damping values is approximately ±0.5 percent for most modes, with a somewhat larger error range for those modes in which modal interference complicated the response, and lesser error for modes with frequencies that are more separated. It should be noted that these values of damping are valid only for the amplitudes of the testing and somewhat higher values are expected in the event of stronger motion.

There seems to be a trend toward increasing damping in the modes with increasing mode number. The trend is so slight, however, that it could be just the effects of the generally increasing response levels associated with the higher modes (see Figures 6, 7 and 8). It appears that the assumption of constant modal damping is the most appropriate of the simpler damping approximations for this building, and the damping ratios are not modeled at all well by mass or stiffness proportional damping, or by a combination of the two.

The frequency ratios given in Table II show a regular increase that is similar to, but slightly more rapid than, the odd numbers that typify the simple shear beam. This property is shared by other tall, framed buildings (Jennings, 1969).

The mode shapes of the higher modes are grouped together in Figures 25, 26 and 27 and the centers of rotation at each floor in the second and third torsional modes are given in Figure 28. It should be realized that the center

of rotation becomes poorly defined near nodes of the mode shapes. It is seen from the figures that the primary components of the second and third modes of each type are determined accurately, whereas the fourth, fifth and sixth mode shapes are less well-defined, with a few exceptions.

Some of the higher N-S and torsional modes in Figures 25 and 27 show a tendency toward large displacements in the upper few floors. This property of the mode shapes, if correctly measured, is thought to be a consequence of the lighter structural frame in the upper few stories, the absence of elevator shafts and one stairwell in the upper story and the large mass of the cooling tower in the southwest corner of the 20th and 21st floors. The large modal displacements in the upper stories were not confirmed by the ambient tests discussed in the next section, and consequently are subject to some doubt.

As can be seen in Table II, some of the frequencies of the higher modes are quite near to those of corresponding modes in other directions. For example, the second, fourth and fifth E-W and corresponding torsional frequencies are all rather close. It is not too surprising then to find that some of the higher modes exhibited coupling qualitatively similar to that found for the fundamental modes of the building. The coupling in the higher modes was not studied as extensively as it was for the fundamental modes, but the nature of the coupling was determined in most cases. The coupling was most pronounced in the case of the fifth torsional mode. This mode, which shows large top-story displacements in Figure 27 is associated with equally large E-W translational components so that translation dominates the motion except near the roof. The coupling in the fourth and sixth torsional modes was similar but the translational components were less, ranging from

about one-tenth to two-thirds of the rotational components. Coupling to this degree makes the identification of the modes as torsional, etc., ambiguous, and the classification used here must be regarded as tentative. The nominally E-W higher modes showed torsional coupling similar to that for the higher torsional modes, but the N-S modes appeared to be relatively uncoupled showing only 5 to 10 percent coupling with rotational motion. An exception was the fourth N-S mode which showed rotational coupling of about one-third. To identify in more detail the three-dimensional character of the higher modes appears feasible in some of the instances in which four response records per floor were obtained, but this extensive analysis was not undertaken in the present study. To be done effectively, such data analysis would have to be done concurrently with the testing so that significant features of the mode shapes and points of question could be examined in greater detail; such an approach is difficult under field conditions, however.

COMPARISON WITH AMBIENT TEST RESULTS

The testing program for the San Diego Gas and Electric Company Building included an ambient vibration experiment in addition to the forced vibration tests. In the ambient testing, statistical analyses of the response to wind, traffic and microtremors (in this case the wind was the dominant excitation) are made to yield the dynamic properties of the building. The ambient testing requires a more sensitive measurement system and more extensive analysis of the data on the computer, but has the advantages of being relatively easy to perform, taking only one day in the present instance, and of not requiring the mounting of heavy equipment which subsequently generates potentially disturbing vibrations. The ambient testing procedures and results have already been made available (Trifunac, 1970a) and are not repeated here with the exceptions of the mode shapes, which are included in Appendix II, and the natural frequencies and damping values which are given in Table III below along with comparative values from the forced vibration tests.

Looking first at the frequency comparisons in Table III, it is seen that there is general agreement with the exception of the first N-S mode and the sixth E-W mode. In the case of the N-S fundamental mode, it appears that N-S components of the fundamental torsional and E-W modes may have been excited sufficiently strongly by the ambient excitation to mask the mode at 0.382 cps. The plausibility of this explanation is supported by the ambient results at the 20th floor (Trifunac, 1970a) which show that the N-S mode, whichever of the two frequencies it might have, was not excited strongly by the ambient excitation. The given identification of the sixth E-W frequency was questioned by Trifunac who stated that the frequency was well defined,

TABLE III

COMPARISON OF FORCED VIBRATION AND AMBIENT TEST RESULTS

Mode No.	N-S Modes				E-W Modes				Torsional Modes			
	FORCED VIB.		AMBIENT		FORCED VIB.		AMBIENT		FORCED VIB.		AMBIENT	
	frequency (cps)	damping (percent)	frequency (cps)	damping (percent)	frequency (cps)	damping (percent)	frequency (cps)	damping (percent)	frequency (cps)	damping (percent)	frequency (cps)	damping (percent)
1	0.382	1.6	0.429	9.5†	0.394	2.5	0.398	11.62†	0.425	2.0	0.429	9.2†
2	1.10	2.7	1.19	3.5	1.20	1.6	1.31	4.0†	1.23	3.4	1.29	5.7†
3	1.99	3.7	1.99	2.6	2.27	3.1	2.45	4.6	2.15	2.9	2.32	
4	3.00	3.9	3.03		3.40	2.8	3.54		3.36	3.0	3.39	
5	4.10	3.1	4.03		4.46	3.0	4.63		4.75	4.4	4.62	
6	5.10	4.4	5.05		5.30	4.0	6.02*		5.78	3.4		

† Large values are a result of modal interference

* See text

but that it was not possible to determine whether it represented E-W or torsional vibrations. From the forced vibration tests, it is seen that it is most probable that the mode is what has been identified herein as the sixth torsional mode (see Table III and Figure 10).

There is a clear trend, also discussed by Trifunac, for the frequencies determined from the ambient testing to be higher than the corresponding values from the forced vibration tests. It is thought that this is another example of the well-established tendency of building frequencies to decrease slightly with amplitude of vibration. The amplitude of the forced vibration response is about 100 times that of the ambient response and the resonant frequency-amplitude relation implied by the numbers in Table III would, if approximately uniform, be imperceptible over the limited range of the forced vibration tests.

Although small differences in the results of the ambient and forced vibration tests do appear, the most significant conclusion is that the two test techniques have yielded substantially the same natural frequencies with either set of results being sufficiently accurate for most practical purposes.

The comparison of the damping values in Table III is not as satisfactory because it was not possible in the ambient tests to determine accurately the damping in the fundamental modes of response. Also, damping in the fourth and higher modes could not be found. The difficulty with the damping in the fundamental modes was caused by the nearness of the three fundamental frequencies. As noted by Trifunac, the close spacing of the frequencies leads to an overlap and broadening of the peaks in the Fourier spectra that are the essential feature of the data analysis in ambient testing. The broadening of the spectrum peaks caused by this modal interference yields misleadingly high values of damping when standard techniques are applied.

For the San Diego Gas and Electric Company Building, the high values of damping and their cause was identified by Trifunac because the number of excited modes in the affected frequency band was known. For more complex structures, however, such as earth dams and nuclear reactors,which tend to have more irregularly spaced frequencies which are difficult to identify, the broadening of spectral peaks by modal interference could easily lead to erroneously high values of damping in important modes of the structure.

Comparison of the mode shapes in Appendix II with those found from the forced vibration tests shows general agreement for the primary component of the fundamental modes, and throughout the higher modes with the exception of the fifth and sixth N-S modes and the fourth and fifth torsional modes. In these four cases, the differences are mainly confined to the upper three floors and involve the amount of "whipping" present in the mode shapes. For the fifth N-S mode, the ambient tests show larger deflections at the top of the structure, whereas in the other three cases the forced vibration tests yield mode shapes with top level deflections significantly larger than those found from the ambient tests. Without further testing, it is not possible to resolve the differences in the mode shapes, and the accuracy of the large top level modal deflections shown in Figures 25 and 27 would appear to be open to question. In this regard, it should be noted that the higher modes are near the limits of the capabilities of both testing techniques.

The comparison of ambient and forced-vibration test results indicates substantial agreement in the dynamic properties determined by the two methods, with the exception of the damping values affected by modal interference. This difficulty is not considered too serious for relatively simple dynamic structures like most tall buildings; it was not observed in a similar

ambient test of a 39-story steel-frame building (Trifunac, 1970b) and, presumably, could be overcome in part by more refined analysis of the data from ambient tests. The advantages of the ambient testing and the results obtained where it has been employed indicate that it is a promising research tool that should be developed further.

COMPARISON WITH RESULTS OF ANALYTICAL STUDY

As noted in the introduction, an analytical study of the San Diego Gas and Electric Company Building has been performed in parallel with the testing program. The complete results of this study have been reported elsewhere (Gobler, 1969) and only a portion of the results are summarized here. In addition to the motivation provided by the vibration experiments on the building, the investigation was prompted by a desire to study the influence of different assumptions concerning the behavior of architectural and structural components upon the computed dynamic properties of a modern high-rise building. The basic parametric studies were made using a program for two-dimensional analysis and then a program for analysis of three-dimensional motion was used for a limited number of cases.

The natural frequencies of the three-dimensional analytical model of the building which was selected on the basis of the parametric studies are summarized in Table IV. The natural frequencies and the dominant directions of the first eighteen modes of vibration are presented and can be compared to the experimentally determined natural frequencies included from Table II. The analytical study shows generally good agreement for the first four or more frequencies of each type, and also predicts the important observed feature of the nearness of the natural frequencies of the two fundamental modes of lateral vibration. Table IV shows that the analytically determined natural frequencies for the lateral modes are somewhat lower than those obtained experimentally, whereas the analytical values of natural frequencies for the predominantly torsional modes are slightly higher than those found from the tests.

It was found in the calculations that the stiffness of the floor beams, floor slabs, fireproofing and nonstructural elements substantially affected

TABLE IV

COMPARISON OF EXPERIMENTALLY AND ANALYTICALLY DETERMINED NATURAL FREQUENCIES

Predominately N-S Modes			Predominately E-W Modes			Predominately Torsional Modes		
Mode No. †	Forced Vib.*	Analysis	Mode No. †	Forced Vib.*	Analysis	Mode No. †	Forced Vib.*	Analysis
1	0.382 cps	0.362 cps	2	0.394 cps	0.385 cps	3	0.425 cps	0.464 cps
4	1.10	1.077	5	1.20	1.168	6	1.23	1.369
7	1.99	1.887	8	2.27	2.179	9	2.15	2.458
10	3.00	2.739	11	3.40	3.230	12	3.36	3.606
13	4.10	3.610	14	4.46	4.359	16	4.75	4.832
15	5.10	4.412	18	5.30	5.527			
17		5.147						

† Numbering system follows Gobler, 1969

* From Table II

the calculated values of the natural frequencies. The agreement among frequencies shown in Table IV is based, in essence, on the analysis of a structure that included the basic structural frame, floor beams, floor slabs, special structural framing and fireproofing, but which neglected both the mass and the stiffness of architectural and special features not included above (including the exterior concrete fins). This approach is based on the assumption that these special elements, whose effects are difficult to ascertain, contribute in approximately the same ratio to both the mass and stiffness of the structure, thereby leaving the natural frequencies essentially unchanged. After the frequencies were established in this manner, the masses of the nonstructural items were added, while changes in the stiffness necessary to preserve the fundamental frequencies were made also. The agreement of the final results indicates this is an approach deserving further study.

The effects of the various elements were approximately as follows: beginning with the basic frame, the addition of the floor beams and floor slabs caused an increase in the fundamental frequencies of 12 percent and the further addition of the fireproofing, primarily on the first two levels, resulted in further increase of the frequencies of 5 percent. The additional consideration of the various architectural and special features in the manner summarized above caused a further increase in the natural frequencies of about 30 percent. This last figure underlines the importance of these elements in the dynamic behavior of the building, at least for the low stress levels of the vibration tests.

The motion of the 20th floor in the first three modes as determined from the analytical study is shown in Figure 29. This result can be compared

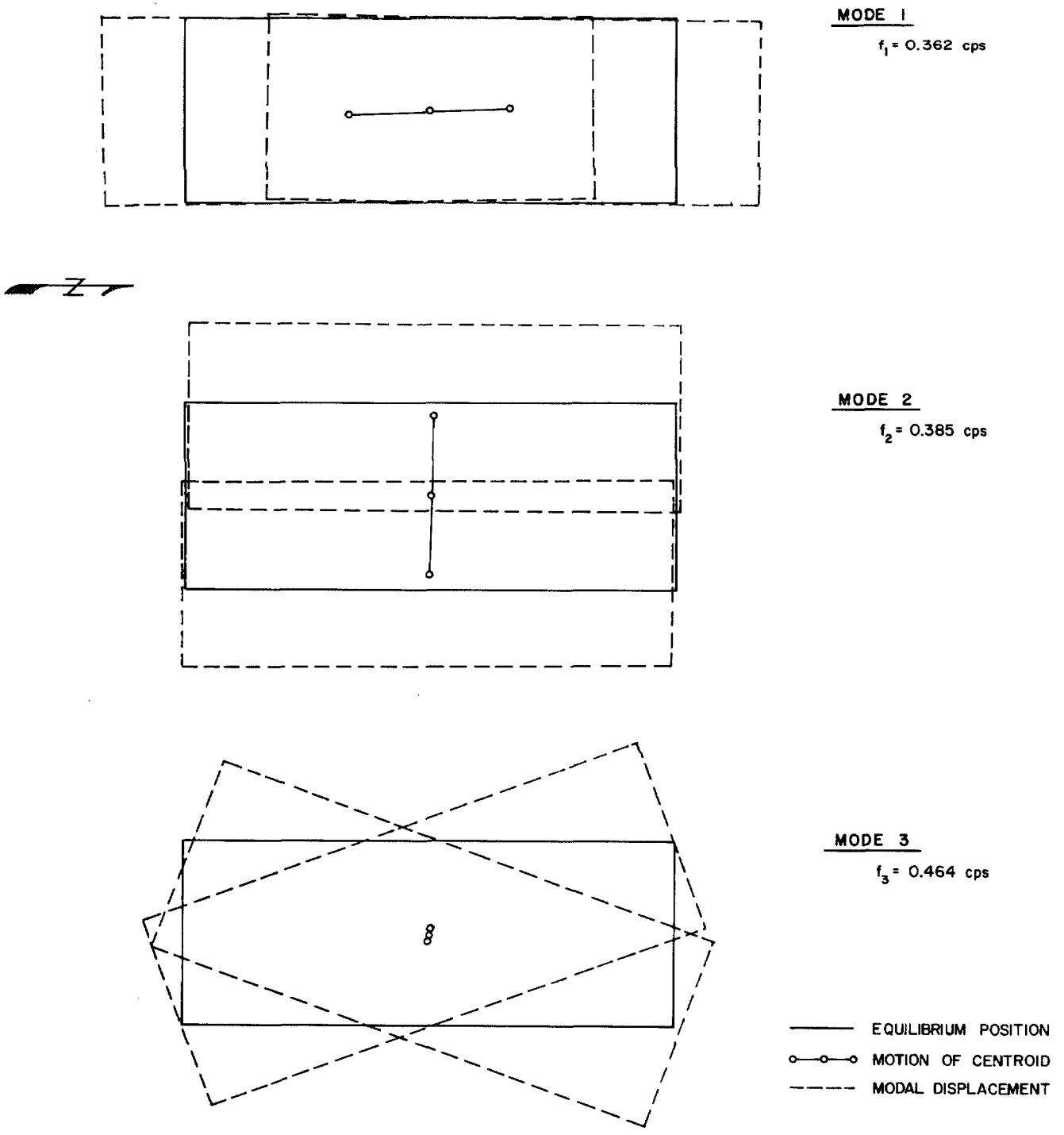

FUNDAMENTAL ANALYTICAL MODES AT THE 20th FLOOR

FIGURE 29. PLAN VIEW OF FUNDAMENTAL MODES AT 20th FLOOR AS DETERMINED FROM ANALYTICAL STUDY. COMPARE WITH FIGURES 17 AND 22.

to the experimentally determined floor motions shown in Figures 17 and 22. The modes agree qualitatively but there is clearly much less coupling of the three components of motion in the analytical mode shapes than in the experimental results. This fact suggests that the analytical model did not adequately represent the eccentricities of the mass and stiffness of the building.

DISCUSSION AND CONCLUSIONS

The test results presented above demonstrate that it is possible to determine the natural frequencies, mode shapes and damping values of a modern tall building to a degree that is satisfactory for most purposes. Many questions still remain, of course, such as the amplitude sensitivity of the results, particularly the damping, and the extent to which the linear dynamic properties can aid in understanding the yielding and nonlinear response expected in most structures during very strong shaking. Unfortunately, these important questions are beyond the capabilities of the type of test reported here and must await records of earthquake response. The major value of the dynamic properties determined in this test lies in the understanding of response to moderate earthquake motions or strong winds, in helping to determine the levels at which strong earthquake motion causes significant departure from linear behavior, and in the improvement of techniques by which dynamic properties of structures are calculated.

The dynamic properties also are useful in a general way in the development of rational methods for the earthquake-resistant design of tall buildings. These methods require estimates of the way dynamic forces would be distributed over the structure during earthquakes. This distribution is determined by the mode shapes and natural frequencies of the structure and values of the forces for design are most logically based on average dynamic properties of similar structures.

Test programs such as the present effort are impractical on a routine basis and one of the goals of structural analysis is the capability for predicting the dynamic properties of structures and their response to earthquakes and other dynamic loadings. In this context, the dynamic properties represent

intermediate results which must be known accurately if confidence is to be placed in subsequent calculations. Although developed fairly well, these analytical techniques have not yet progressed to the point where natural frequencies and mode shapes of buildings can be calculated consistently and accurately, and techniques for calculating damping values for complex structures are in their infancy. As a part of the effort to improve the methods of analysis, an analytical determination of the mode shapes and frequencies of the San Diego Gas and Electric Company Building has been made by G. C. Hart and H. W. Gobler (Gobler, 1969) and a summary of some of the results was presented in the previous section.

The conclusions which follow are divided into those pertaining to the dynamic properties of the building and those relating to techniques for testing and data analysis.

Dynamic Properties of the Building

The mode shapes and natural frequencies of the San Diego Gas and Electric Company Building showed, in general, the regularity and uniformity that appears to typify most tall buildings and reflect the fact that for the first few modes, at least, these structures are relatively simple dynamic systems. The most significant special feature of the dynamic properties of this structure is the extent to which the motion of the building in its three fundamental modes is a mixture of translational and rotational components. This amount of coupling of modal components, expected in asymmetrical structures, is somewhat surprising in a building which is essentially symmetrical in its structural plan. It is thought that the coupling tendencies of small eccentricities in the building have been amplified strongly by the fortuitously small differences among the first three fundamental frequencies.

It seems clear that strong coupling in the fundamental modes will make the structure respond to earthquake motion in a manner different than envisaged in most design approaches, including that embodied in building codes, but it is not yet established that the complexity of the fundamental modes necessarily implies more severe response during an earthquake. The significance of the earthquake response of highly coupled and correlated modes is a topic that needs more research.

This is one of the few tests in which a large enough number of modal damping values have been determined to allow the identification of trends in the results. The damping values, shown in Table II, vary from 1.6 percent to 4.4 percent over the first 18 modes of the structure. Although there is a small tendency for the damping to be greater for the higher modes, there is no strong trend in the values. Of the simpler damping assumptions that might be used to study the response of the building to dynamic excitation, the choice of constant modal damping is most appropriate and mass or stiffness proportional damping is not realistic. The values of damping found are for response of the order of 0.001g and it is not known how these damping values can be extrapolated to greater response levels. The records obtained in future strong earthquakes from the accelerographs in the building should help to answer this question.

Although the forced vibration and ambient tests are not in agreement on this point, it appears probable that one or two of the fourth, fifth or sixth modes of the building may have large modal displacements in the upper two or three floors. This effect, termed "whipping" is particularly evident for the torsional modes shown in Figure 27. If these mode shapes are accurate and if the modes are excited strongly by earthquake motions, then large

displacements are to be expected in the upper two levels. Two factors, however, tend to reduce the potentially large displacements indicated by these modes. First, the higher modes are less important to the overall earthquake response than the lower modes, especially the fundamentals. Second, modes which are primarily torsional in nature are excited less by earthquake motions than modes which are primarily translational. Whipping is not present in any of the first, second or third modes of the building, and any whipping in the higher modes is expected to have a relatively minor effect in the overall earthquake response of the building.

The results of the analytical study of the building showed generally good agreement with the test results, including the important feature of the nearness of the two fundamental translational frequencies. The predicted mode shapes were qualitatively similar to those found from the tests, but showed significantly less coupling than observed experimentally. The analysis demonstrated again the need to consider nearly all structural and nonstructural elements of the building in order to achieve results of acceptable accuracy. The inclusion of the floor beams and slabs caused a 12 percent increase in the frequencies calculated using the structural frame; the considerations of the fireproofing caused an additional increase of 5 percent; and the further inclusion of the nonstructural masses and stiffnesses by an approximate technique gave an additional increase in the frequencies of about 30 percent. The importance of the nonstructural elements in determining the dynamic properties, at least for small strains, is emphasized by this last result.

Testing Techniques and Data Analysis

When assessing the techniques of dynamic testing and the methods for the subsequent data analysis, it must be borne in mind that the experiments are done under field, rather than laboratory, conditions. Thus, it is rarely

possible for anything but the most rudimentary data analysis to keep pace with the experiment, nor for the testing equipment to remain installed for periods long enough to allow reinvestigation of points which the data are insufficient to resolve. In fact, much of the early portions of tests such as these are devoted to learning, in a general way, what the dynamic properties of the building are so that informative measurements can be taken.

The closeness of the natural frequencies of the building provided a severe test of the techniques for data analysis. In this effort, the measurement of the relative phase between force and response and the subsequent resolution of the response into in-phase and 90° out-of-phase components proved to be extremely valuable. As can be seen from Figures 10 and 13, for example, this approach materially assists in understanding the building response. In addition, as can be seen from Figure 9, the technique allows a more accurate measurement of the damping because the unconservative effects of modal interference are largely avoided. Although less important, the phase measurements also permitted a somewhat more precise determination of the natural frequencies. This useful technique appears capable of further exploitation, for example, by the development of a method of direct determination and recording of the 90° out-of-phase component of response.

Many tests of this type, including the present one, are performed under the assumption that the floor moves as a rigid body. This assumption seems to be acceptable for the San Diego Gas and Electric Company Building for the first few modes, but the data show that it is much better for translational modes than for torsional modes. Different rotations were found for the torsional modes from N-S and E-W pairs of accelerometers, indicating deformation of the floor system. A detailed study of torsional modes of a

building of this type would have to be accompanied by measurements establishing the extent of deformation of the floor systems.

Comparison of the results from the ambient and forced vibration tests showed generally the same natural frequencies and mode shapes and, where modal interference was not significant, approximately the same values of damping. The ambient test results were not as extensive as those from the forced vibration tests, but are sufficiently complete for most purposes. The advantages of the ambient testing and the encouraging results support further development of this approach. In particular, techniques should be found to overcome the spectral overlap, and the associated high damping values caused by modal interference.

A comparison of the results from the data reduction technique applied to the fundamental modes and the related, computer-aided approach to the same problem show general agreement in the major features, with the best agreement between the derived mode shapes at the 20th floor as shown in Figures 17 and 22. The comparison of the computed response to the data (Figures 19-21) was less satisfactory, particularly for N-S excitation, and the calculations were found to be particularly sensitive to the assumed properties of the structure, presumably as a consequence of the nearness of the three fundamental frequencies. This difficulty has not been observed to this degree in other applications of the method (Ibañez, et al., 1970) and the computer-aided approach to the data analysis problem, in general, appears promising.

The cooperative approach employed in this research project was successful in bringing to bear a variety of analytical and experimental techniques on the problem of determining the dynamic properties of a building. The increased scope of the resulting joint effort demonstrates the advantage of a joint approach to field testing of large structures.

REFERENCES

1. Benton Engineering, Inc. (1965), Soils Investigation Proposed Multistory Building, San Diego Gas and Electric Company, San Diego, California, San Diego, California.

2. Benya, J. S., (1967), A Forced Vibration Study of a Steel Framed Building, M.Sc. Thesis, School of Engineering, University of California, Los Angeles.

3. Gobler, H. W., (1969), Three-Dimensional Modeling and Dynamic Analysis of the San Diego Gas and Electric Company Building, M.Sc. Thesis, School of Engineering, Univ. of California, Los Angeles.

4. Hoerner, J. B. and Jennings, P. C., (1969), Modal Interference in Vibration Tests, Journal of the Engr. Mech. Div., ASCE, Vol. 95, EM4, pp. 827-839.

5. Hudson, D. E. (1962), Synchronized Vibration Generators for Dynamic Tests of Full-Scale Structures, Earthquake Engr. Res. Lab., Calif. Inst. of Tech., Pasadena.

6. Ibañez, I., Matthiesen, R. B., Smith, C. B. and Wang, G. S. C., (1970), San Onofre Nuclear Generating Station Vibration Tests, Nuclear Energy Lab. and Earthquake Engr. and Structures Lab., Univ. of Calif., Los Angeles.

7. Jennings, P. C., (1969), Spectrum Techniques for Tall Buildings, Proceedings of the Fourth World Conference on Earthquake Engineering, Vol. II, pp. 61-64, Santiago, Chile.

8. Jennings, P. C. and Kuroiwa, J. H., (1968), Vibration and Soil-Structure Interaction Tests of a Nine-Story Reinforced Concrete Building, Bull. Seism. Soc. of Am., Vol. 58, No. 3, pp. 891-916.

9. Keightley, W. O., (1964), A Dynamic Investigation of Bouquet Canyon Dam, Earthquake Engr. Res. Lab., Calif. Inst. of Tech., Pasadena.

10. Kuroiwa, J. H. (1967), Vibration Test of a Multistory Building, Earthquake Engr. Res. Lab., Calif. Inst. of Tech., Pasadena.

11. Matthiesen, R. B. and Smith, C. B., (1969), Forced Vibration Tests of the Carolinas-Virginia Tube Reactor (CVTR), Earthquake Engr. and Structures Lab. and Nuclear Energy Lab., Univ. of Calif., Los Angeles.

12. Nielsen, N. N., (1964), Dynamic Response of Multistory Buildings, Earthquake Engr. Res. Lab., Calif. Inst. of Tech., Pasadena.

13. Rea, D., Bouwkamp, J.G., and Clough, R.W. (1966), The Dynamic Behavior of Steel Frame and Truss Buildings, Struct. Engr. Lab. Report No. 66-24, University of Calif., Berkeley.

14. Shanman, R. D. (1969), A Forced Vibration Study of a Completed Five-Story Steel Frame Building, M.Sc. Thesis, School of Engineering, University of California, Los Angeles.

15. Smith, C.B., and Matthiesen, R. B., (1969), Forced Vibration Tests of the Experimental Gas-Cooled Reactor (EGCR), Earthquake Engr. and Structures Lab. and Nuclear Energy Lab., Univ. of Calif., Los Angeles.

16. Trifunac, M.D., (1970a), Wind and Microtremor-Induced Vibrations of a Twenty-Two Story Steel Frame Building, Earthquake Engr. Res. Lab., Calif. Inst. of Tech., Pasadena.

17. Trifunac, M. D. (1970b), Ambient Vibration Test of a Thirty-Nine Story Steel Frame Building, Earthquake Engr. Res. Lab., Calif. Inst. of Tech., Pasadena.

APPENDIX I

SUMMARY OF FORCED VIBRATION TESTING

The forced vibration tests of the San Diego Gas and Electric Company Building were conducted on weekends in the period from May 24 through June 28, 1969 and included a total of 10 days on which testing was done. During the testing the vibrators remained on the 20th floor in the positions shown in Figures 5 and I-1, whereas the accelerometers were positioned throughout the building as required for the purposes of the various tests, subject to the geometrical constraints imposed by the building. The directions of the forces generated by the vibrators were adjusted to produce N-S, E-W or torsional excitation as desired.

The testing program is summarized in Table I-1 which includes the test number, date, machine loading and resulting force, and the scale factor for the frequency measurement system. Also included are brief descriptions of the purpose of each test and shorthand descriptions of the accelerometer locations. The accelerometer locations are detailed in Table I-2 and shown approximately in Figures I-1 and I-2.

The personnel used to perform the forced vibration tests varied from a minimum of four to a maximum of eight.

TABLE I-1

SUMMARY OF TESTING
SAN DIEGO GAS AND ELECTRIC COMPANY BUILDING

Test	Date	Purpose	Weights per Unit[1]	Force lbs/Unit	Frequency Scale counts/cycle	Accelerometer Locations[3] (Figures I-1, I-2)
1	May 24, 1969	N-S low frequency sweep	S1, L1	$241f^2$ [2]	1000	1′-S-20-a 2′-W-20-c 3′-S-20-b 4′-W-20-y 1 -S-20-c 2 -S-20-d 3 -S-20-f 4 -S -20-g
2	May 24	N-S low frequency sweep	Full(S4, L4)	$804f^2$	1000	Same as test 1
3	May 24	E-W low frequency sweep	Full	$804f^2$	1000	1-W-20-k, 2-W-20-j, 3-W-20-i, 4-W-20-h, UCLA same as test 1
4	May 24	Torsional low frequency sweep	Full	$804f^2$	1000	1-W-20-k, 2-W-20-j, 3-E-20-i, 4-E-20-h, UCLA same as test 1
5a	May 25	Torsional high frequency sweep	S4	$227f^2$	300	1-W-20-k, 2-W-20-j, 3-E-20-i, 4-E-20-ℓ, UCLA same as test 1
5b	May 25	Torsional high frequency sweep	S2	$140f^2$	300	Same as test 5a
5c	May 25	Torsional high frequency sweep	Empty	$53f^2$	300	Same as test 5a
6a	May 25	E-W high frequency sweep	S4	$227f^2$	300	1-W-20-k, 2-W-20-j, 3-W-20-i, 4-W-20-ℓ, UCLA same as test 1
6b	May 25	E-W high frequency sweep	S2	$140f^2$	300	Same as test 6a
6c	May 25	E-W high frequency sweep	Empty	$53f^2$	300	Same as test 6a
7a	May 30	N-S high frequency sweep	S4	$227f^2$	300	1-S-20-c, 2-S-20-d, 3-S-20-f, 4-S-20-g, UCLA same as test 1
7b	May 30	N-S high frequency sweep	S2	$140f^2$	300	Same as test 7a
7c	May 30	N-S high frequency sweep	Empty	$53f^2$	300	Same as test 7c
8a	June 7	Detailed N-S frequency sweep	Full	$804f^2$	1000	CIT same as test 7a, UCLA accelerometer not used in 8a or later tests
8b	June 7	Geometry of 1st, 2nd and 3rd N-S modes	Full	$804f^2$	1000	First setup: 1-S-R-n, 2-S-21-m, 3-S-20-m, 4-S-19-m, 5-S-20-d. Second setup: 5-S-20-d; 1-S-m on floors 18, 14, 10, 6 and 2; 2-S-m on floors 17, 13, 9 and 5, and 2-S-1-o; 3-S-m on floors 16, 12, 8 and 4, and 3-S-A-n; 4-S-m on floors 15, 11, 7 and 3, and 4-S-B-n.
9	June 8	Geometry of 1st, 2nd and 3rd N-S modes	Full	$804f^2$	1000	First setup: 1, 2, 3 and 4-S-12-r, (dynamic calibration) and 5-S-20-d. Second setup: 1-S-12-p, 2-S-12-q, 3-S-12-s, 4-S-12-t, 5-S-20-d.
10	June 8	Geometry of 1st, 2nd and 3rd N-S modes	Full	$804f^2$	1000	1-S-R-u, 2-S-R-w, 3-S-21-v, 4-S-21-b, 5-S-20-d.

[1] Hudson, D. E. (1962)

[2] f = frequency in cycles/sec

[3] 1, 2, 3, 4 = CIT accelerometers; 1′, 2′, 3′, 4′ = UCLA accelerometers; N. S. E. W. = directions; R=Roof; A=first basement; B= second basement

TABLE I-1 (Continued)

Test	Date	Purpose	Weights per Unit	Force lbs/Unit	Frequency Scale counts/cycle	Accelerometer Locations (Figures I-1, I-2)
11	June 8	Geometry of 1st, 2nd and 3rd E-W modes	Full	$804f^2$	1000	First setup: 1, 2, 3, 4 and 5-W-20-e (dynamic calibration) Second setup: 1-N-20-g, 2-W-20-c, 3-S-20-z, 4-W-20-y, 5-W-20-x.
12	June 14	Detailed torsional low frequency sweep	Full	$804f^2$	1000	1-N-20-g, 2-W-20-e, 3-S-20-z, 4-E-20-y, 5-W-20-x
13	June 14	Geometry of 1st, 2nd and 3rd torsional modes	Full	$804f^2$	1000	First setup: 1, 2, 3, 4 and 5-W-20-bb (dynamic calibration) Second setup: 1-N-R-aa, 2-W-R-aa, 3-S-R-cc, 4-E-R-cc, 5-W-20-dd Third setup: 1-N-aa and 2-W-aa on floors 21 through 7; 3-S-ee and 4-E-ee on floors 21 through 7, 5-W-20-dd.
14	June 15	Geometry of 1st, 2nd and 3rd torsional modes	Full	$804f^2$	1000	First setup: 1, 2, 3 and 4-W-aa (dynamic calibration) 5-W-20-dd Second setup: 1-N-aa and 2-W-aa on floors 7 through 2; 3-S-ee and 4-E-ee on floors 7 through 2, 5-W-20-dd Third setup: 1-N-1-aa, 2-W-1-aa, 3-S-1-hh, 4-E-1-hh, 5-W-20-dd Fourth setup: 1-N-A-aa, 2-W-A-aa, 3-S-A-ff, 4-E-A-ff, 5-W-20-dd Fifth setup: 1-N-B-aa, 2-W-B-aa, 3-S-B -gg, 4-E-B-gg, 5-W-20-dd
15	June 15	Geometry of 1st, 2nd and 3rd E-W modes	Full	$804f^2$	1000	First setup same as Fifth setup, test 14; Second setup same as Fourth setup, test 14; Third setup same as Third setup test 14; Fourth setup 1-N-aa, 2-W-aa, 3-S-ee, and 4-E-ee on floors 2 through 21 and 5-W-20-dd; Fifth setup same as Second setup, test 13.
16	June 21	Measurement of two-story portion during E-W vibration	Full	$804f^2$	1000	Two locations on roof of two-story building
17a	June 21	E-W high frequency sweep	S4	$227f^2$	300	1-W-16-aa, 2-W-16-ee, 3-W-18-aa, 4-W-18-ee, 5-W-20-dd
17b	June 21	E-W high frequency sweep	S2	$140f^2$	300	Same as test 17a.
18a	June 21	Torsional high frequency sweep	S4	$227f^2$	300	1-W-16-aa, 2-E-16-ee, 3-W-18-aa, 4-E-18-ee, 5-W-20-dd
18b	June 21	Torsional high frequency sweep	S2	$140f^2$	300	Same as test 18a
19a	June 21	N-S high frequency sweep	S4	$227f^2$	300	1-S-16-aa, 2-S-16-ee, 3-S-18-aa, 4-S-18-ee, 5-S-20-dd
19b	June 21	N-S high frequency sweep	S2	$140f^2$	300	Same as test 19a
20	June 22	Geometry of higher N-S modes	S3	$184f^2$	300	1-S-aa on floors 21, 19, 17, . . . , 3, 1, B; 2-S-ee on floors 21, 19, 17, . . . , 5, 3; 3-S-aa on floors R, 20, 18, . . . , 4, 2, A; 4-S-ee on floors R, 20, 18, . . . , 4, 2; and 5-S-20-dd.

TABLE I-1 (Continued)

Test	Date	Purpose	Weights per Unit	Force lbs/Unit	Frequency Scale counts/cycle	Accelerometer Locations (Figures I-1, I-2)
21a	June 28	Torsional and E-W high frequency sweeps	S1	$96f^2$	300	First setup: 1-E-13-aa, 2-W-13-ee, B-E-14-aa, 4-W-14-cc 5-W-20-dd Second setup: 1-W-13-aa, 2-W-13-ee, 3-W-14-aa, 4-W-14-ee, 5-W-20-dd
21b	June 28	Geometry of higher E-W modes	S3	$184f^2$	300	1-W-aa on floors 21, 19, 17, . . . , 5, 3, 1, B; 2-W-ee on floors 21, 19, 17, . . . , 5, 3; 3-W-aa on floors R, 20, 18, . . . , 4, 2, A; 4-W-ee on floors 20, 18, . . . , 4, 2 and 4-W-R-ii; 5-W-20-dd.
22	June 28	Geometry of higher Torsional modes	S2	$140f^2$	300	1-N-aa on floors R, 21, 20, . . . , 1, A, B; 2-S-R-ii and 2-S-ee on floors 21, 20, 19, . . . , 3, 2; 3-W-aa on floors R, 21, 20, 19, . . . , 3, 2; 4-E-R-ii and 4-E-ee on floors 21, 20, . . . , 1, A, B; 5-W-20-dd.

TABLE I-2
ACCELEROMETER LOCATIONS
SAN DIEGO GAS AND ELECTRIC COMPANY BUILDING

Location Code	Floor(s)	Location (Figure I-1, I-2)
a	20	On line 3, 1' E of row A
b	20, 21	1' N of line 3, 1' W of row C
c	20	1' N of line 2, 26' W of row B
d	20	1' N of line 2, 15' W of row B
e	20	1' N of line 2, on row B
f	20	1' N of line 2, 15' E of row B
g	20	1' N of line 2, 1' W of row C
h	20	2' N of line 7, on row B
i	20	2' S of line 5, 1' W of row B
j	20	2' S of line 3, 1' W of row B
k	20	3' S of line 1, on row B
l	20	3' N of line 7, on row B
m	21, 20, . . . , 2	West landing of south stairwell, 1' S and 1' E of NW corner
n	R, A, B	6' N of line 4, 1' E of row B
o	1	6' S of line 3, 10' E of row B
p	12	2' N of line 4, 24' W of row B
q	12	2' N of line 4, 10' W of row B
r	12	2' N of line 4, on row B
s	12	2' N of line 4, 10' E of row B
t	12	2' N of line 4, 24' E of row B
u	R	On line 4, 36' W of row B
v	21	1' N of line 3, 1' E of row A
w	R	On line 4, 36' E of row B
x	20	On line 4, 1' W of row B
y	20	1' S of line 6, 1' E of row B
z	20	On line 6, 1-1/2' E of row A
aa	R, 21, 20, . . . , 1, A, B	Center of east landing of north stairwell
bb	20	2' N of line 2, 4' W of row B
cc	R	58' S of line 4, 36' W of row B
dd	20	2' N of line 2, on row B
ee	21, 20, . . . , 3, 2	Center of west landing of south stairwell
ff	A	On line 5, 2' W of row B
gg	B	2' N of North wall of freight elevator foyer, 10' W of elevator
hh	1	Center of west landing of N stairwell
ii	R	3' N of line 5, 1' E of row A

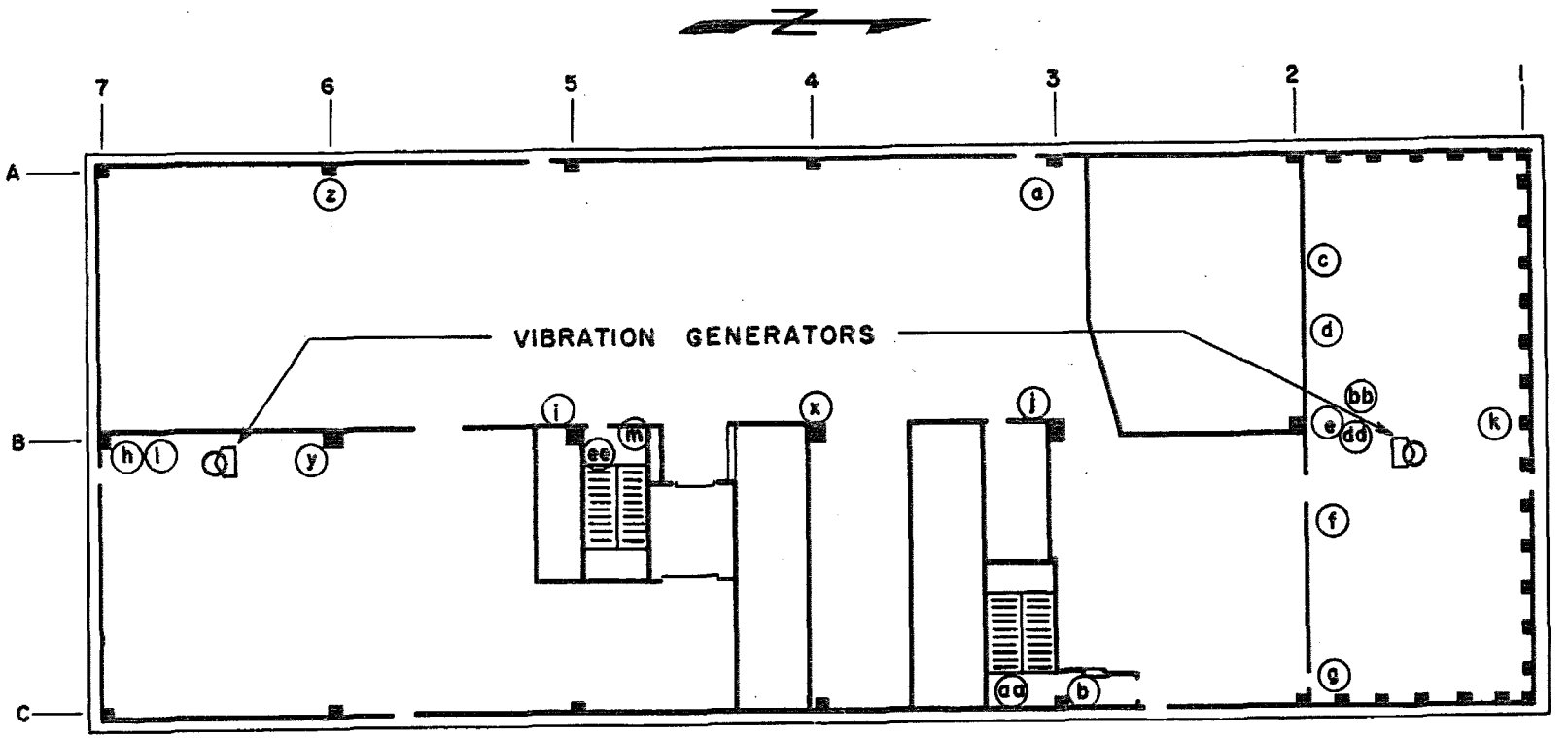

APPROXIMATE ACCELEROMETER LOCATIONS
20th FLOOR
SAN DIEGO GAS & ELECTRIC BUILDING

FIGURE I-1.

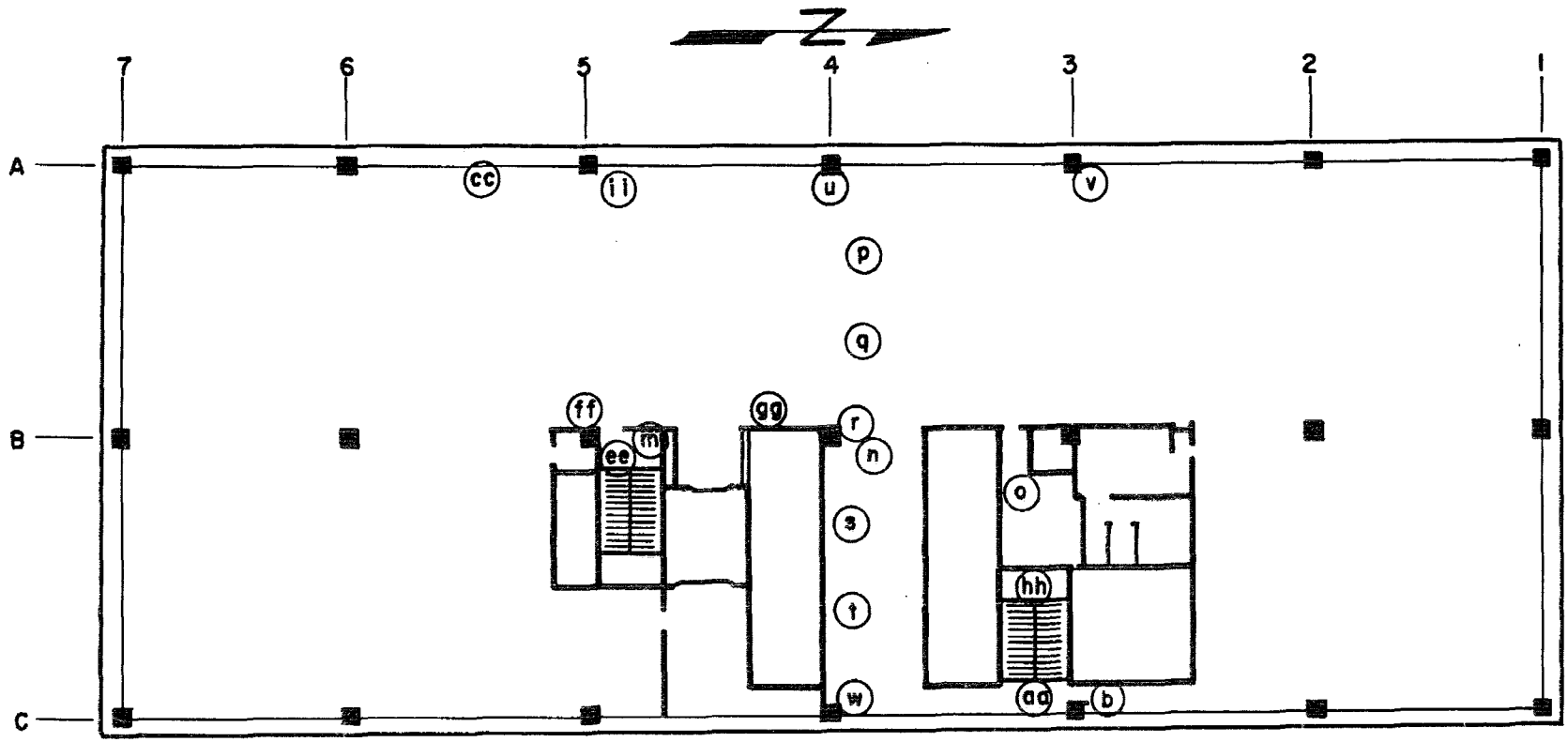

APPROXIMATE ACCELEROMETER LOCATIONS

ALL FLOORS EXCEPT 20th

SAN DIEGO GAS & ELECTRIC BUILDING

FIGURE I-2.

APPENDIX II

MODE SHAPES FROM AMBIENT TESTS

The following natural periods and mode shapes were determined from ambient vibration tests of the San Diego Gas and Electric Company Building. The ambient, or wind-excited, experiment was conducted in conjunction with the forced-vibration tests described in the text of this report. The details of the ambient tests have been presented previously (Trifunac, 1970a) and only the mode shapes are repeated here for purposes of comparison with similar results from the forced vibration of the building. Natural frequencies and damping ratios determined from the ambient tests have already been included in the text in Table III.

Some of the figures include comparison of the mode shapes with those found from the forced-vibration tests. Because the results from the forced-vibration experiment were preliminary when they were made available to Dr. Trifunac, some small differences exist between mode shapes given in this appendix and those presented in the body of the report. Also, since preliminary data analysis did not reveal clearly the complexity of the fundamental modes, the fundamental mode shapes ascribed to forced vibration given in this appendix include only the primary component of the motion.

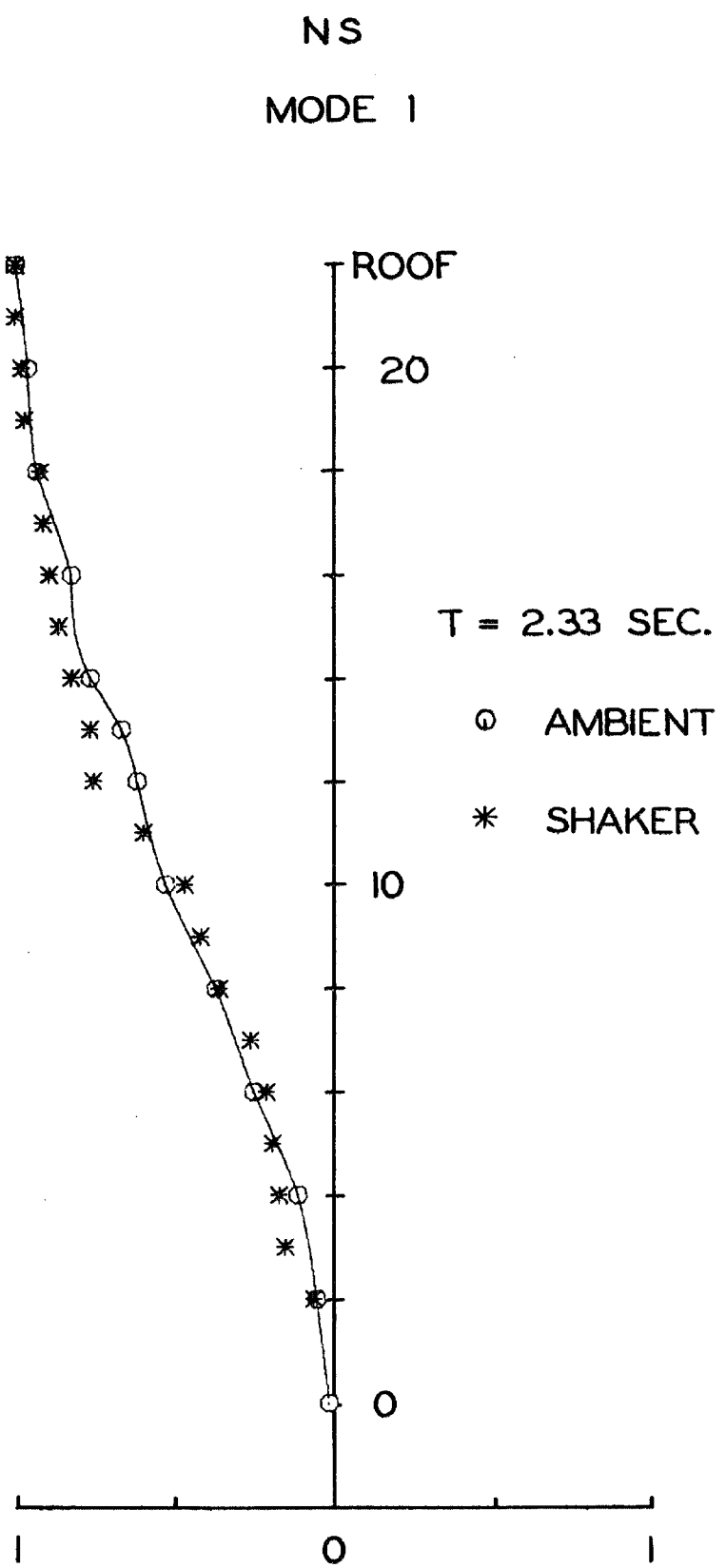

FIGURE II-1. FIRST N-S MODE

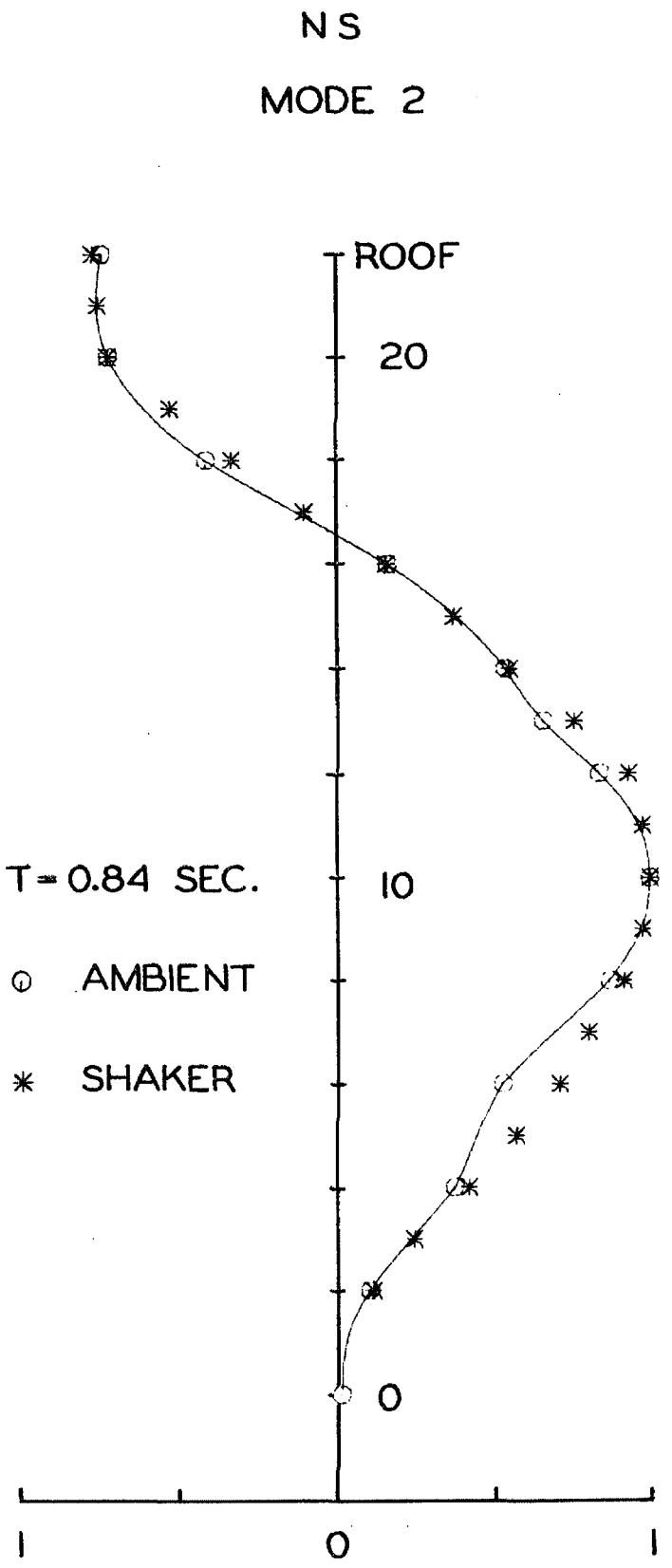

FIGURE II-2. SECOND N-S MODE

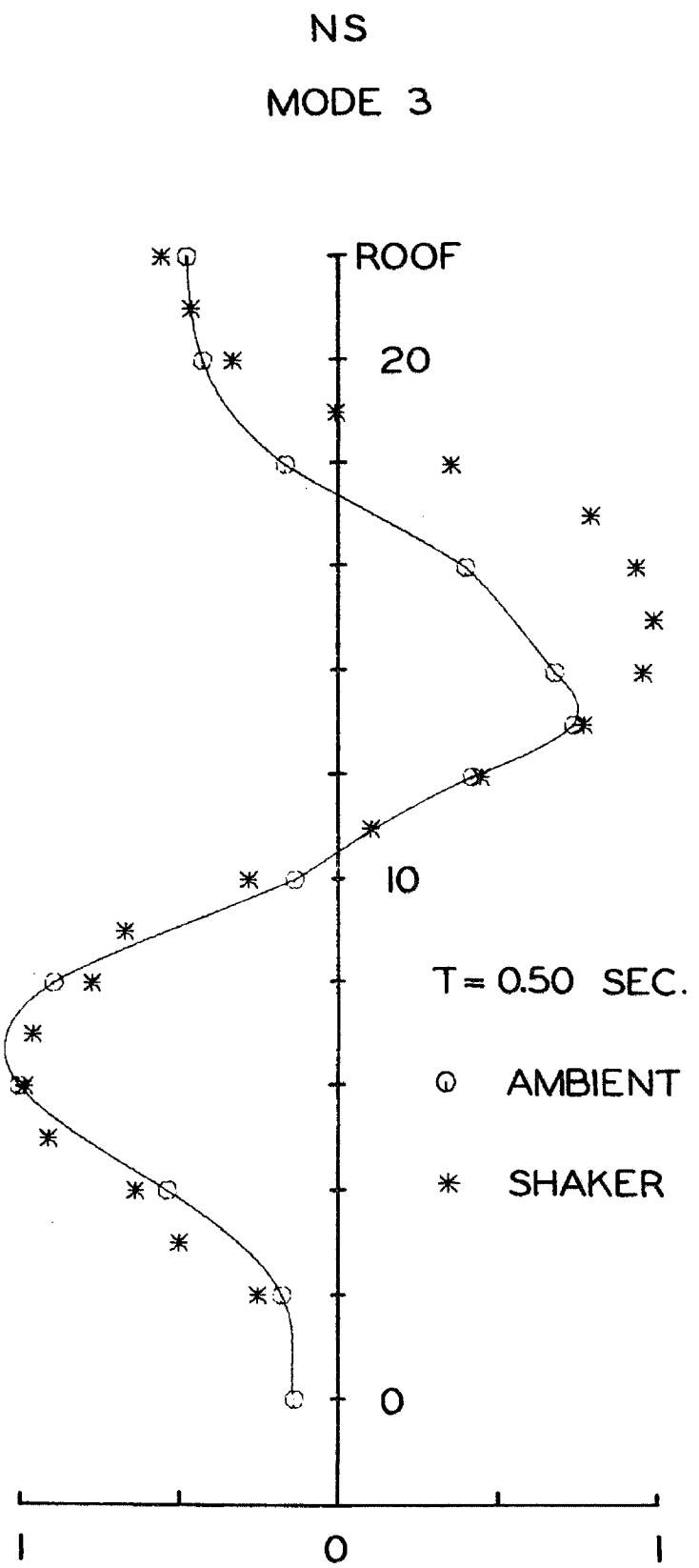

FIGURE II-3. THIRD N-S MODE

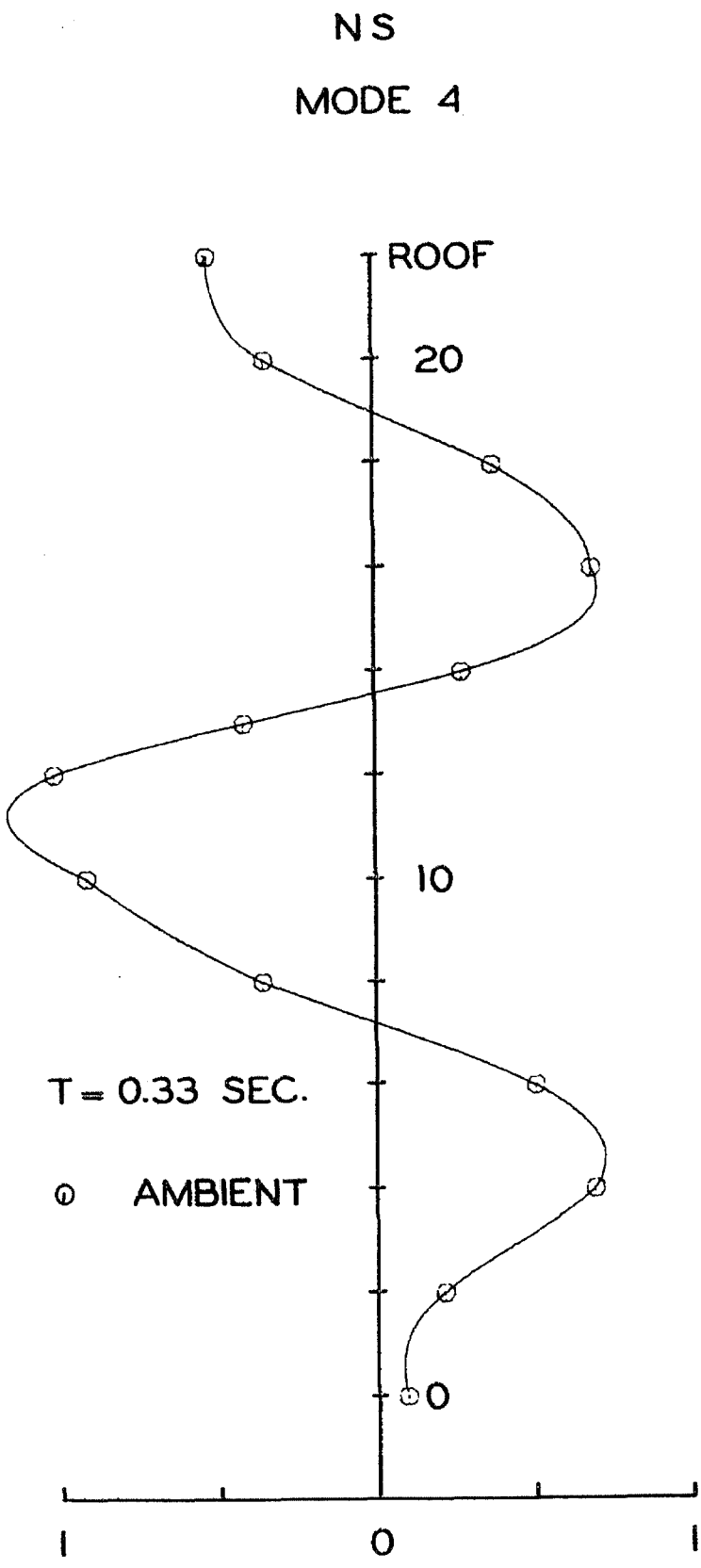

FIGURE II-4. FOURTH N-S MODE

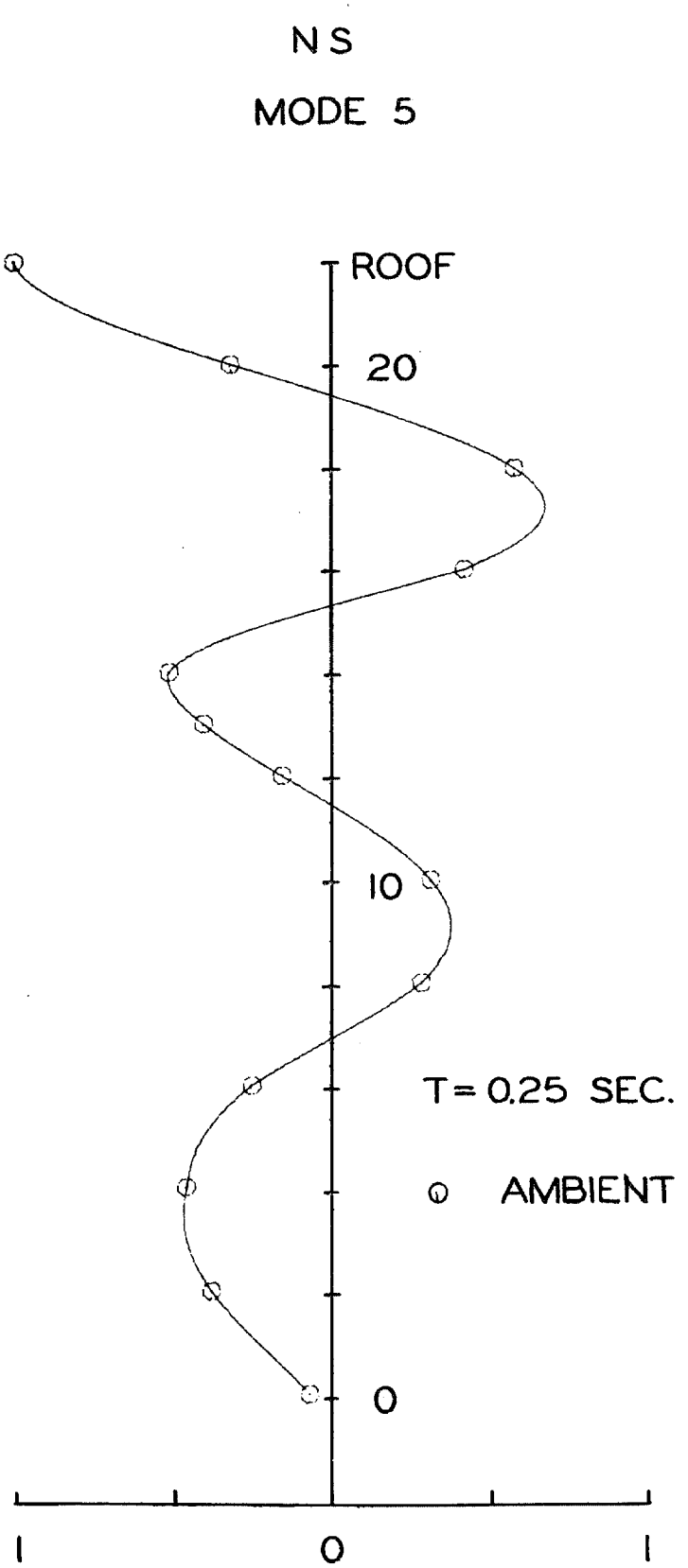

FIGURE II-5. FIFTH N-S MODE

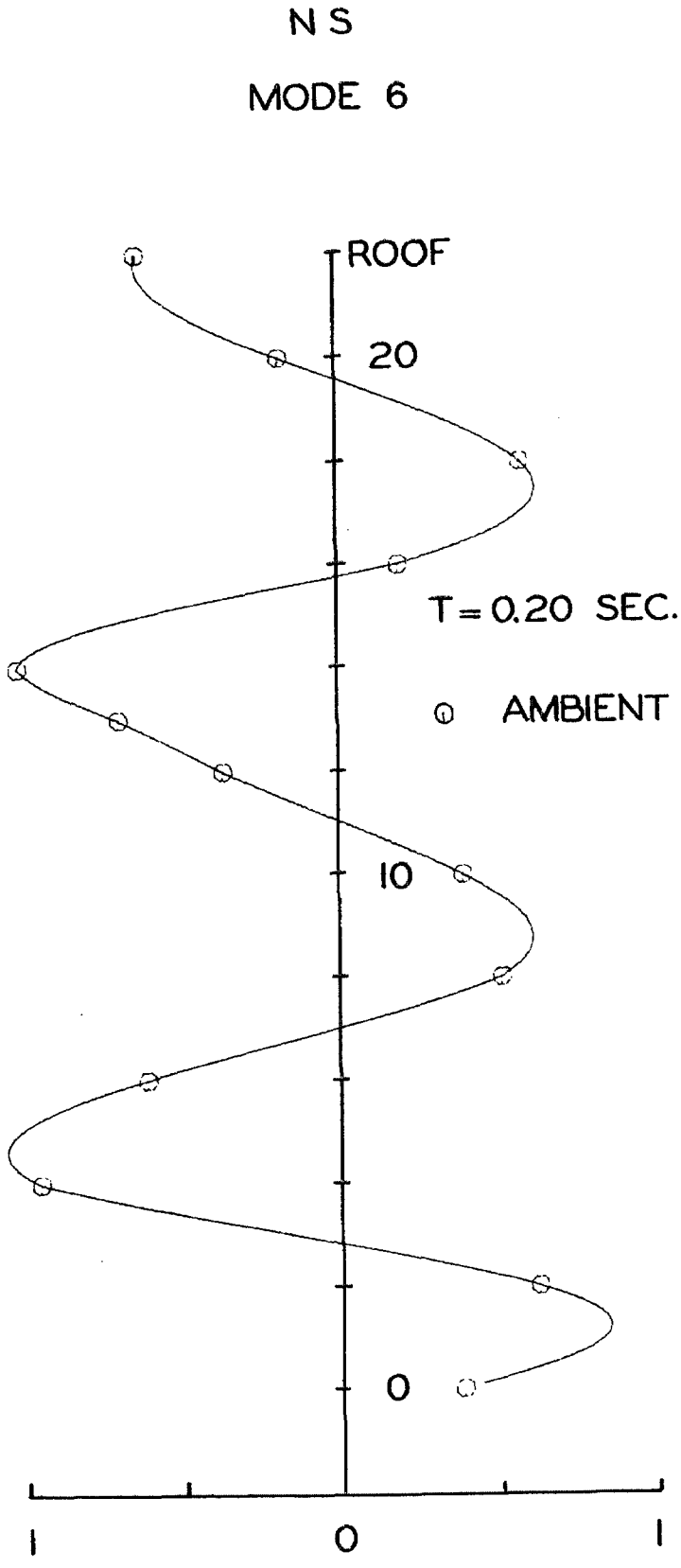

FIGURE II-6. SIXTH N-S MODE

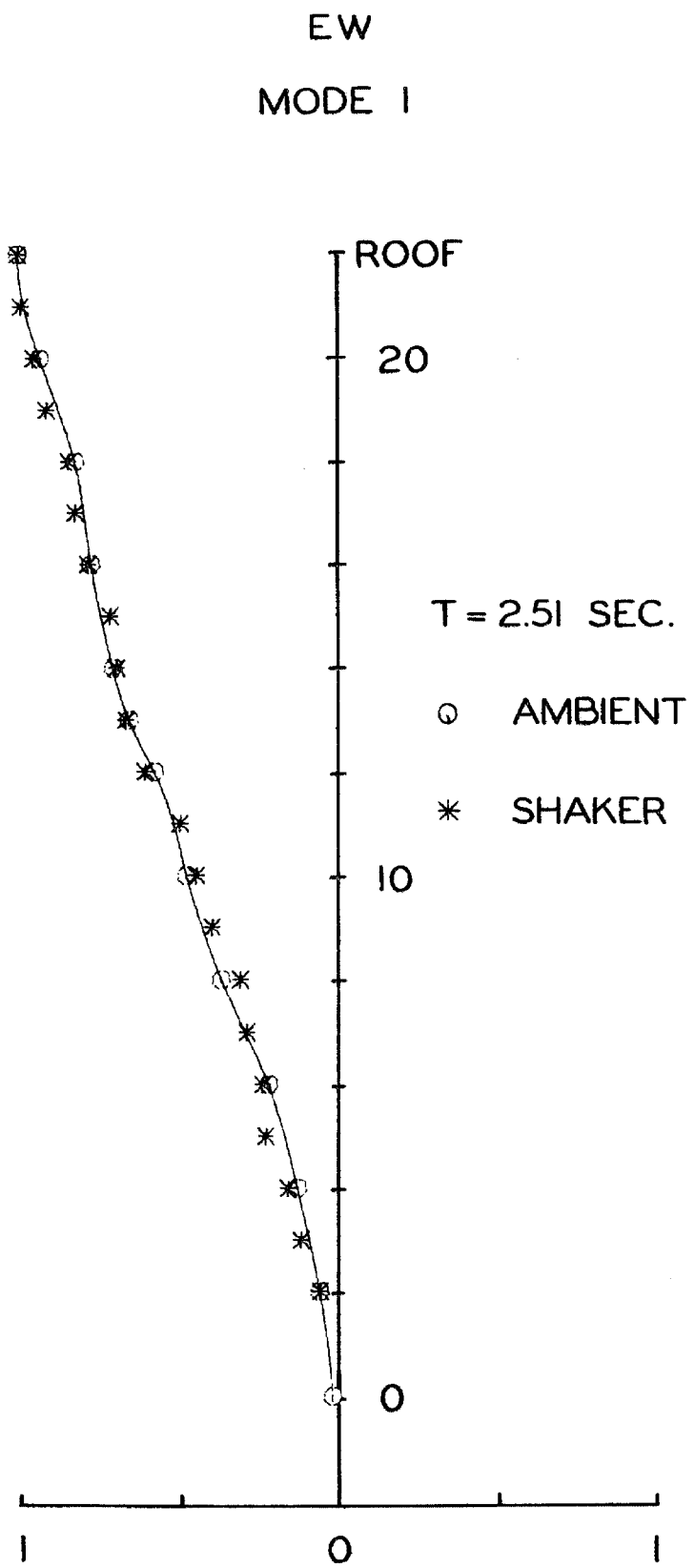

FIGURE II-7. FIRST E-W MODE

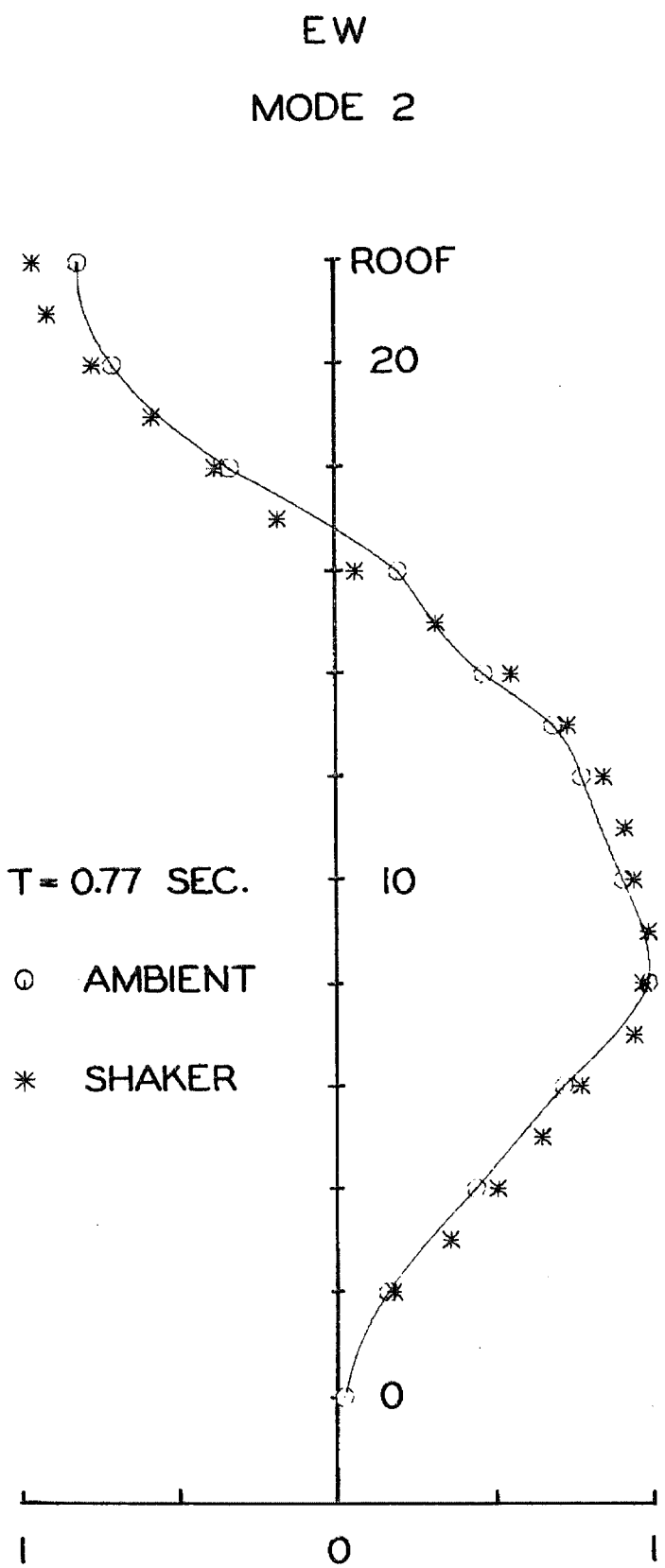

FIGURE II-8. SECOND E-W MODE

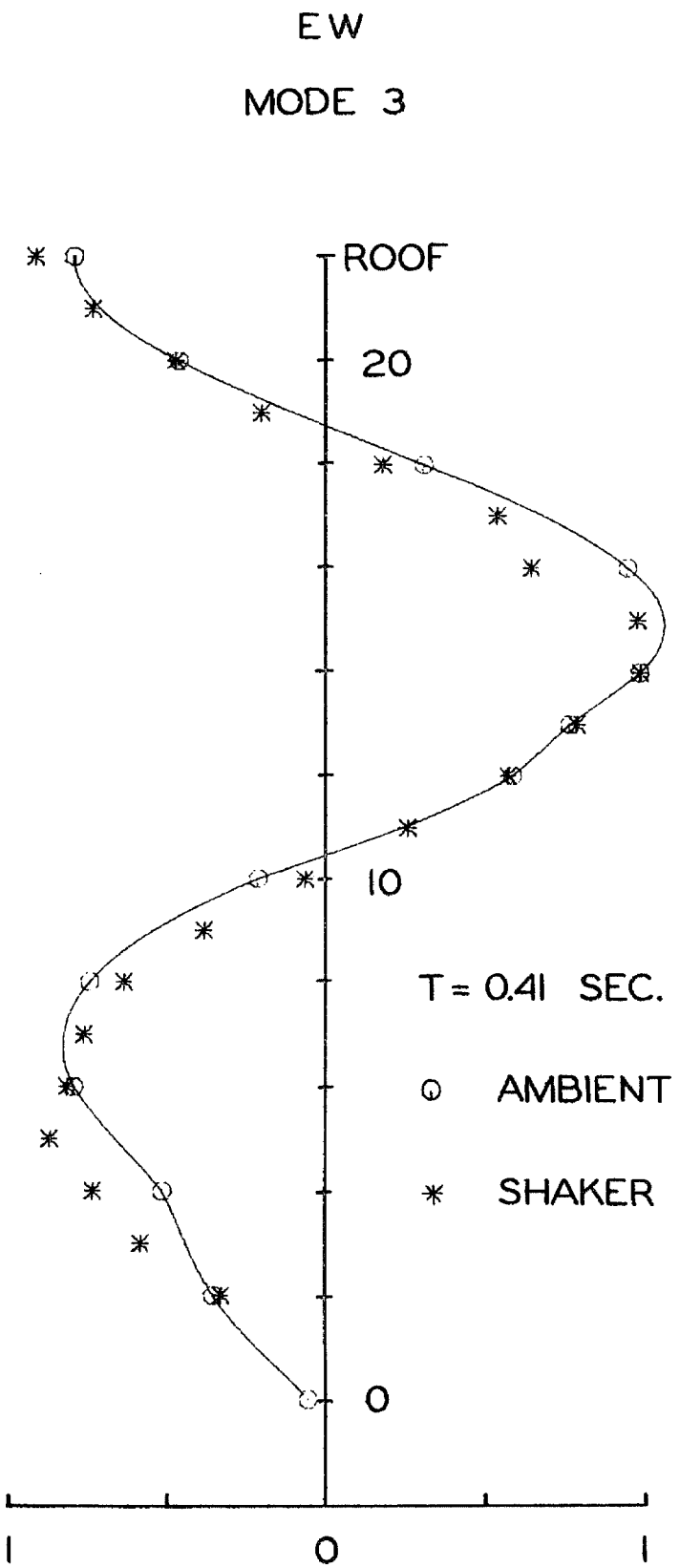

FIGURE II-9. THIRD E-W MODE

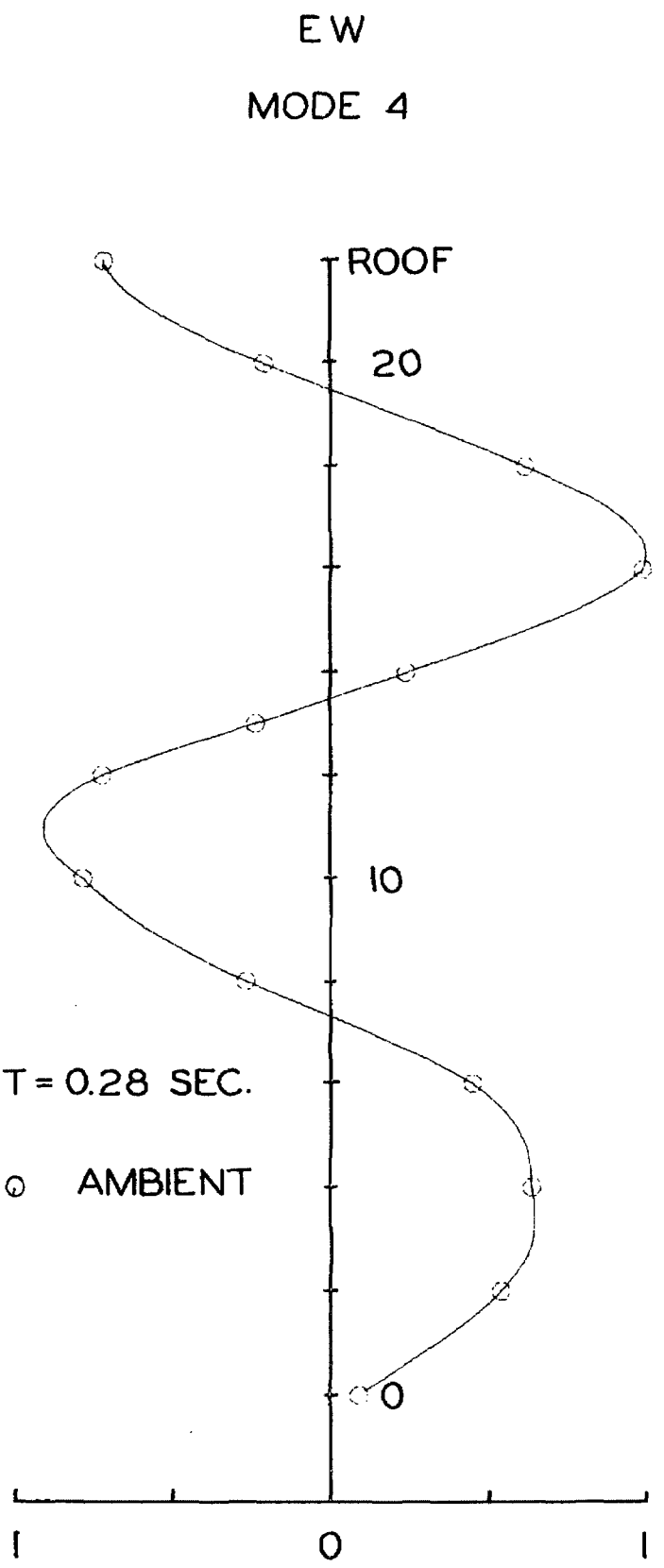

FIGURE II-10. FOURTH E-W MODE

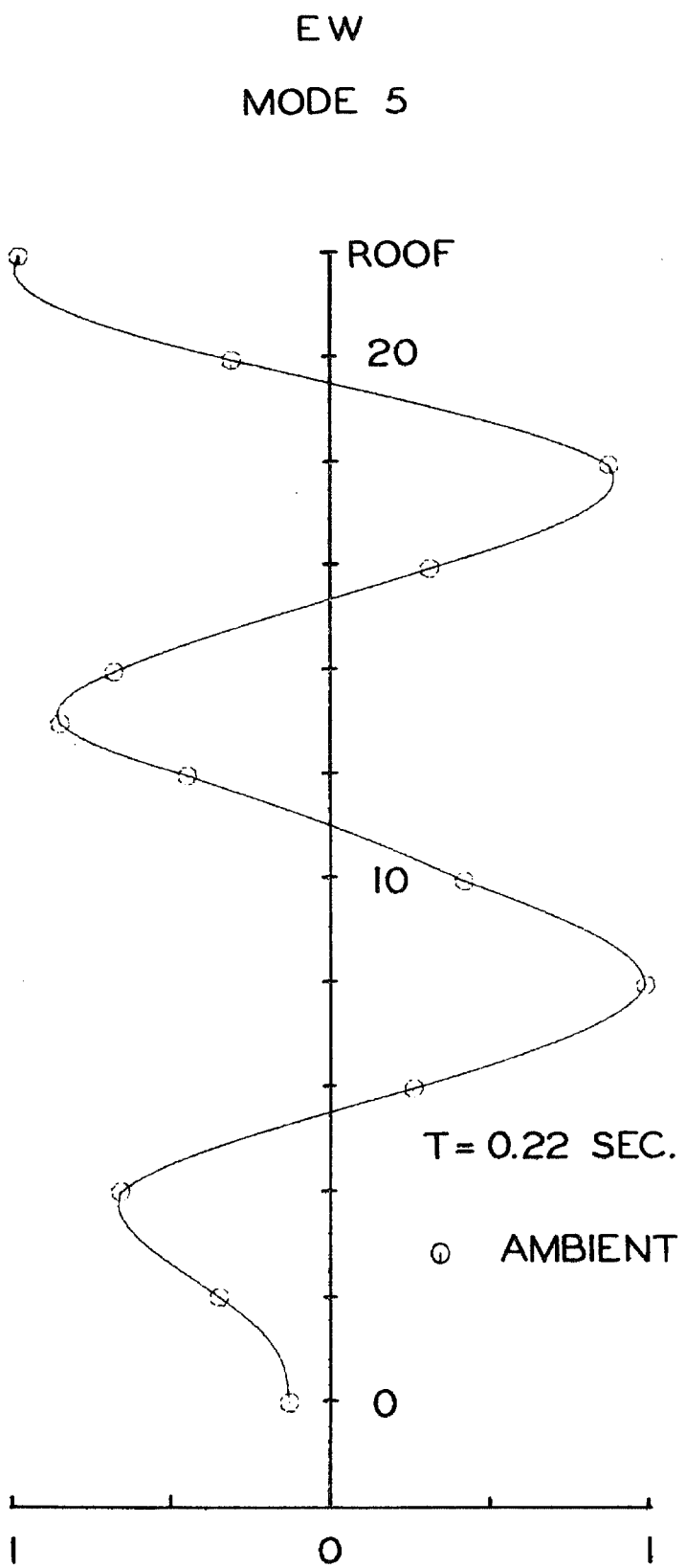

FIGURE II-11. FIFTH E-W MODE

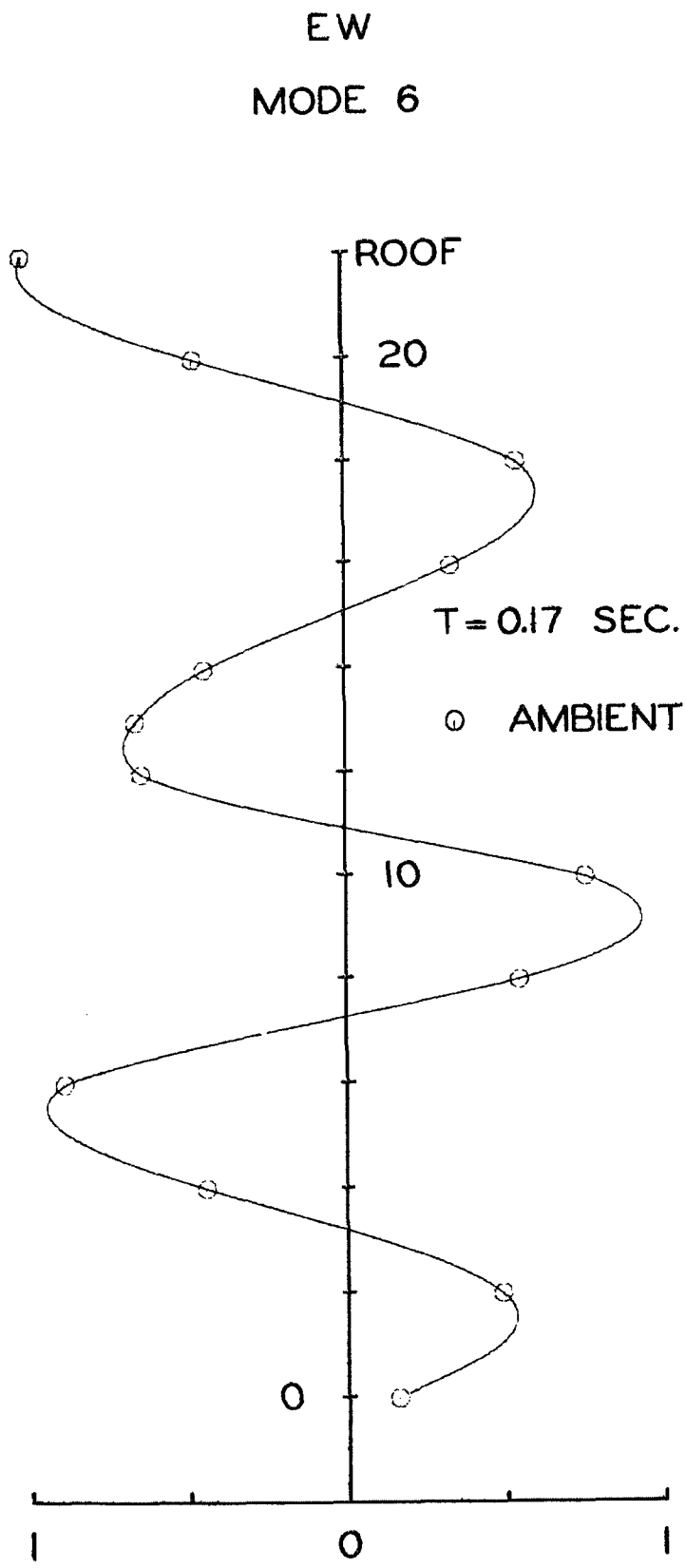

FIGURE II-12. SIXTH E-W MODE

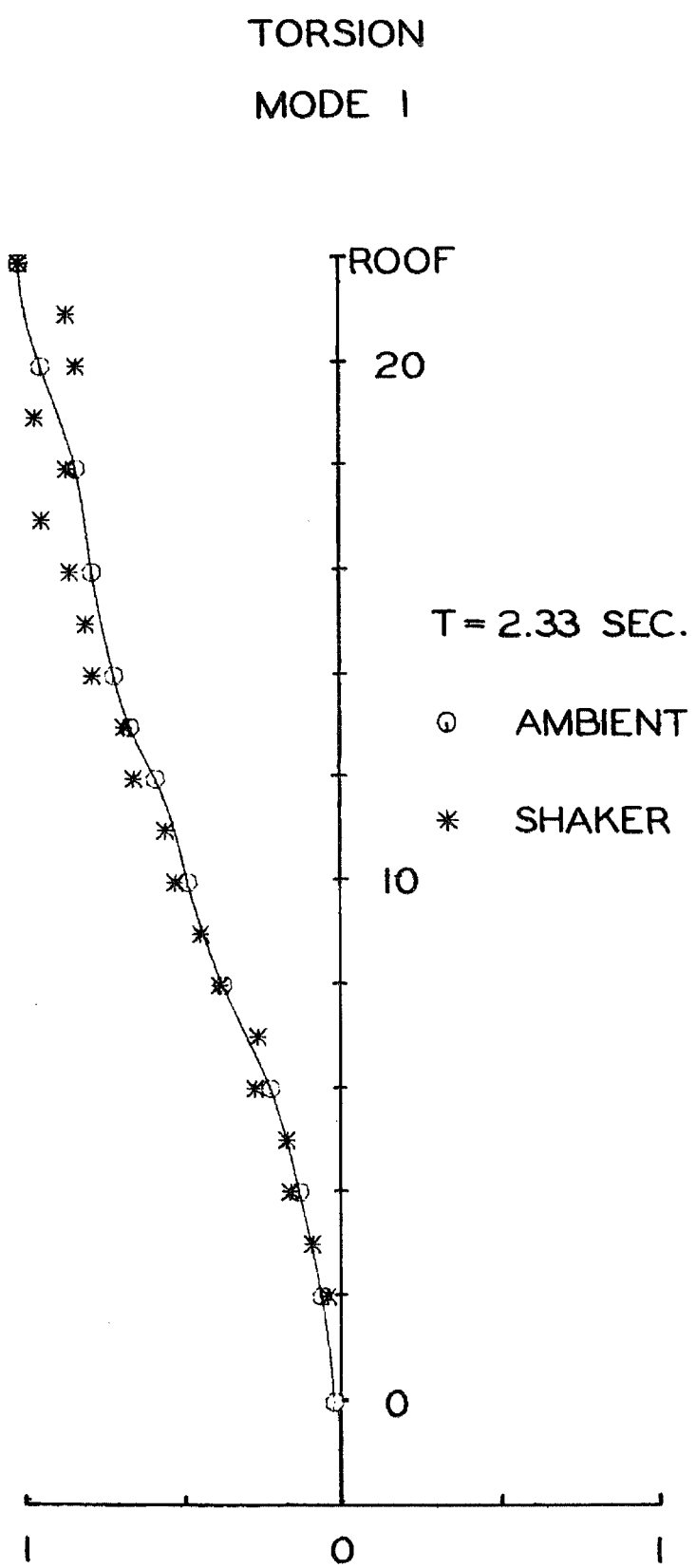

FIGURE II-13. FIRST TORSIONAL MODE

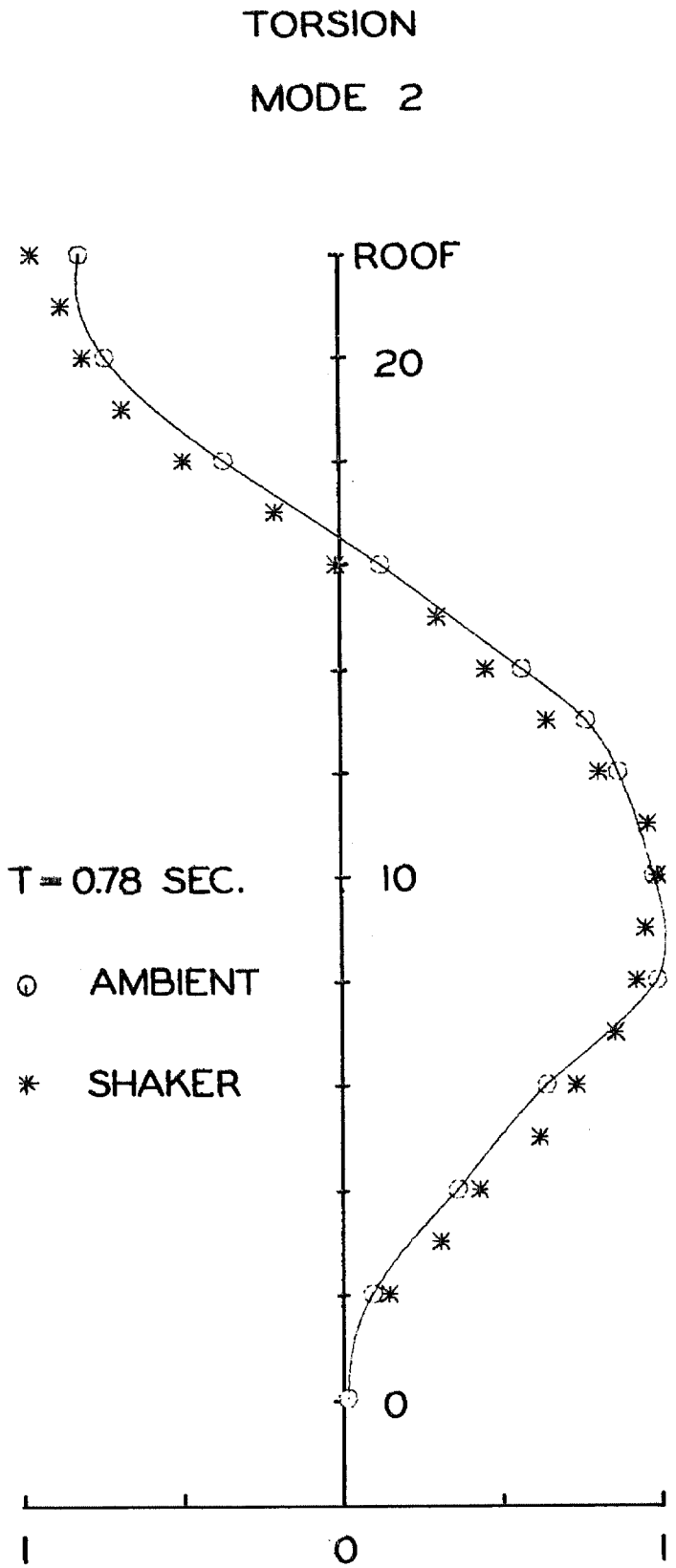

FIGURE II-14. SECOND TORSIONAL MODE

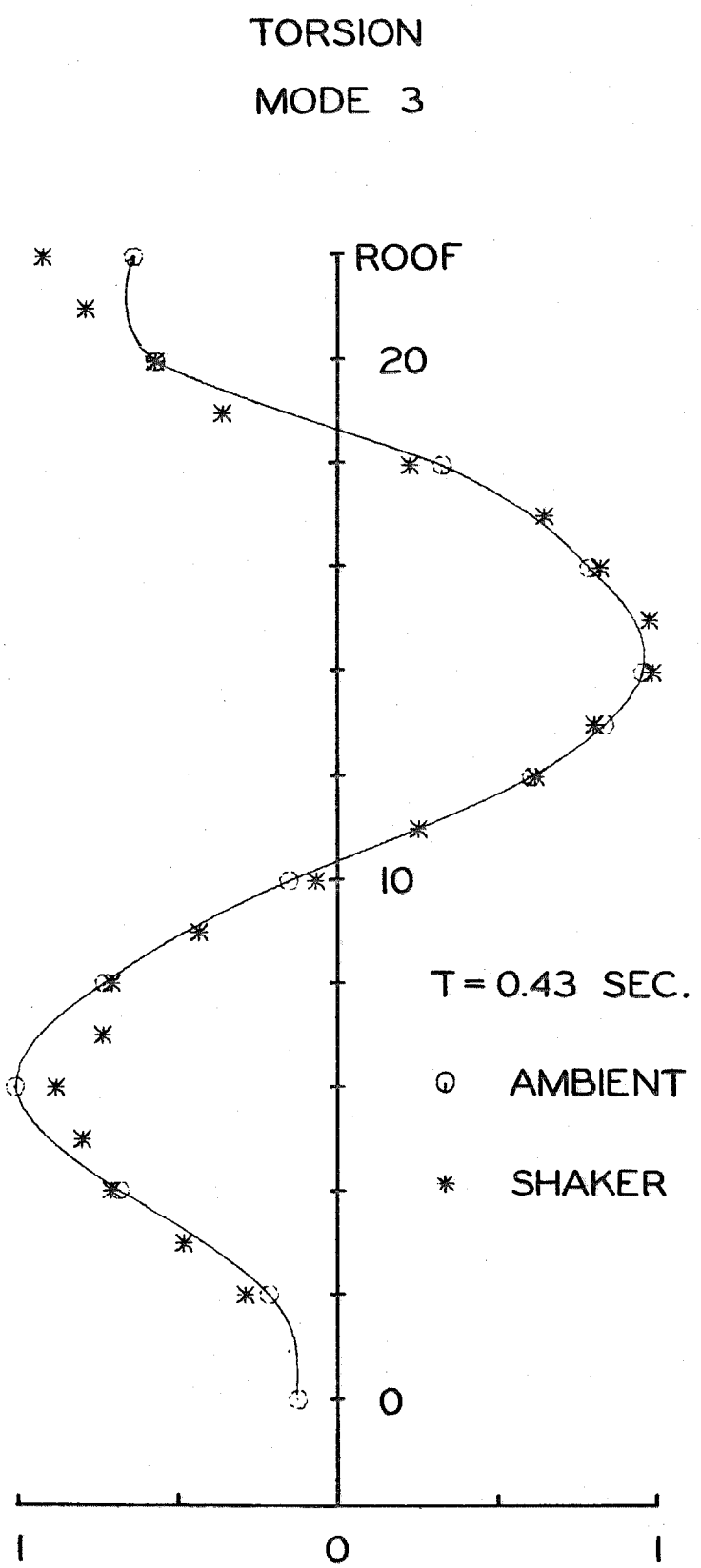

FIGURE II-15. THIRD TORSIONAL MODE

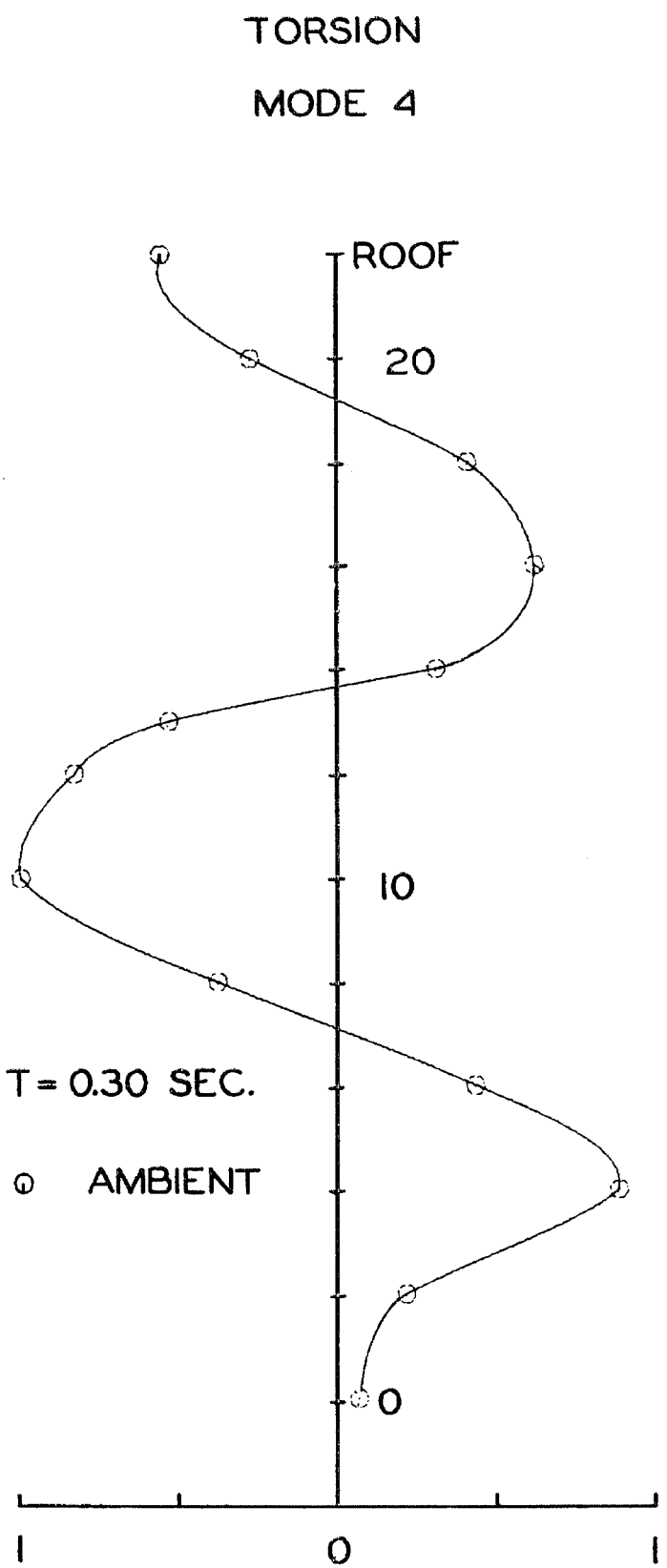

FIGURE II-16. FOURTH TORSIONAL MODE

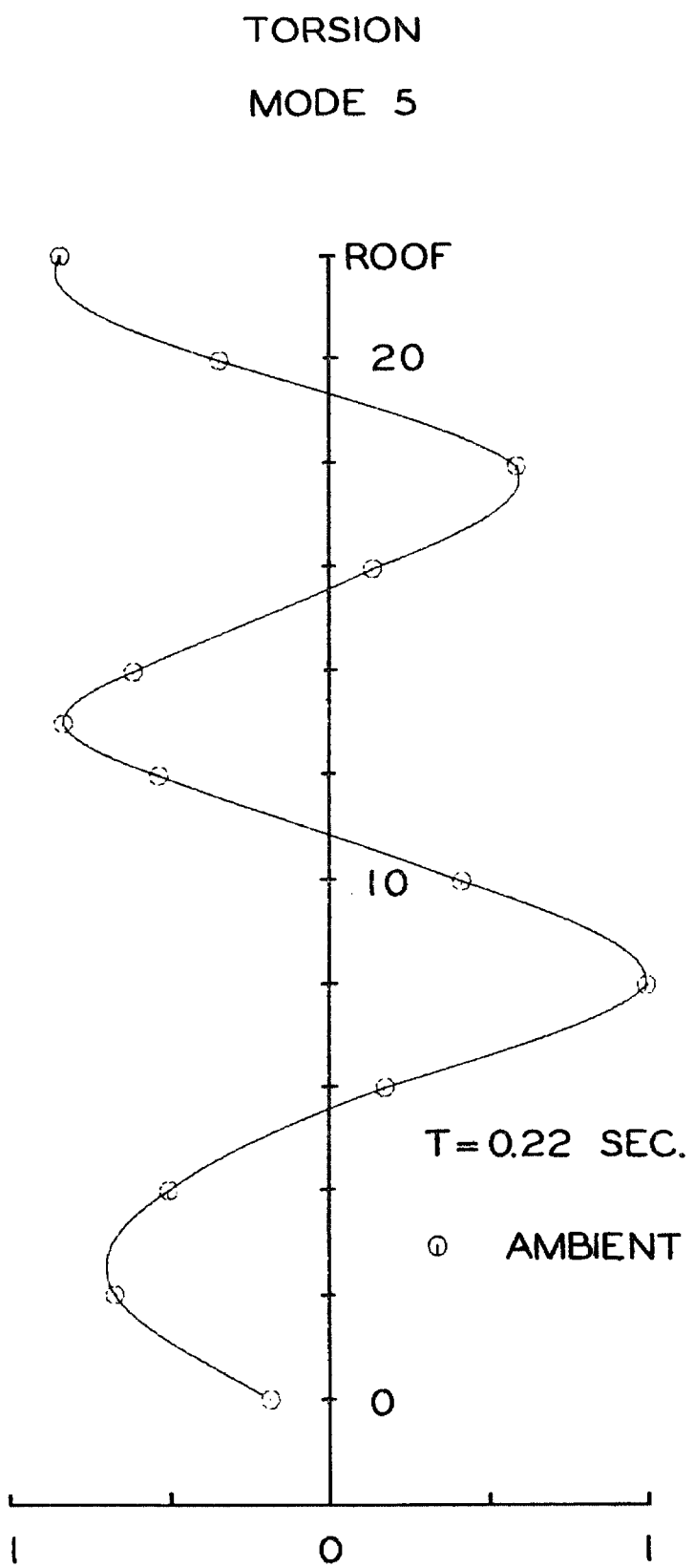

FIGURE II-17. FIFTH TORSIONAL MODE